An investigation into the biochemical effects of Kojic acid (KA) on human hepatocellular carcinoma (HepG2) cells

By

Kimera Tamzin Suthiram

BSc. B. Med. Sci. (Hons) (UKZN)

Submitted in fulfilment of the requirements for the degree of

Master of Medical Science

In the Discipline of Medical Biochemistry

School of Laboratory Medicine and Medical Sciences

College of Health Science

University of KwaZulu-Natal

Durban

2020

DECLARATION

I, Miss, Kimera Tamzin Suthiram, declares as follows:

i. The research reported in this thesis, except where otherwise indicated, is my original work.

ii. This thesis has not been submitted for any degree or examination at another university.

iii. This thesis does not contain other persons' data, pictures, graphs, or other information, unless specifically acknowledged as being sourced from other persons.

iv. This thesis does not contain other person's writing, unless specifically acknowledged as being sourced from other researchers. Where other written sources have been quoted, then:
a. their words have been re-written but the general information sourced has been referenced to the authors;

b. where their exact words have been used, their writing has been placed within quotation marks, and referenced.
v. Where I have reproduced a publication of which I am an author, co-author, or editor, I have indicated in detail which part of the publication was written by myself alone and have fully referenced such publications.

vi. This thesis does not contain text, graphics, or tables copied and pasted from the internet, unless specifically acknowledged, and the source being detailed in the thesis and reference section.

The research described in this study was carried out in the Discipline of Medical Biochemistry, School of Laboratory Medicine and Medical Science, College of Health Sciences, University of KwaZulu-Natal, under the supervision of Prof Anil A. Chuturgoon and Dr Terisha Ghazi.

1/02/2021

_____ _____

Miss K.T. Suthiram Date

ACKNOWLEDGEMENTS

To My Supervisor and Co-supervisor

Prof A.A. Chuturgoon, you have been a constant inspiration and source of knowledge. Your advice and teachings are forever etched in my mind. Dr T. Ghazi, I cannot express my gratitude as to how much I appreciate your constant guidance throughout the year. Thank you for your devotion, excellent work ethic, and allowing me to learn from my mistakes.

To my mother

You have been the greatest inspiration in my life. I thank you for your selfless and unequivocal love, devotion and tireless efforts to afford me every dream I've ever had. I am so grateful for every piece of advice and motivation you have given me. You have been there through all the challenges that I have faced and always reminded me to look beyond the challenge and enjoy the moments of development. For this I cannot thank you enough.

To my siblings

Nastassia, you have been supportive in every endeavour that I have ever embarked on. Though we were apart, I never felt the distance due to your loving advice and motivation. You have imparted so much of knowledge onto me while growing up that at times I didn't understand, but as I grow, I understand every lesson more and more. You have made this journey easier and I appreciate it immensely. Bradley, you have been my stress reliever and have motivated me to do better in so many ways. You have always believed in my abilities and taught me so much throughout the years. I thank you both for always believing in me even when I had set boundaries for myself. Both of you have inspired and encouraged me to take leaps that I often found daunting.

To the Medical Biochemistry department

I'd like to thank everyone in the department for all their helpful advice and assistance. All of you have left a lasting impression and I am so grateful to have met such remarkable, motivating and intelligent individuals.

Funding

I would like to thank the National Research Foundation for the financial support during the research.

TABLE OF CONTENTS

LIST OF ABBREVIATIONS

α	Alpha
β	Beta
%	Percentage
µg	Microgram
µl	Microlitre
4-HNE	4-Hydroxy-4-nonenal
8-OHdG	8-hydroxy-2-deoxyguanosine
AA	Arachidonic acid
AP-1	Activating protein-1
APS	Ammonium persulfate
ATP	Adenosine triphosphate
BCA	Bicinchoninic acid
BSA	Bovine serum albumin
CA	California
cDNA	Complementary DNA
cm^3	Centimetre cube
CO_2	Carbon dioxide
Cu^+	Cuprous ion
Cu^{2+}	Cupric ion
CYP450	Cytochrome P450
dH_2O	Distilled water
DMSO	Dimethyl sulfoxide
DNA	Deoxyribose nucleic acid
EDTA	Ethylene diaminetetraacetic acid
ELISA	Enzyme-linked immunosorbent assay

EMEM	Eagle’s minimum essential medium
ETC	Electron transport chain
g	Gravitational force
h	Hours
H_2O_2	Hydrogen peroxide
HepG2 cells	Human hepatocellular carcinoma cell line
HQ	Hydroquinone
HRP	Horseradish peroxidase
IC_{50}	Maximal inhibition concentration
KA	Kojic acid
KEAP1	Kelch-like ECH-associated protein 1
LDH	Lactate dehydrogenase
L-DOPA	L-3,4-dihydroxyphenylalanine
M	Molar
MAPK	Mitogen-activated protein kinase
MAPKK	Mitogen-activated protein kinase kinase
MAPKKK	Mitogen-activated protein kinase kinase kinase
MDA	Malondialdehyde
MDM2	Murine double minute 2
mg	Milligram
min	Minute
MITF	Microphthalmia-associated transcription factor
ml	Milliliitre
mM	Millimolar
MN	micronuclei

NFDM	Non-fat dry milk
NFκB	Nuclear factor kappa B
Nrf2	Nuclear factor-erythroid 2-related factor 2
º C	Degrees Celsius
O_2	Superoxide
OD	Optical densities
OH^-	Hydroxyl radical
OXPHOS	Oxidative Phosphorylation
PARP1	Poly [ADP-ribose] polymerase 1
PBS	Phosphate Buffer Saline
PCE	Polychromatic erythrocytes
p53	Tumour suppressor protein 53
p-NFκB	Phosphorylated- nuclear factor kappa B
p-Nrf2	Phosphorylated-nuclear factor-erythroid 2-related factor 2
p-ser47-Sirt1	Phosphorylated-serine47-sirtuin1
PUFA's	Polyunsaturated fatty acids
qPCR	Quantitative Polymerase Chain Reaction
RBD	Relative Band Density
RLU	Relative light units
ROS	Reactive oxygen species
RT	Room temperature
SA	South Africa
SDS-PAGE	Sodium dodecyl-sulphate polyacrylamide gel electrophoresis
Sirt-1	Sirtuin 1
Taq	*Thermus aquaticus*

TBARS	Thiobarbituric acid reactive substances
TEMED	N, N, N', N'-Tetramethylethylenediamine
TTBS	Tris buffer saline
USA	United States of America
UV	Ultraviolet
WI	Wisconsin

LIST OF FIGURES

CHAPTER 1

CHAPTER 2

CHAPTER 3

APPENDIX

LIST OF TABLES

Abstract

Kojic acid (KA) is a secondary metabolite and divalent metal chelator that is widely used in the beauty industry as a skin lightener. However, KA toxicity is not well-established in humans. This study aimed to determine the toxicity of KA by assessing oxidative stress, nuclear factor kappa B (NFκB) signalling, and mitogen-activated protein kinase (MAPK) signalling in human hepatoma (HepG2) cells following 24 h exposure. Cell viability was assessed using the methylthiazol tetrazolium (MTT) and crystal violet assays. To confirm cell death, apoptosis (caspase -8, -9, -3/7 luminometry), and Lactate dehydrogenase (LDH) leakage were assessed. Oxidative stress (TBARS), DNA damage (8-OHdG), and protein oxidation (protein carbonyls assay) to determine macromolecule damage. An assessment of inflammatory and oxidative stress markers were carried out using mRNA expression (*GPx, NFκB, IκB;* qPCR) and miRNA expression (*miRNA-29a, miRNA-29b and miRNA-155*; qPCR). Protein expression of nuclear factor erythroid-2 factor-2 (Nrf2), phospho-Nrf2 (ser40), catalase (CAT), c-Jun-N-terminal kinase (JNK), p38, phospho-Sirtuin 1 (ser47) (phospho-sirt1), NFκB, phospho-NFκB (ser536), and activator protein 1 (AP-1) were assessed using Western Blot in HepG2 cells. KA decreased cell viability in HepG2 cells and elevated the activities of caspase -9 ($p < 0.0001$), caspase -8 ($p = 0.0003$) and caspase 3/7 ($p < 0.0001$) at lower concentrations [4.22 & 8.02 mM] which served as confirmation of apoptosis. Necrosis at the higher concentration [12.67 mM] was confirmed by the presence of LDH leakage indicating membrane damage. Increased cell death was further correlated with increased *miRNA-29b* expression ($p = 0.009$), a miRNA responsible for elevated apoptotic activity. Adenosine Triphosphate (ATP) production was increased significantly at 12.67 mM ($p < 0.0001$), while oxidative stress (Malondialdehyde (MDA) levels) was increased significantly at 4.22 mM ($p < 0.0001$). Macromolecules are susceptible to damage in the presence of oxidative stress. Due the elevation of MDA levels, DNA damage and protein oxidation assays were carried out. Protein carbonyls were significantly decreased ($p < 0.0001$), suggesting a potential cytoprotective effect. Due to the presence of oxidative stress, Nrf2, is activated and is responsible for the transcription of antioxidant genes. This was illustrated by an increase in activated Nrf2 at lower concentrations (4.22 & 8.02 mM), whilst at higher a concentration (12.67 mM) decreased phospho-Nrf2 ($p > 0.0001$). CAT was decreased significantly ($p = 0.0002$) and GPx significantly increased at lower concentration [4.22 mM] (1.51-fold). A key function of the MAPK pathway is the initiation of stress-activated protein kinases, p38 and JNK, in response to oxidative stress. KA significantly increased, p38 at lower concentration ($p = 0.0011$) and significantly decreased JNK1 ($p = 0.0039$) and JNK2 ($p < 0.0001$) activity. Regulation of reactive oxygen species (ROS) production by Sirt-1 occurs via the alteration of immune responses through NFκB signalling and AP-1. Inflammatory mediators, phospho-Sirt1 was significantly decreased ($p < 0.0001$), while AP-1 expression was elevated ($p = 0.0003$). The decrease in phospho- Sirt1 resulted in decreased phospho- NFκB expression ($p < 0.0001$). To further illustrate inflammation repression and alteration in MAPK signalling, *MiRNA-155* expression was increased ($p = 0.0018$). There was elevation of *miRNA-29a* expression ($p = 0.0002$)

which is in agreement with repressed inflammatory responses reflected by decreased NFκB expression. KA treatment resulted in increased MDA levels and antioxidant responses. MAPK signalling was elevated in response to oxidative stress suggesting the involvement in cell death, whilst inflammation was suppressed. In conclusion, KA displayed low toxicity in HepG2 cells.

Introduction

Kojic acid (KA; 5-hydroxy-2-(hydroxymethyl)-4H-pyran-4-one), is a fungal metabolite produced by *Aspergillus and Penicillium* species (Parrish et al., 1966). KA is a hydrophilic acid and a recognised chelating agent that is widely used in the medicinal, cosmetic and food industry (Azami et al., 2017), known to inhibit tyrosinase activity in melanocytes leading to the reduction of melanin and lightening of skin pigmentation (Choi et al., 2012).

Toxicity studies by Rodrigues et al. (2011) found that KA's ability to produce reactive oxygen species (ROS) enhances the phagocytic activity of mice peritoneal cells leading to cell damage. In contrast, KA was found to have an antioxidant effect on cells by scavenging ROS in leukocytes *in vitro* (Niwa and Akamatsu, 1991). *In vivo*, KA studies found increased lipid peroxidation, expressed as elevated MDA levels, in liver homogenates (Kotyzova et al., 2004). Oxidative stress is a result of the imbalance between antioxidants and oxidants (free radicals). The molecular oxygen can react to form products such as water (H_2O), hydrogen peroxide (H_2O_2), and superoxide anions (O_2^-). The equilibrium required for the normal functioning of biological systems is altered when oxidants exceed the cells antioxidant capacity (Ott et al., 2007). Macromolecules exposed to excess ROS form DNA adducts, protein carbonyls, and are prone to lipid peroxidation (Wiesmüller et al., 2002, Cooke et al., 2003, Dalle-Donne et al., 2003, Ayala et al., 2014).

The increase of ROS results in an antioxidant response by nuclear factor erythroid-2 related factor 2 (Nrf2). Majority of ROS is produced in the mitochondria (Murphy, 2009). Nrf2 is termed the master regulator of antioxidant responses due to its function in the transcription of antioxidant genes, namely superoxide-dismutase 2 (SOD_2) and catalase (CAT). These enzymes play key roles in the alleviation of oxidative stress (Basak et al., 2017). O_2 is converted by SOD_2 to H_2O_2 and later decomposed by CAT to hydrogen peroxide (H_2O_2) and O_2. Dysregulations in the antioxidant response have been linked to several diseases (Liguori et al., 2018).

ROS acts as a secondary messenger which initiates an immune response. KA inhibits tyrosinase activity; hence, the mitogen-activated protein kinase (MAPK) pathway could be a potential target. ROS has been found to activate the MAPK signalling pathway to initiate cell death due to toxic insult (Kim et al., 2014). The MAPK family comprises of serine/threonine protein kinases, namely, extracellular signal-regulated kinase (ERK), c-Jun-N-terminal kinase (JNK) and p38. The oxidative stress that cells experience can influence the MAPK pathway affecting the stress-activated protein kinases (SAPK), namely, JNK and p38. MAPK is responsible for the phosphorylation of transcription factors and cellular functions such as cell survival and cell death. The MAPK pathway has been implicated in the activation of Nrf2; however, the mechanism in which regulation is initiated remains elusive. Studies to date have favoured indirect phosphorylation of Nrf2 as a point of regulation by the MAPK pathway (Sun et al., 2009). Previous KA studies have shown that MAPK expression was

upregulated in injured *Hypsizygus marmoreus* as a response to the increase of oxidative stress. The expression of CAT was upregulated as well as extracellular ATP (eATP) as a stress signal to facilitate mycelial regeneration (Zhang et al., 2017). Previous studies have not investigated Nrf2 and MAPK signalling following treatment with KA in HepG2 liver cells.

Immune responses result in the activation of the inflammatory pathway in the case of oxidative stress. Sirtuin 1 (Sirt1) interacts with MAPK proteins in the presence of oxidative stress. Sirt1 is a protein deacetylase, responsible for alleviating oxidative stress and promoting cell survival (Salminen et al., 2013). Regulation of ROS production by Sirt1 occurs via the alteration of immune responses through nuclear factor kappa B (NFκB) signalling and activator protein-1 (AP-1) (Salminen et al., 2013, Xie et al., 2013a). Inflammation is a contributing factor to several pathologies. NFκB and IκBα (nuclear factor of kappa light polypeptide gene enhancer in B-cells inhibitor, alpha) are found in the cytoplasm; IκBα is phosphorylated and free for ubiquitin-dependent proteasome degradation while NFκB translocates to the nucleus for the transcription of pro-inflammatory cytokines (Yang et al., 2012). KA has shown anti-inflammatory effects in transfected HaCaT keratinocyte cells (Moon et al., 2001)

MAPK proteins activate pro-inflammatory cytokines such as the tumour necrosis factor (TNF) family, and interleukin-1 (IL-1) to enhance AP-1 activity (Shaulian and Karin, 2002). AP-1 is made up of dimeric basic region leucine-zipper (bZIP) proteins, Fos, Jun, Maf and ATF sub-families. Of the subfamilies, c-Jun (potent transcription activator) and Fos hetero-dimerize which allow for more efficient DNA binding activity. AP-1 participates in many processes in cells including cell proliferation , differentiation, inflammation and cell death (Fisher and Voorhees, 1998).

MicroRNAs (miRNA's) are a class of post-transcriptional repressors of gene expression (Reinhart et al., 2000). MiRNA's play key roles in the regulation of inflammation, oxidative stress, immune response and cell death. Examples of these miRNA's are miRNA-155, miRNA-29a and miRNA-29b. MiRNA-155 expression can repress NFκB and MAPK signalling (Wang et al., 2015). MiRNA-29a expression is also inhibited by NFκB and decreases apoptosis by targeting proapoptotic mediators such as bcl-2-like protein 4 (Bax), poly(ADP-ribose) polymerase (PARP), phospho-Fas-associated protein with death domain (phospho-FADD), cleaved caspase 8, and caspase 3 (Tiao et al., 2014). MiRNA-29b functions include the regulation of oxidative stress by increasing apoptosis and decreasing cell viability (Hou et al., 2017).

The level and duration of oxidative stress determines the degree of damage and the initiation of cell death. Apoptosis plays a key role in the maintenance of cellular homeostasis by removing injured cells. Apoptosis is executed via the intrinsic and extrinsic apoptotic pathways by caspases; initiator (caspase -8 and -9) and the executioner (caspase -3/7) (Elmore, 2007). KA has known functions in the

inhibition of cell proliferation and the reduction of tumour growth (Chen et al., 2013). Although KA is known to inhibit cell proliferation, little is known on its inhibitory mechanism.

Research determining the effects of KA on oxidative stress, MAPK signalling, and inflammation have been established in some animal and human models, however, liver toxicity remains neglected. This study investigates the effect of KA on oxidative stress, MAPK signalling pathway and NFκB inflammatory responses in the human liver (HepG2) cell line. Results from this study provide insights into the role of KA in liver toxicity.

CHAPTER 1

LITERATURE REVIEW

1.1. Kojic acid

Kojic acid (KA) is a secondary metabolite formed by aerobic respiration in several fungal species belonging to the genera *Penicillium* and *Aspergillus* (Parrish et al., 1966, Mohamad et al., 2010, El-Kady et al., 2014). Several carbon sources are used in KA production, such as glucose, sucrose, arabinose, xylose, acetate, and ethanol (Burdock et al., 2001). There are several uses of KA in the agricultural, food, cosmetic, and medicinal industries. KA has been used as a pesticide and insecticide due to its antifungal and antibacterial properties (Lee et al., 1950, Beard and Walton, 1969, Uher et al., 1994, Kim et al., 2012, Wu et al., 2019). It inhibits melanin production to reduce skin conditions for example melasma (Bandyopadhyay, 2009). KA is also used to preserve food by preventing the discolouration of fruits and acting as a flavour-enhancing additive (Chen et al., 1991, Burnett et al., 2010, Deri et al., 2016).

1.1.1. Chemical structure of Kojic acid

KA is known by the chemical nomenclature 5-hydroxy-2-hydroxymethyl-γ-pyranone ($C_6H_6O_4$). KA was first discovered in 1907 in mycelia of *A. oryzae*, but the structure was later discovered in 1924 (Beelik, 1956, Belsito et al., 2009). KA is a weak acid with a hydroxyl group on the C5 position of the heterocyclic structure (Fig 1.1). KA has an amylene oxide ring structure similar to that of glucose; however, the KA ring structure is stable. The compound structure allows for the formation of salts by the chelation of metals (Beelik, 1956, Saeedi et al., 2019). KA can form salts with metals such as sodium, copper, zinc, calcium, nickel, and cadmium (Coupland and Niehaus, 1987a, Saeedi et al., 2019). This attribute has been exploited in the inhibition of melanin (Azami et al., 2017).

KA was considered a mycotoxin due to its contamination of maize and poultry feed and co-existence with aflatoxins (Parrish et al., 1966, Souza et al., 2013). With the emergence of more research into KA, it was suggested that KA does not exhibit mycotoxin risks to human health (Bentley, 2006). The lack of research in some aspects of the efficacy of KA on human health may be the reason for KA's varying classification. This draws attention to the need for more research into the health effects of KA.

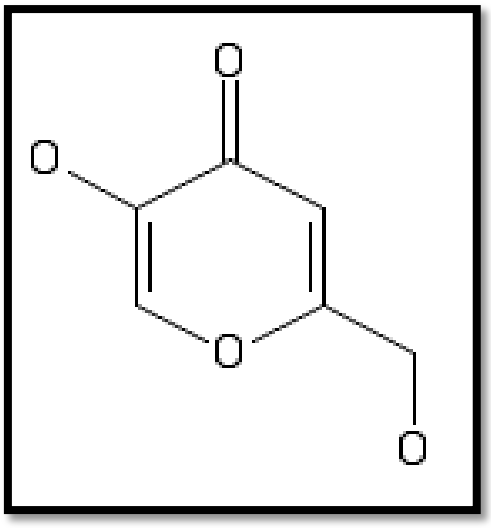

Figure 1.1 The chemical structure of KA derived from *Aspergillus oryzae* fungi. Chemical structure was drawn using PubChem Sketcher Version 2.4.

1.2.2. Absorption, distribution, and metabolism of Kojic acid

KA is absorbed and distributed in the body through the dermal, transdermal, and oral routes of exposure. An *in vitro* study by Sansho Seiyaku Co., Ltd determined that the percutaneous absorption of 2 mg/cm^3 KA administered to human dermatomed skin, with 16.98% of the administered KA percutaneously absorbed following 16 h incubation. This study was further validated in humans. Women who applied creams containing 1% KA to their skin for a period of 0.5, 1, 1.5, 3, 6, 12 and 24 h were found to have 1 ng/ml KA in their plasma. This study found low penetration of KA into the bloodstream; however, no adverse effects were identified (Sansho Seiyaku Co., 2001).

The consumption of fermented food containing undetermined quantities of KA showed blood plasma concentrations of 1-8 µg/ml within 12-24 h. This, as well as other studies, indicated that KA was absorbed by the gastrointestinal tract (Niwa and Akamatsu, 1991, Higa et al., 2000). According to the International Agency for Research on Cancer (IARC), studies into the metabolism of KA have not been established. KA's structure allows for a metabolism similar to that of dietary hexoses (Burdock et al., 2001). The *in vitro* metabolism of KA to comenic aldehyde has been carried out in *Anthrobacter ureafaciens* (K-1), a soil-dwelling microorganism that utilises KA as a sole carbon source. The proposed enzyme responsible for the degradation of KA was hypothesized to be a non-heme iron protein-containing ferric ion responsible for accepting hydrogen (H^+) released from KA (Imose et al., 1970). The ferrous ion formed is oxidised by oxygen (aerobic conditions) or nicotinamide adenine dinucleotide (NAD) (anaerobic conditions) to produce hydrogen peroxide (H_2O_2) and reduced NAD, respectively (Fig 1.2) (Imose et al., 1970).

Limited data is available on the absorption, distribution, metabolism, and excretion of KA in humans; however, more information is available on the distribution and metabolism of KA in rat models. [^{14}C] KA was used to dose JCL Wistar rats with 10 µCi/100g via oral, subcutaneous, and dermal routes. The study found that KA was rapidly distributed in tissues and organs within 30 mins of administering a single oral dose. Additionally, very high levels of KA were found in the liver, kidney, and pancreas, while high levels were found in the lung, heart, and spleen. Blood KA levels were assessed after 0.5, 1, 3, 6, 24, and 48 h of KA administration. In the blood, a 20.63% and 25.05% decrease in administered KA doses was observed at 30 min and 1h, respectively. Assessment of bile revealed 0.5 µCi/10µCi of the administered dose within 24 h and no enterohepatic circulation occurred. The elimination of KA from the body was assessed in rats following a single oral dose; it was found that approximately 70% was in urine, and 0.82% of the administered quantity was excreted in faeces within 48 h (Sansho Seiyaku Co., 2001).

Subcutaneous and dermal exposures, showed high levels of KA in the kidney within 30 min and 1h; however, there was no significant KA was found in the liver (Sansho Seiyaku Co., 2001, Burnett et al., 2010). Blood KA levels were found to be 13.29% and 21.67% of the administered dose within 30 min and 1 h of subcutaneous exposure and 5% detected through dermal exposure after 30 min. Assessment of bile found 0.76 µCi/10 µCi for subcutaneous and dermal exposures, respectively. The excreted doses were more significant in urine samples within 48 h measuring 50% and 56% of the subcutaneous and dermal administered doses. Expired air was assessed within 5 h and found 1.4% of the subcutaneous single administered dose (Sansho Seiyaku Co., 2001).

A repeated dose for subcutaneous exposure in JCL Wistar rats for a period of 7 days was assessed. Observation of the relationship between [^{14}C] KA and blood and urine samples revealed an increase in the concentration of KA detected until equilibrium was reached. The distribution of KA significant in organs and tissues, namely the intestinal tract, pancreas, and adipose tissue was assessed at 10 min, 1, 6, 24, and 48 h. The excreted concentration was assessed in urine and bile. Metabolites such as sulphate conjugated to KA (35.6-93.7%) and glucuronides (6.4-39.6%) were detected in urine and bile (Sansho Seiyaku Co., 2001). In a review by the Scientific Committee of Consumer Products (SCCP), repeated doses of KA showed a significant increase in concentrations distributed and excreted compared to a single dose.

The pregnant rats and nursing rats were dosed with 10 µCi/100g to illustrate KA's transfer from nursing JCL Wistar rats and pups via milk, amniotic fluid, uterus, and placenta. The pregnant rats were dosed subcutaneously on the 11th and 20th day of gestation. Foetuses were examined following removal at 10 min, 30 min, and 3 h after treatment. After treatment, very high KA levels were observed in the kidney, liver, pancreas, spleen, salivary glands, and lungs. KA levels were detected

within 30 min in the uterus, placenta, amniotic fluid, and foetus. The distribution of treatment in the foetus was similar to that of the adults displaying elevated KA levels in the liver and gastrointestinal tract. The milk transfer study was dosed on the 3rd day of lactation, and pups were examined at 30 min, 1 h and 3 h. The pups' stomach wall and contents had 0.02% KA after a 3 h incubation. KA is distributed freely to the foetus, uterus, reproductive organs, and secreted milk in JCL Wistar rats (Sansho Seiyaku Co., 2001, SCCP, 2008).

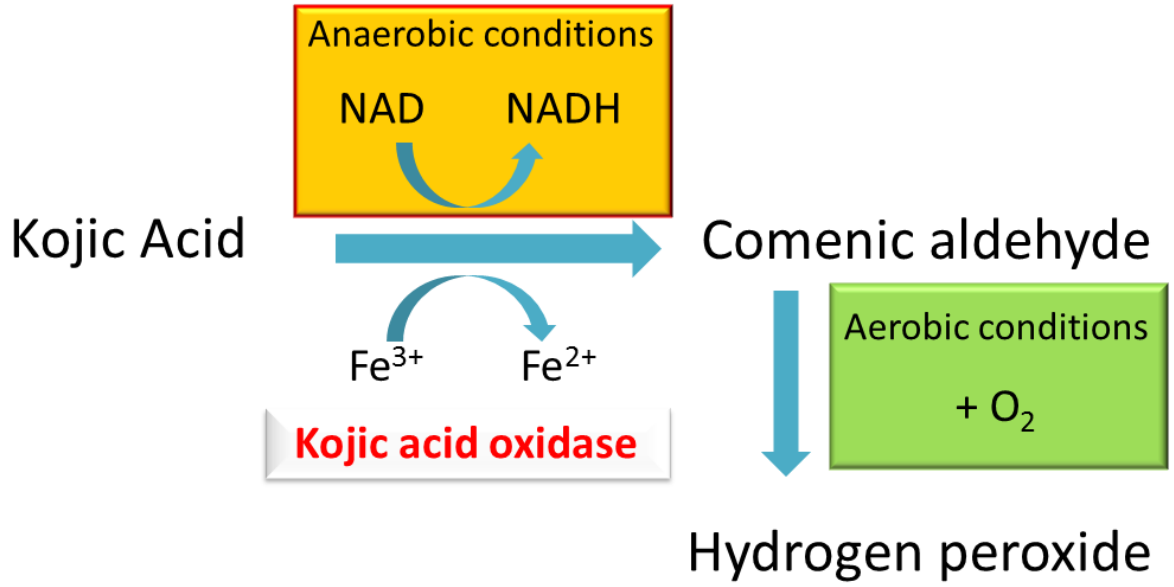

Figure 1.2 Proposed metabolism of KA in microorganisms (prepared by author)

1.2.3. Mechanism of tyrosinase inhibition

Melanin is produced by the transportation of structural proteins from the endoplasmic reticulum (ER) and the fusion of melanosome-specific regulatory glycoproteins. These glycoproteins are released as coated vesicles from the Golgi apparatus. They are sorted and transported to the melanosome. Melanin is produced in melanocytes and then transferred to keratinocytes hence forming pigmentation. Melanogenesis is important for protecting the skin from ultraviolet radiation (UV) (Brenner and Hearing, 2008, Zolghadri et al., 2019).

Polyphenol oxidase (tyrosinase) is widely found in plant and animal tissue (Pawelek and Körner, 1982, Mayer, 1986). It is a metallo-protein enzyme-containing histidine residue that binds copper ion at its active site (Gillbro and Olsson, 2011). The enzyme is responsible for the colour of epidermal cells such as skin, eyes, and hair of animals (Pekkarinen et al., 1999). Tyrosinase catalyses two steps in melanogenesis; the hydroxylation of tyrosine to 3, 4-dihydroxyphenylalanine (L-DOPA) as monophenolase and the oxidation of L-DOPA to dopaquinone (Fig 1.3) (Kim et al., 2003).

There are two types of melanin in skin, namely pheomelanin and eumelanin. Depending on the type of melanin being produced, either dopachrome or cysteinyldopa can be formed. Cysteinyldopa produces pheomelanin, whereas dopachrome is used to produce eumelanin with the assistance of tyrosinase-related protein 1 (TRP-1) and tyrosinase-related protein 2 (TRP-2). The melanosomes are transferred to keratinocytes by TRP-1 and TRP-2 (Masum et al., 2019). KA has the ability to form salts with metals such as sodium, copper, zinc, calcium, nickel, and cadmium (Coupland and Niehaus, 1987b, Saeedi et al., 2019). KA chelating properties are crucial in the inhibition of tyrosinase activity. KA inhibits the process by chelating the copper ion (II) found in tyrosinase hence decreasing melanin production (Chen et al., 2013). KA is a slow-binding inhibitor that binds to active tyrosinase present (Chang, 2009). KA inhibits melanosis by inhibiting oxygen uptake that aids in browning. The competitive inhibition of tyrosinase has led to its use as a preservative in food products and as a skin lightening agent in the beauty industry (SCCP, 2008).

Other skin lightening compounds are also tyrosinase inhibitors, such as hydroquinone (HQ). HQ is a preferred treatment for hyperpigmentation; however, it has chronic side effects such as nephrotoxicity and carcinogenesis (Findlay et al., 1975, Kooyers and Westerhof, 2004). Due to safety concerns, HQ is no longer used to treat hyperpigmentation, and KA has become a more popular option due to its similar mechanism of action. A study by Azami et al. (2017) evaluated KA's tyrosinase inhibition potency by assessing KA's interaction with mushroom tyrosinase binding sites. KA bound to the histidine at sites, His263, His259, His296, His94, His85, and His61. It was found that tyrosol and KA bind to region 1 of tyrosinase and therefore, compete for binding. KA is a potent inhibitor of tyrosinase, displaying more interactions, and better binding with tyrosinase (Azami et al., 2017).

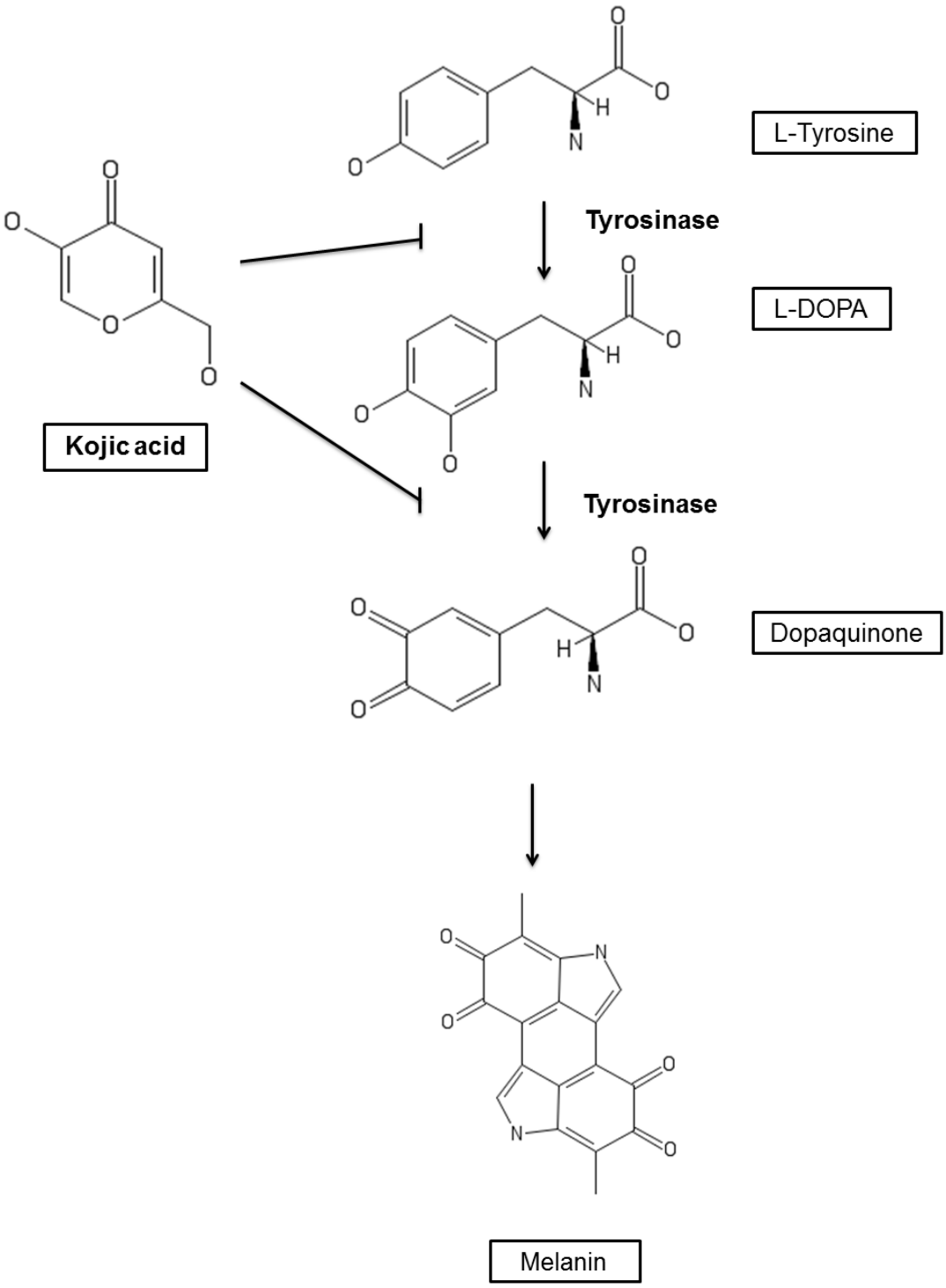

Figure 1.3 KA inhibits tyrosinase activity in animals and humans. Chemical structures were drawn using PubChem Sketcher Version 2.4.

1.2.4. Effects of KA in vitro and in vivo

1.2.4.1. Biological effects of KA in vitro

KA is commonly referred to as an anti-tumour and anti-cancer treatment. A study assessing the proliferative nature of KA and its derivatives in HeLa cells found that KA (25 µg) did not induce cell

cycle arrest in the absence and presence of 50 µM copper ion (Chen et al., 2013). A proteomic assessment of KA [8 µg/ml] (safe recommended concentration) was used to treat A375 cells for 24, 48, and 72 h. At 72 h, a significant fold-change of 16 differentially expressed proteins responsible for apoptosis and cell signalling, namely p53, Ras/mitogen-activated protein kinase kinase (MEK)/ the extracellular-regulated kinase (ERK), RAF-1, and B-cell lymphoma 2 (Bcl-2), was observed. KA suppressed heat-shock proteins (HSP), which are proteins found to facilitate tumour growth and survival (Nawarak et al., 2008), validating KA's anti-cancer potential.

KA is well-established as a skin lightener due to the inhibition of tyrosinase activity. The inhibition of tyrosinase activity has been associated with proliferation due to microphthalmia-associated transcription factor (MITF) functions in cell survival and differentiation (Hodgkinson et al., 1993, Hughes et al., 1993). KA-induced cytotoxic effects on B16F1 melanoma cells at higher concentrations [125- 500 µg/ml] but not at lower concentrations [7.81- 31.25 µg/ml] (Lajis et al., 2012). Inflammatory mediators play a role in melanocyte proliferation, differentiation, and pigmentation (Lin and Fisher, 2007). KA [0.2 mM] inhibited melanogenesis by stimulating interleukin-6 (IL-6) in keratinocyte and melanocyte co-cultures (Choi et al., 2012).

KA's ability to treat skin conditions was determined on human transfected-HaCaT and SCC-13 cells. It was found that 10 mM KA was a potential inhibitor of nuclear factor kappa B (NF-κB) activation in human epithelial cells for 24 h (Moon et al., 2001). Many skin-related conditions, such as psoriasis and keloids, exhibit elevated inflammatory markers during the condition's development and progression. KA [100 µM] was found to be a potential inhibitor of senescence through NF-κB and p21 pathways in HCEC cells following treatments at 1, 3, 5, and 7 days (Wei et al., 2019). The p21 plays a role in the cell cycle, apoptosis, and transcriptional regulation after DNA damage has occurred. The p21 protein was found to inhibit caspase 3 and 9 activations, resulting in apoptosis prevention (Karimian et al., 2016).

KA is known to be a chemo-sensitising agent of complex III inhibitors in the electron transport chain (ETC) (Kim et al., 2013). As a result of the sensitisation of complex III inhibitors, cellular energy production may be disrupted, resulting in the escape of electrons leading to reactive oxygen species (ROS). A study by Oncul et al. (2019), highlighting the initiation of the intrinsic pathway of apoptosis by KA derivatives, found an approximate IC_{50} of KA > 100 µM. It was also found that KA derivatives had increased ROS production in HepG2 cells. Pro-apoptotic factors such as c-Jun-N-terminal kinase (JNK) and Bax were not upregulated; however caspase 3 was activated. KA did not produce the same effects in HepG2 cells at 100 µM (Oncul et al., 2019). Studies by Niwa and Akamatsu (1991) on neutrophils and lymphocytes have shown a reduction in ROS following KA exposure [5 and 20 µg/ml] in both xanthine oxidase systems and neutrophils.

1.2.4.2. In vivo studies

1.2.4.2.1. Animal Toxicity

Skin lightening treatments such as HQ have been found to cause DNA adducts and promote carcinogenesis. Research into the effect of KA on carcinogenesis in rats measured the DNA adduct formation and cell proliferation in hepatocytes. A study by Higa et al. (2007) investigated carcinogenic initiation potential in 2% KA orally treated F344 rats for 4 weeks with sodium phenobarbital (PB), a carcinogenic promotor, and found no significant increase in pre-neoplastic legions shown by biomarker glutathione S-transferase placental (GST-P) positive foci (> 0.2 mm). An increase was observed in a group initiator treatment without promotion treatment (Higa et al., 2007). The result showed an increase in proliferation but no significant 8-oxodeoxyguanosine levels (8-OxodG) in male F344 rats receiving 2% KA doses for periods of 3, 7, and 28 days. F344 rats dosed with KA once [0, 1000, 2000 mg/kg body weight] for 2 weeks showed no liver tumour initiating capacity, but some data showed that liver tumours may occur. Interestingly, KA did not exert rat liver initiation in tumours following a single dose (Watanabe et al., 2005); however prolonged dietary intake showed increased tumour promotion. Contrary to *in vitro* studies, *in vivo* mice studies found no data suggesting KA has potential to initiate tumours following liver assessments (Ishikawa et al., 2006, Moto et al., 2006, Ogiwara et al., 2015). With contrasting results in *in vivo* and *in vitro* models regarding KA, no conclusive deductions could be obtained.

The genotoxic tumour initiating potential of KA (0, 0.002, 0.02 and 2%) was assessed in rat thyroid at various periods (2-31 weeks), and found that oxidative stress was decreased accompanied by the absence of DNA-adducts. It was established that there was low to no genotoxicity of KA in the thyroid (Tamura et al., 2006). Similarly, Fujimoto et al. (1999) determined KA proliferative effect in the thyroid was not influenced by KA genotoxicity.

KA toxicity in terms of lipid peroxidation and iron chelation was assessed in CD-1 mice dosed [100 mg/kg in 0.25% methylcellulose] for 7 days, and male Wistar rats dosed *ad libitum* [0.5% KA] in water for 4 weeks. Oral doses of 100 mg/kg for 7 days did not affect iron levels accumulated in the liver compared to the control (iron chelator- deferoxamine); however, increased lipid peroxidation was observed. Oral doses of 0.5% KA for 4 weeks did not have any effect. KA showed minimum effect with no protective effect against reperfusion injury (Kotyzova et al., 2004). This result was validated in rabbit hearts dosed with 30 µM, displaying no protective function after reperfusion illustrated by any improvement in left ventricular function (Katoh et al., 1992).

The teratogenic capabilities of KA are not fully established; however, Choudhary et al. (1992) found an increase in mortality and decreased litter size, implantation sites, and viable litters following KA

exposure. The study was conducted in Sprague Dawley rats dosed from day 1-5 (female) post-coitum with KA (50 µg/day/rat). The rats were laparotomised at day 8, and the corpora luteum comparison found no change compared to the control. The study concluded an increase in mortality with no teratogenic effects (Choudhary et al., 1992).

A risk assessment of KA in feed due to mycotoxin contamination was assessed in broiler chickens [> 2 g/kg] between hatchlings and 21-day old chickens. A decrease in growth rates in 21-day old birds as well as effects on pro-ventriculus, gizzard, pancreas, and Bursa of the Fabriculus following KA treatment [4 - 8 g/kg] was observed (Giroir et al., 1991). Notably, KA was a gastrointestinal irritant and inflammatory promotor of the pro-ventriculus and gizzards. Liver toxicity was observed by the increase in relative weight and serum glutamic oxaloacetic transaminase (GOT) activity. The Bursa of Fabricius' immune activity was altered along with pancreas toxicity. Haematological effect included increased red blood cells and decreased mean corpuscular volume. This was hypothesized to be due to the stimulation of erythropoiesis and hemoconcentration (Giroir et al., 1991).

Previous studies by Klein and Olsen (1947) stated that low KA concentrations inhibit oxidation enzymes in rat livers, namely D-amino acids, L-phenylalanine, and L-methionine. Giroir et al. (1991) further proved the altered activity of serum GOT, alkaline phosphatase, and creatine kinase. It was established that KA increased total protein, cholesterol, albumin, and triglycerides due to alterations in lipid and protein metabolism; however, more research is required to deduce the mechanisms by which KA causes these serum concentration changes.

Kidney dysregulation was observed by the increased concentration of uric acid and serum glucose concentrations, possibly, due to damage to the Islets of Langerhans in the pancreas. The alteration of glucose could explain the decreased colon temperature in the 8 g/kg KA-treated chickens (Giroir et al., 1991). Notably, 2 g/kg and above concentrations caused toxicity detrimental to broiler chicken health. Contaminated feed was found to contain KA concentrations of 1 to 25 mg/g; however, Wilson (1966) found only trace amounts of KA that do not pose a risk to chicken health.

1.2.4.2.2. Human Toxicity

KA is commonly used in creams for beauty applications. To determine sensitivity, 107 patients with chloasma were treated with KA creams [2.5% KA] twice daily for an average of 9.5 months. Two individuals developed facial dermatitis due to hypersensitivity. No sensitivity was detected in 66 patients with chloasma (Nakayama, 1982) and 31 healthy subjects when treated with the cream [1% KA] (Hira et al., 1985). According to studies carried out by Nakayama (1982), no sensitivity was detected following the use of KA creams.

In a similar study by Nakagawa et al. (1995), the frequency of sensitisation to KA was assessed in patch tests of 220 female patients with suspected cosmetic-related dermatitis. Of the total patients, 8 used one skin product with KA. Five reacted to KA and one or more products containing 1% KA. Three remaining patients showed no reaction to products containing KA. The 212 patients who did not use KA previously showed no adverse results (Nakagawa et al., 1995).

.

1.3. Cell Death

Cell death is a process employed by the body to maintain physiological and pathological homeostasis during cellular stress. Cell death also allows for the release of chemicals (danger signals) by the dying cells to alert the organism or colony of a potential threat (Galluzzi et al., 2018). The process of cell death can be categorised into two categories: programmed cell death and accidental cell death. However, some overlap of characteristics does exist (Galluzzi et al., 2018).

1.3.1. Apoptosis (Programmed cell death)

Apoptosis is a regulated, genetically determined process that occurs when the cell undergoes self-destruction. The process ensures the elimination of damaged cells that may exhibit protein cross-linking, protein cleavage, and DNA breakdown (Hengartner, 2000, Elmore, 2007).

The mechanism of apoptosis is an energy-requiring process that initiates alterations in biochemical features of the cell. When apoptosis occurs in a cell, there are characteristic changes such as chromatin condensation, nuclear fragmentation, reduction of cellular volume, reduction of pseudopods, and the rounding of the cell (Hanahan and Weinberg, 2000). The condensation of chromatin occurs at the periphery of the nucleus and can be visualised as a ring structure. The chromatin further condenses and breaks up by a process termed karyorrhexis. Throughout this process, the cell membrane remains intact. Loss of membrane integrity and membrane blebbing occurs at later stages of apoptosis. In normal functioning cells, phagocytic cells engulf apoptotic cells as soon as detected.

Caspases (cysteine aspartic proteases) are proteolytic enzymes that cleave aspartic residues on proteins, resulting in apoptosis induction (Shalini et al., 2015). There are ten main categories of caspases that are responsible for different specificities. They are categorised into initiators (caspases -2, -8, -9 and -10), executioners (caspases -3, -6 and -7) and inflammatory caspases (caspases -1, -4 and -5) (Cohen, 1997). The two main pathways of apoptosis are the extrinsic (death receptor) pathway and the intrinsic (mitochondrial) pathway (Fig 1.4).

1.3.1.1. The intrinsic apoptotic pathway

The intrinsic pathway is stimulated by external stimuli that include DNA damage, ischemia, and oxidative stress. The activation of the intrinsic pathway occurs via the mitochondria and is affected by both pro-apoptotic and anti-apoptotic members of the Bcl-2 family. Under stress conditions, the inner

mitochondrial membrane (IMM) permeability increases, allowing molecules to enter into the mitochondrial matrix leading to the disruption of the oxidative phosphorylation (OxPHOS). Osmotic swelling and the compression of vesicles cause unfolding of the inter-cristae space (Redza-Dutordoir and Averill-Bates, 2016). An increase in the outer mitochondrial membrane permeabilisation (MOMP) results in the release of pro-apoptotic proteins, namely cytochrome C, apoptosis-inducing factor (AIF), endonuclease G (endo G), and secondary mitochondria-derived activator of caspases/direct inhibitor of apoptosis (IAP)-binding protein with low pI (Smac/Diablo). In the cytosol, cytochrome C forms an apoptosome complex with apoptotic protease-activating factor 1 (Apaf-1) and procaspase-9 (Redza-Dutordoir and Averill-Bates, 2016). The hydrolysis of adenosine triphosphate (ATP) by the apoptosome complex allows for the cleavage of caspase-9, which in turn cleaves caspase -3, -6, and -7. The activation of executioner caspases results in apoptosis (Loreto et al., 2014).

Members of the Bcl-2 family responsible for exerting anti-apoptotic functions are mainly located at the outer mitochondrial membrane (OMM). They form heterodimers with pro-apoptotic proteins (Bax, Bim, Bak, Bad), thus inhibiting pro-apoptotic signalling (Redza-Dutordoir and Averill-Bates, 2016)

1.3.1.2. The Extrinsic apoptotic pathway

The extrinsic pathway of apoptosis occurs through the transmembrane receptor-mediated interaction. These receptors are involved in transmitting death signals from the cell surface to the intracellular signalling pathway (Wong, 2011). The death receptors and ligand pairs include FasL/FasR, TNFα/TNFR1, Apo3L/DR3, Apo2L/DR4, and Apo2L/DR5 (Elmore, 2007). Binding of ligands to respective receptors results in the recruitment of cytoplasmic adaptors; fatty acid synthetase ligand (FasL) binding to the fatty acid synthetase receptor (FasR) results in the recruitment of Fas-associated death domain (FADD). Tumour necrosis factor-alpha (TNF-α) binds to the tumour necrosis factor receptor-1 (TNFR1) resulting in the binding of TNF receptor-associated death domain (TRADD) and recruitment of FADD and receptor interacting protein (RIP). FADD dimerizes with procaspase-8 at the death effector domain. A death-inducing signalling complex (DISC) is formed, which activates pro-caspase 8 (Elmore, 2007).

The execution of apoptosis is the final pathway initiated by the activation of execution caspases -3, -6, and -7. These caspases activate cytoplasmic endonucleases and proteases, which degrade nuclear material and cytoskeleton and nuclear proteins, respectively (Elmore, 2007). Caspase 3 plays a crucial role in the execution pathway by the cleavage of the inhibitor of caspase-activated DNAse (CAD), known as ICAD. CAD degrades chromosomal DNA leading to chromatin condensation. Caspase 3 also plays a role in inducing apoptotic body formation (Elmore, 2007).

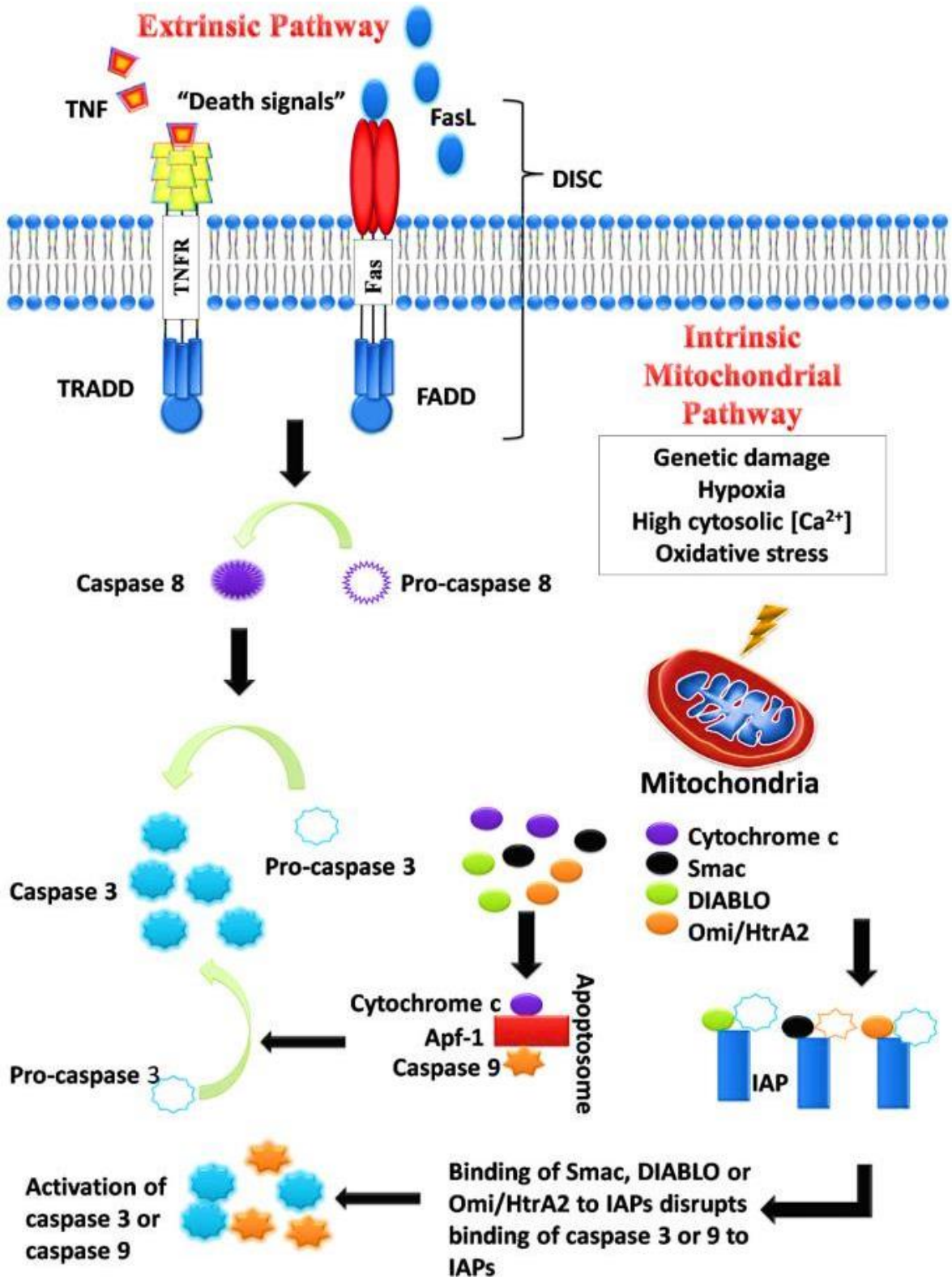

Figure 1.4 Overview of the intrinsic and extrinsic apoptotic pathways (Wong, 2011)

1.3.2. Necrosis

Necrotic cell death is characterised as the swelling and rupturing of intracellular organelles resulting in plasma membrane breakdown. The cell contents, such as cytoplasmic enzymes, are released into the extracellular matrix (Chan et al., 2013). The plasma membrane leakage results in the mediation of inflammatory responses. Cytokines in the TNF family have been found to trigger necrosis. The defining difference between necrosis and apoptosis is plasma membrane lysis before the activation of catabolic enzymes in necrotic cell death as opposed to activation of proteases and endonucleases before lysis of the cell (Kroemer et al., 1998). A key marker of necrotic death and membrane damage is the leakage of lactate dehydrogenase (LDH), found in the cells' cytoplasm (Chan et al., 2013).

1.4. Liver

1.4.1. Function and hepatotoxicity

The liver is often affected by toxic insult due to its role as a hub of metabolic activity. The liver uses lysosomes for the detoxification of xenobiotics via biotransformation. Liver metabolism converts lipophilic compounds into a hydrophilic compound in a two-phase process. Biotransformation occurs primarily in the endoplasmic reticulum in hepatocytes. The reactions in phase I are carried out by cytochrome P450 (CYP450) enzymes. In phase I, the product undergoes oxidation, reduction, or hydrolysis, resulting in an oxygen species' addition. The addition of the oxygen species allows for greater reactivity of enzymes with the xenobiotic. Phase II involves the conjugation of glucuronate, glutathione, or sulphate to the compound enabling the secretion into blood or bile (Kalra et al., 2020).

Due to the liver's relationship with the gastrointestinal tract and its functions in the detoxification of xenobiotics, the liver is prone to toxic insults (Abou Seif, 2016). Injury or impairment of the liver can be severe for an individual's health. Hepatotoxicity is dependent on the dose, type of xenobiotic, and frequency of exposure (Casas-Grajales and Muriel, 2015).

1.5. Oxidative stress

The overproduction of reactive species can cause an electrochemical imbalance resulting in oxidative stress. ROS is a term used to refer to metabolic by-products such as superoxide radicals ($O_2^{\bullet-}$), H_2O_2, and hydroxyl radicals (•OH) of biological processes (Pizzino et al., 2017). The majority of intracellular ROS is produced in the mitochondria (Murphy, 2009); however, the organelle is also a target of ROS damage (Ott et al., 2007). Oxidative stress has been associated with diseases due to oxidative damage to biomolecules, such as DNA, lipids, and proteins (Liguori et al., 2018).

1.5.1. Mitochondrial production of reactive oxygen species (ROS)

The mitochondrion, commonly referred to as the 'powerhouse of the cell', is a double-membrane structure that provides energy in the form of ATP for intracellular metabolic processes. The

mitochondria also have various roles in nicotinamide adenine dinucleotide phosphate (NADPH) synthesis, DNA repair, metabolic pathways, and cell death (Kakkar and Singh, 2007). The ETC consists of transmembrane complexes (I-IV), ubiquinone, and cytochrome c, present in the cristae (folded inner membrane of mitochondria).

The mitochondrial ETC complexes may leak electrons to molecular oxygen leading to the production of superoxides. Superoxide radicals are produced by NADPH oxidase, xanthine oxidase, and peroxidases and non-enzymatic electron transfers to molecular oxygen (Pizzino et al., 2017). Superoxide production occurs in the IMM. In the ETC, electrons are transferred by NADH and flavin adenine dinucleotide ($FADH_2$) to complex I and II, and electrons are transferred to complex III by coenzyme ubiquinone (Zhao et al., 2019). Ubiquinone plays a role in linking complexes I and III, complex I and II, and superoxide production by complex III (Fig 1.5) (Ott et al., 2007). The superoxide anion is a precursor for most ROS and yields hydrogen peroxide, peroxynitrite, and hypochlorous acid. The reaction occurs in the presence of catalysts such as Fe^{2+} and Cu^{+} (Fenton reaction) (Pizzino et al., 2017).

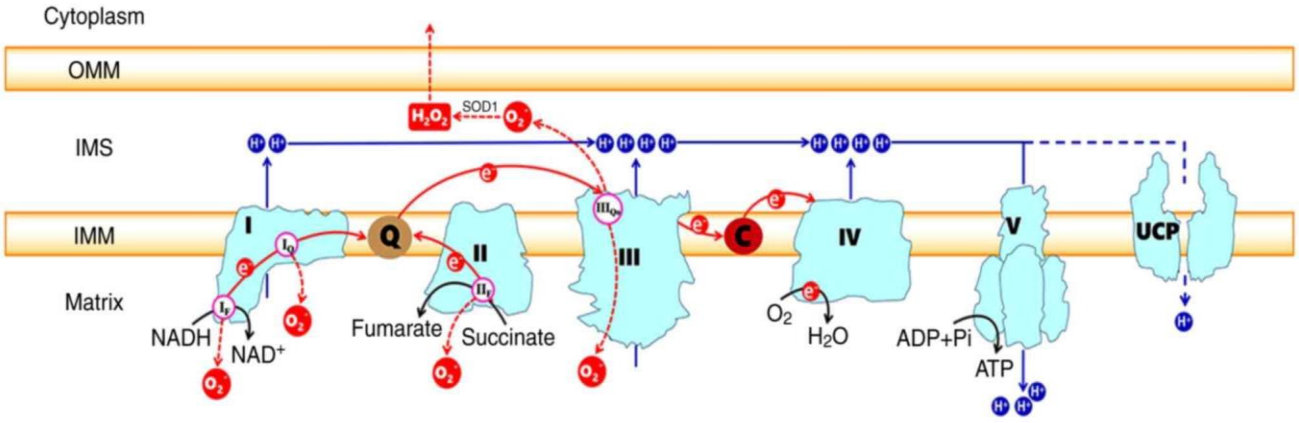

Figure 1.5 Overview of the ETC present in mitochondria and responsible for producing ATP in the cell (Zhao et al., 2019)

1.5.2. Lipid peroxidation

Lipid peroxidation is a process that involves reactive species oxidising lipids to form aldehydes and peroxides. The products formed in lipid peroxidation are more stable than parent reactive species and exit the site of generation and inflict tissue damage and dysfunction. The lipid peroxidation products are highly reactive and can exert their effects on DNA, protein, and cell signalling (Ramana et al., 2013). Reactive species attach lipids with carbon-carbon double bonds, especially polyunsaturated fatty acids (PUFAs).

Lipid peroxidation is a 3-step process that involves an initiation, propagation, and termination step. The initiation step consists of hydrogen abstraction whereby peroxidants abstract allylic hydrogen to

form a carbon-centered lipid radical. The propagation step involves the lipid radical reacting with oxygen to form lipid peroxy radicals that further abstracts hydrogen from another lipid, thus forming a new lipid radical. This initiates a chain reaction between neighbouring lipid molecules. The chain reaction continues until a donor antioxidant, such as vitamin E, donates hydrogen to a lipid radical to form a nonradical product (Fig. 1.6). This is known as the termination step in lipid peroxidation (Ayala et al., 2014).

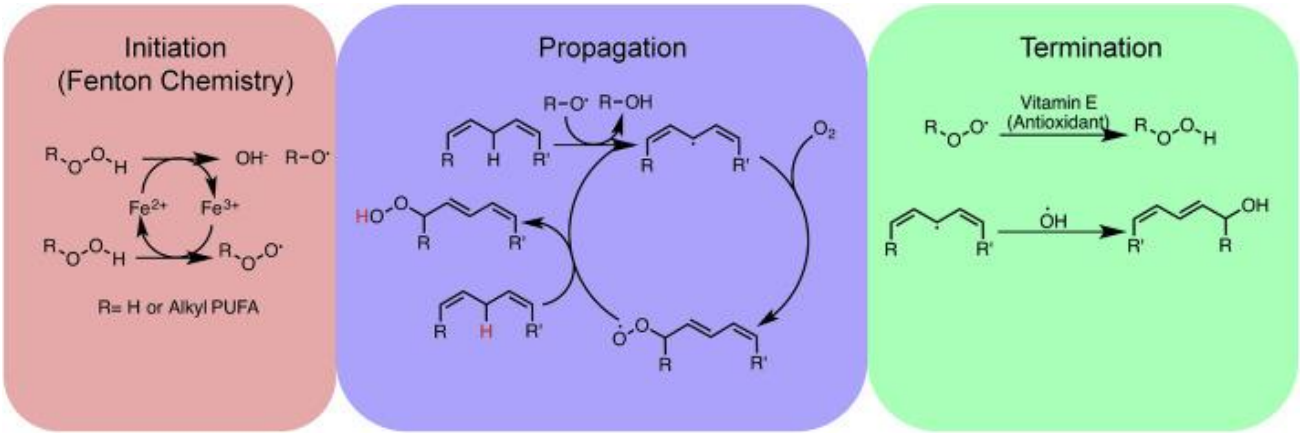

Figure 1.6 The chain reaction that occurs in lipid peroxidation illustrating the key steps i) initiation, ii) propagation, and iii) termination (Gaschler and Stockwell, 2017)

1.5.3. Oxidative DNA damage

DNA plays a crucial role in transferring genetic information in living organisms. DNA structural damage can occur due to endogenous and exogenous factors. A common cause of DNA modifications is ROS, while external factors such as ultra-violet radiation can also play a role (Wiesmüller et al., 2002). The effect of DNA damage, depending on where in the cell the damage occurs, can cause cell cycle arrest resulting in cell death. In the event of oxidative DNA damage, modifications of purine and pyrimidine bases, deoxyribose backbone, single and double-strand breaks, and cross-links with other molecules occur (Ott et al., 2007). DNA modifications have been implicated in premature aging, cancer, and neurodegenerative diseases. Mitochondrial DNA (mtDNA) is particularly susceptible to damage by ROS potentially due to the absence of a complex chromatin organisation which functions as a barrier to ROS, proximity of the OxPHOS, inadequent DNA repair mechanisms in the mitochondria and the effect of secondary ROS reactions on mitochondrial membranes due to lipid peroxidation (Yakes and Van Houten, 1997, Ott et al., 2007, Singh et al., 2015).

A common reactant with DNA is the $OH^{\bullet}$ that adds double bonds and abstracts H^{+} from the methyl group of thymine and the CH bond at the 2'-deoxyribose. Oxidative DNA damage occurs at the C5, C6, and C8 positions, which results in the C5-OH and C6-OH pyrimidine adduct radicals (Cooke et al., 2003). The DNA adduct radicals formed is dependent on redox capabilities. A common adduct formed due to ROS is 8-hydroxydeoxyguanine (8-OHdG) and is generated by eliminating the OH^{--} at

the C4 position of guanine. The pH determines the occurrence of deprotonation, which could lead to a guanine $(H^{-})^{\bullet}$ product. The resultant cation forms a C8-OH, and subsequently, oxidation occurs to form DNA modified products (Fig 1.7). An H abstraction between 8-oxoguanine and 2'-deoxyribose results in DNA strand breaks (Cooke et al., 2003).

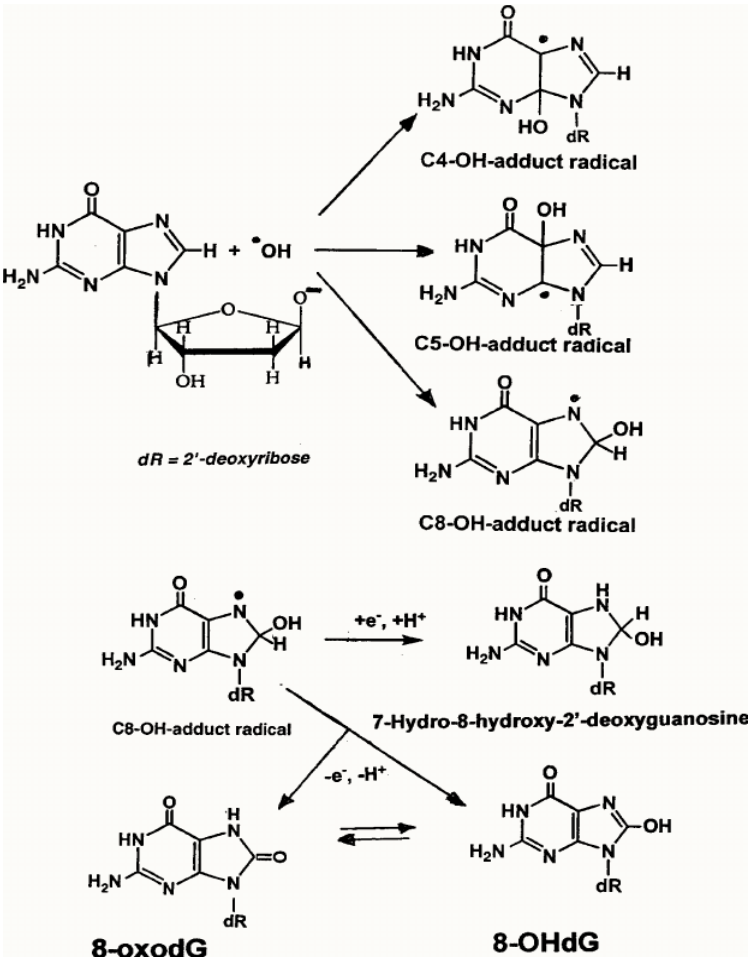

Figure 1.7 The formation of 8-OHdG DNA adduct due to oxidative stress (Valavanidis et al., 2009)

1.5.4. ROS-mediated cell signalling

ROS functions as a secondary messenger to signalling pathways responsible for cell proliferation and differentiation. A change in ROS levels initiates the transduction of signalling molecules from the plasma membrane to the cell nucleus to exert their functions. ROS interacts with protein kinases, protein phosphatases, and transcription factors such as mitogen-activated protein kinase (MAPK) and NFκB (Sauer et al., 2001, Zhang et al., 2016).

1.6. Response to oxidative stress

1.6.1. Nuclear factor erythroid-2 factor 2 (Nrf2) pathway

Antioxidants scavenge free radicals and reduce their reactivity to maintain the balance of oxidants and antioxidants (Casas-Grajales and Muriel, 2015). Mammalian cells have defence mechanisms to facilitate the intracellular environment's decontamination to return to homeostasis within cells by scavenging ROS (Basak et al., 2017). Nrf2 is responsible for the induction of the phase 2 response when oxidative stress is detected as a cellular defence mechanism. This process is dependent on the dissociation of kelch-like ECH-associated protein-1 (KEAP-1) from Nrf2. Nrf2 has a high affinity for KEAP-1 dimers and therefore binds to each other. KEAP-1 is a repressor that contains zinc that is bound to a reactive cysteine thiol. Nrf2 release from KEAP-1 requires the phosphorylation of Ser40 by protein kinase C (PKC) and oxidation of the cysteine thiol groups of KEAP-1 (Basak et al., 2017). Free Nrf2 then translocates into the nucleus, where it acts as a transcription factor that activates the antioxidant response element (ARE) and initiates the transcription of antioxidant genes such as catalase (CAT) and superoxide dismutase (SOD_2) (Fig 1.8). CAT neutralises free radicals by reducing peroxides to water and oxygen (Zhang et al., 2017). SOD_2 converts superoxide into H_2O_2 and oxygen (Wang et al., 2018).

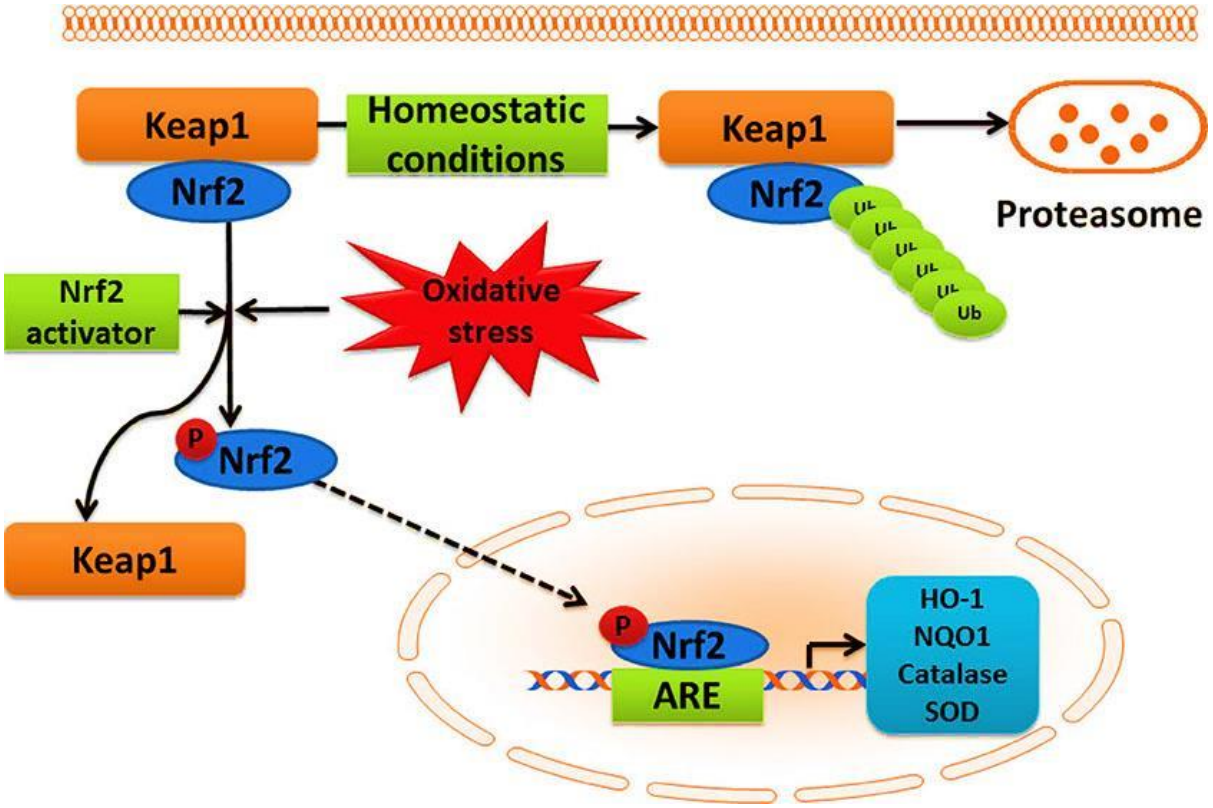

Figure 1.8 Nrf2-KEAP1 pathway illustrating antioxidant regulation in the cell. Nrf2 is dissociated from KEAP1 upon oxidation and translocates to the nucleus. While in the nucleus, Nrf2 binds to the ARE that facilitates the transcription of genes that play a role in antioxidant response (Chen et al., 2014)

1.7. Immune response

1.7.1. MAPK pathway

The MAPK is an intracellular signalling pathway consisting of serine/threonine kinases involved in cell differentiation, growth, development, cell cycle, cell survival, and cell death (Junttila et al., 2008). The general mechanism of MAPK cascade involves stimuli-induced activation of upstream kinases by cell receptors. This leads to sequential action (MAPKKK → MAPKK → MAPK) (Junttila et al., 2008). MAPK downstream kinase activation occurs at the tripeptide motif, which forms the basis of the classification of the ERK, p38, and JNK. The classification of kinases is based on the sequence of the tripeptide. JNK and p38 are termed stress-activated protein kinases (SAPK) due to their roles in inflammatory and environmental stress responses (Fig 1.9) (Plattner and Bibb, 2012).

The p38 protein has physiological roles in both the cytoplasm and nucleus. MAPK p38 has shown functions in cell cycle progression, chromatin remodelling, mRNA stability, cytoskeleton reorganisation, metabolism, and many other cellular processes. In apoptotic pathways, P38 has been implicated in the delayed response to apoptosis by activating p21 and tumour suppressor protein (p53), resulting in cell death (Debacq-Chainiaux et al., 2010). The activation of p38 occurs via the

dual phosphorylation of Thr-Gly-Tyr by mitogen-activated protein kinase kinase 3 (MKK3) and mitogen-activated protein kinase kinase 6 (MKK6). These MKK's are highly selective to p38 and are unable to phosphorylate JNK and ERK1/2. P38 has been associated with the regulation of pro-inflammatory cytokines such as IL-1, IL-6, IL-8, TNF-α, and cyclooxygenase-2 (COX-2) (Cuenda and Rousseau, 2007).

JNK has a wide array of functions from neuronal and immunological functions to gene expression, cell death, and survival pathways (Zeke et al., 2016). Protein kinase mitogen-activated protein kinase kinase 4 (MKK4) and mitogen-activated protein kinase kinase 7 (MKK7) activate JNK via dual phosphorylation at Tyr and Thr (Weston and Davis, 2002). JNK is responsible for the activation of c-Jun, which leads to increased expression of activator protein-1 (AP-1). AP-1 (c-Jun & c-Fos) regulates cell growth, differentiation, and cytokines transcription (Fisher and Voorhees, 1998, Xie et al., 2013b).

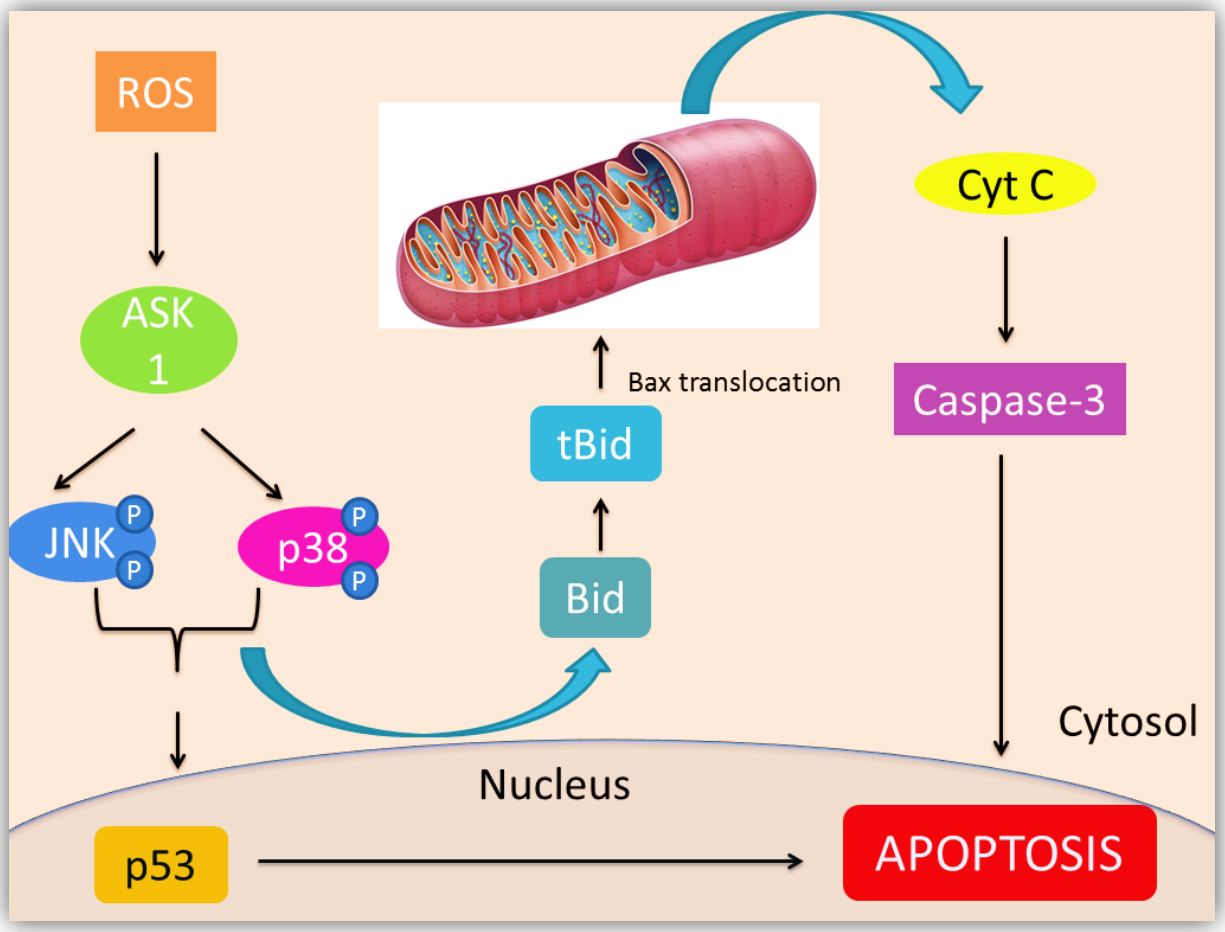

Figure 1.9 Overview of the MAPK pathway and oxidative stress (prepared by author)

1.7.2. Inflammation

Inflammation is the immune system's response to toxic insult, pathogens, and damaged cells. Inflammation is not only a defence mechanism to remove dangerous stimuli and initiate healing, but also a consequence of several diseases (Chen et al., 2017).

1.7.2.1. Sirtuin 1(Sirt1) and inflammatory regulation

Sirt1 expression has been linked to inflammatory regulation and cytoprotection in different cell lines (Xie et al., 2013a). Sirt1 undergoes phosphorylation by JNK1 and JNK2 at multiple serine and threonine residues. JNK and other kinases regulate Sirt1 expression; however, it is unknown which regulatory mechanism is involved in Sirt1 alteration of inflammatory responses (Xie et al., 2013a). Studies carried out by Alcendor et al. (2007) revealed that Sirt1 regulates ROS levels by elevating CAT expression. The increase in CAT expression was induced by forkhead box protein O1 (FoxO1); Sirt1 deacetylates FoxO1, FoxO3a, and FoxO4, which in turn, activates antioxidants such as CAT, SOD_2, and thioredoxin (Trx) (Salminen et al., 2013). Nevertheless, upregulation of Sirt1 also caused oxidative stress by deacetylating the Lys588 and Lys591 residues of Nrf2 and repressing its antioxidant function (Kawai et al., 2011). Sirt1 is also responsible for the regulation of ROS by controlling immune responses via NFκB. Sirt1 inhibits the activation of NFκB by the deacetylation of Lys310 residues found on RelA/p65 (Fig 1.8) (Yeung et al., 2004). Furthermore, Sirt1 expression has been associated with the deacetylation of transcription factors of AP-1 (Xie et al., 2013a).

1.7.2.2. Nuclear factor-kappa β (NFκB)

NF-κB is a transcription factor responsible for the induction of an immune response and inflammation. NFκB is induced in response to stimuli from the environment. NFκB, when unstimulated in cells, can form a complex with IκB (nuclear factor of kappa light polypeptide gene enhancer in B-cells inhibitor, alpha), an inhibitory protein. Activator molecules such as TNF-α, interleukin 1 (IL-1β), lipopolysaccharide (LPS), and UV radiation can lead to the phosphorylation of NF-κB and the degradation of IκBα. The activated NF-κB translocates to the nucleus and alters the expression of target genes (Ahn et al., 2003). Chelators of iron and copper were found to inhibit the activation of NF-κB (Schmilz, 1995). Exposure to TNF-α, IκBα can become phosphorylated by IκB kinases (IKK). IKK comprises of IKKα and IKKβ (Chen et al., 2017). This may result in the ubiquitination or degradation of the freed NFκB. The NFκB transcription genes' repression or activation is responsible for mediating inflammatory and immune responses by Th2 cytokines, chemokines, COX-2, matrix metallopeptidases (MMP's), and apoptotic factors (Fig 1.10) (Messadi et al., 2004).

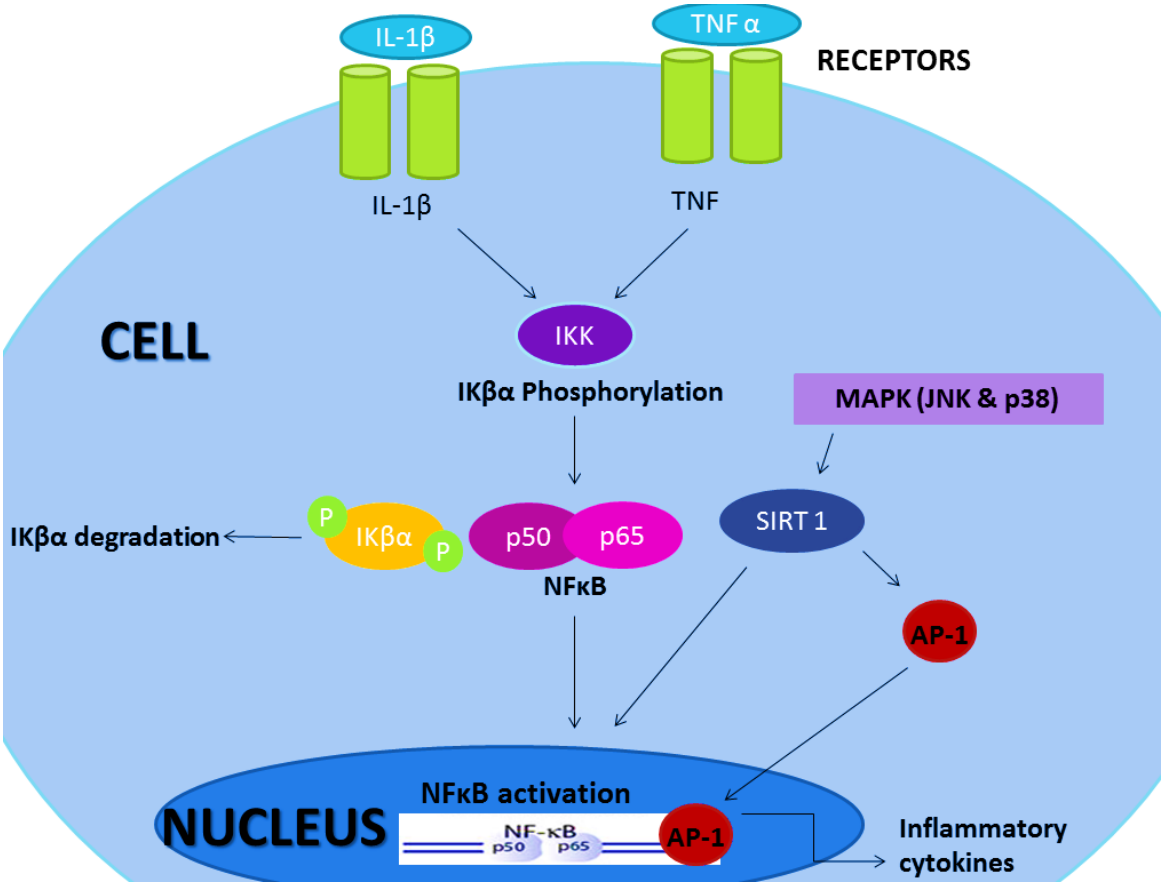

Figure 1.10 Overview of the NFκB pathway activation. Stimuli, such as ROS, can induce the activation of NFκB and degradation IKβ. NFκB translocates to the nucleus and transcribes for inflammatory and immune responses. MAPK regulates NFκB and AP-1 via Sirt 1 expression (prepared by author).

1.8. MicroRNAs (miRNAs)

MiRNAs are small, non-coding RNAs that interact with the 3' untranslated region (UTR) region of mRNA for the post-transcriptional regulation of gene expression. However, some miRNAs may interact with the 5' UTR region, gene promoters, and coding sequences (O'Brien et al., 2018). The formation of mRNA-miRNA complex results in translational repression or mRNA degradation (Fig 1.11) (Maurer et al., 2010). MiRNAs are involved in biological processes, including proliferation, apoptosis, and differentiation (Maurer et al., 2010). MiRNAs have been found to regulate approximately 30% of the human genome. The dysregulation of miRNAs has been associated with cancer, neurological, cardiovascular, and autoimmune diseases (Wiemer, 2007, Lukiw et al., 2008, Carè et al., 2007, Stanczyk et al., 2008).

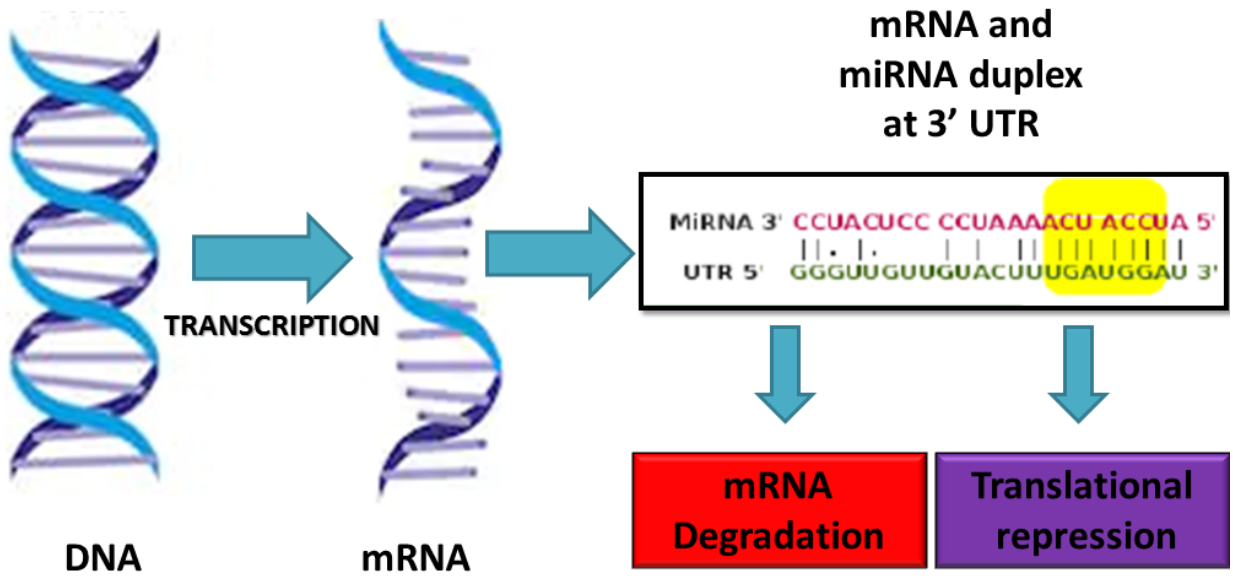

Figure 1.11 MiRNA function in mRNA degradation and translational repression (prepared by author)

1.8.1. MiRNA biogenesis

MiRNA biogenesis is classified into two pathways namely the canonical pathway and non-canonical pathway. MiRNA is generated predominantly from the canonical pathway.

1.8.1.1. Canonical miRNA biogenesis pathway

This pathway involves the transcription of primary miRNA (pri-miRNA) from their genes into precursor miRNA (pre-miRNA). The canonical pathway is dependent on the microprocessor complex which consists of the nuclease III enzyme, Drosha and an RNA binding protein, DiGeorge Syndrome Critical Region 8 (DGCR8) (O'Brien et al., 2018). DGCR8 recognises motifs within the pri-miRNA such as N6-methyladenylated GGAC. Drosha is responsible for the cleavage at the base of the hairpin structure of the pri-miRNA duplex. The resultant pre-miRNA is exported to the cytoplasm by an exportin 5 (XP05)/RanGTP complex. The pre-miRNA is processed by RNase III endonuclease Dicer by removing the terminal loop producing a mature miRNA. The miRNA is assigned a name based on its directionality (O'Brien et al., 2018). The miRNA hairpin comprises of a 5p strand arising from the 5' region and the 3p strand arises from the 3' region end. The mature duplex comprising of both 3p and 5p can be loaded into the Argonaute (AGO) family of proteins and the process is ATP dependent. The amount of AGO-loaded 3p and 5p is dependent on the cell type, cellular environment and thermodynamic stability. Strands with lower 5' stability or a uracil at the 5' region is preferential and is AGO loaded and serves as a guide strand while the unloaded strand (passenger strand) unwinds through various mechanisms (O'Brien et al., 2018).

1.8.1.2. Non-canonical miRNA biogenesis pathway

This pathway involves Drosha, Dicer, exportin 5 and AGO2. Non-canonical pathway differs from the canonical pathway due to Drosha/DGCR8 and Dicer independent pathways. Pre-miRNA's are produced by Drosha/DGR8 independent pathways resembling Dicer substrates. Mirtrons (pre-miRNA's produced from introns of miRNA splicing) and 7-methylguanosine-capped-premiRNA's (m^7G) are examples of premiRNA's (O'Brien et al., 2018). The RNA's are exported to the cytoplasm by exportin 1 independent of Drosha cleavage. There is a 3p bias which prevents the 5p strand loading on AGO. Alternately, Dicer independent miRNA's are processed by Drosha and require AGO2 due their insufficient length which excludes them as a Dicer substrate. The entire miRNA is loaded into AGO2 and the maturation process is completed by 3'-5' trimming of the 5p strand (O'Brien et al., 2018).

1.8.2. MiRNAs role in immune responses

1.8.2.1. MiRNA-29a

Studies have shown apoptosis regulation by the downregulation of pro-apoptotic proteins, namely Bax, PARP, phospho-FADD, cleaved caspase 8, and caspase 3. It was also determined that miRNA-29a repressed the expression of NFκB and, in this manner, protects cells from injury and apoptosis (Tiao et al., 2014).

1.8.2.2. MiRNA-29b

Study carried out by Luna et al. (2009), showed the regulation of extracellular matrix (ECM) genes following oxidative stress in HTM (human trabecular meshwork) cells suggesting miRNA-29b is a common oxidative stress-modulated miRNA. Moreover, miRNA-29b regulates oxidative stress by negatively regulating Sirt1 expression in ovarian cancer cells (Hou et al., 2017). MiRNA-29b expression initiated apoptosis by downregulating Bax mRNA expression in cardiomyocytes (Jing et al., 2018). Therefore, miRNA-29b plays a role in oxidative stress responses via sirt1 and apoptosis.

1.8.2.3. MiRNA-155

Studies have shown miRNA-155 as a potential target for cancer treatment due to the ubiquitous oncogene characteristics and promotion of proliferation in human cancer. Of importance was the elevated proliferation rate of hepatocellular carcinoma (HCC) when miRNA-155 expression was upregulated (Gao et al., 2015). Furthermore, miRNA-155 upregulated MAPK signalling and NFκB expression in pancreatic cancer cells leading to increased proliferation and ROS production.

1.9. Problem statement, aims, and objectives

1.9.1. Problem statement

Due to KA's extensive use in the beauty industry and as a food preservative, the effects on organs involved in metabolism of KA such as the liver are potential targets. *In vitro* and *in vivo* studies have

demonstrated KA's effect in multi-organ systems; however, the liver is often neglected. The liver is the main organ responsible for the detoxification of toxins and thus susceptible to damage; therefore, it is important to assess KA's toxicity in liver cells. To date, research on the effects of KA in liver cells cells remains limited. Understanding the potential effects of KA may provide insight on the concentrations posing minimal risk (Fig 1.12).

1.9.2. Alternate Hypothesis

It was hypothesized that KA induced oxidative stress, inflammation, and activated the MAPK signalling pathway in HepG2 cells following 24 h exposure

1.9.3. Aim

The study aims to determine the effects of KA on oxidative stress and subsequent alteration on immune responses related to NFκB inflammation and MAPK signalling in a human liver (HepG2) cell line.

1.9.4. Objectives

The effects of KA on HepG2 cells was determined by measuring:

- mitochondrial output (MTT assay) and ATP luminometry
- apoptosis using caspase luminometry
- oxidative stress
  - Lipid peroxidation (TBARS) assay
  - DNA integrity using 8-OHdG ELISA
  - Protein integrity using Protein carbonyl assay
- MAPK signalling and NFκB inflammatory responses using
  - Western blots of p38, JNK, Nrf2, phosphorylated-Nrf2 (ser40), CAT, phosphorylated-NFκB (ser536), NFκB, phosphorylated-Sirt1 (ser47) and AP-1
  - qPCR of *GPx, NFκB, IκBα* and miR-29a, miR-29b and miR-155 expression

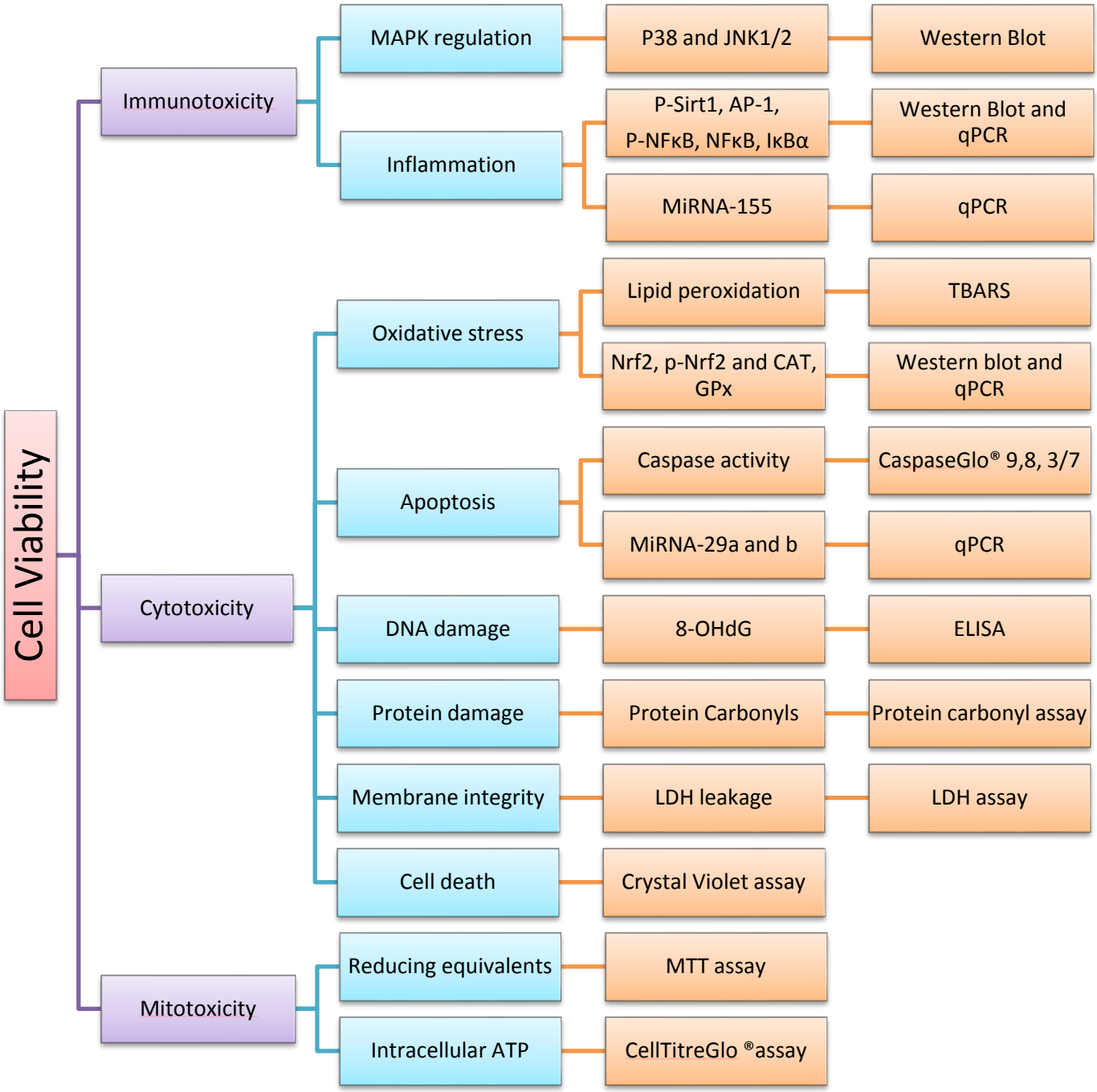

Figure 1.12 The experimental approach employed to investigate the toxicity of KA in HepG2 cells (prepared by author)

CHAPTER 2

METHODS AND MATERIALS

2.1. Materials

HepG2 cells (HB-8065) were purchased from the American Type Culture Collection (ATCC; Johannesburg, South Africa). Cell culture reagents were purchased from Whitehead Scientific (Johannesburg, South Africa). Luminometry kits were purchased from Promega (Madison, WI, USA). Western Blot reagents were purchased from Bio-Rad (Hercules, CA, USA). All other reagents and consumables were purchased from Merck (Darmstadt, Germany) unless otherwise stated.

2.2. Cell culture

2.2.1. Introduction

The HepG2 cell line is derived from the liver tissue of a 15-year-old Caucasian male with differentiated hepatocellular carcinoma (Donato et al., 2015b). HepG2 cells are commonly used for drug metabolism and hepatotoxicity studies. Favourable characteristics include an unlimited life span, stable phenotype, readily available, and easy to handle. HepG2 cells have an epithelial-like appearance and have a high proliferation rate with the ability to perform differentiated hepatic functions (Donato et al., 2015a). Due to the wide use of the cell line, extensive research into the functional characteristics of HepG2 has been carried out. Although a cancer cell line, HepG2 cells have retained characteristics of differentiated hepatocytes such as lipoprotein secretion, albumin secretion, glycogen synthesis and glutathione detoxification (Kammerer and Küpper, 2018). HepG2 is extensively used in toxicity studies due to the presence of biotransformation enzymes such as Phase I (cytochrome P450 monooxygenase) and Phase II (glucuronic and sulphate conjugation), which play a role in detoxification (Dehn et al., 2004).

2.2.2. Protocol

HepG2 cells were cultured (37ºC, 5% CO_2) in 25 cm^3 cell culture flasks containing Eagle's Minimum Essentials Medium (EMEM) supplemented with 10% foetal calf serum (FCS), 1% penicillin-streptomycin-fungizone, and 1% L-glutamine. FCS provides essential albumin and growth factors required for cell attachment, growth, and proliferation (Gstraunthaler et al., 2013). Penicillin-streptomycin-fungizone is a combination of antibiotics and fungicides that are used to prevent bacterial and fungal contamination. Glutamine is an essential amino acid required as a building block for proteins involved in cell growth and physiological functions (Cruzat et al., 2018).

The trypan blue cell exclusion technique is used to determine viable cells in cell culture. The cells are incubated with trypan blue dye and visualised using a light microscope. The trypan blue cell exclusion technique is based principle in which viable cells with intact, selectively permeable cell membranes

exclude the dye, whereas damaged cells take up the blue dye (Strober, 2015). This method was used to enumerate cells and determine cell viability prior to conducting each assay (Fig 2.1).

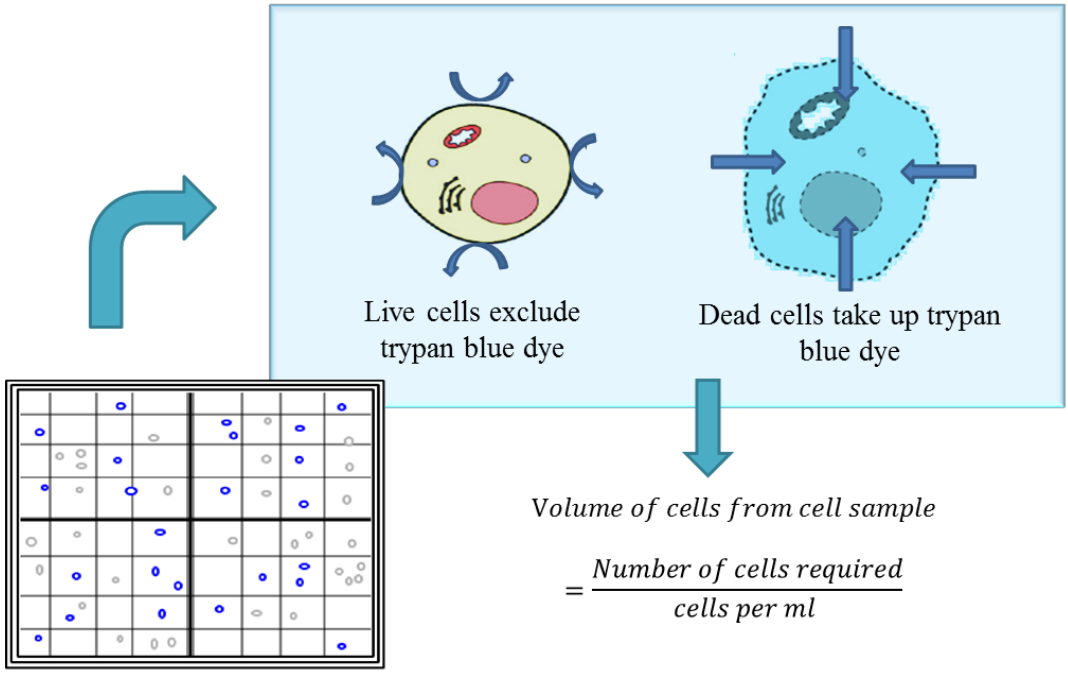

Figure 2.1 Trypan exclusion method used for the enumeration of viable cells (prepared by author)

2.3. KA preparation and treatment

A stock solution of KA (20 mg/ml) was prepared in 0.1 M Phosphate buffered saline (PBS). The cells were allowed to reach 80% confluency before incubation with KA [4.22, 8.02, or 12.67 mM]. All experiments were performed 3 independent times and in triplicate.

2.4. 3-(4, 5-Dimethylthiazol-2-yl)-2, 5-diphenyltetrazolium bromide (MTT) assay

2.4.1. Introduction

The MTT assay is one of the most commonly used assays to assess the anti-proliferative properties of compounds in cells. The assay utilises tetrazolium salts to assess the cell's mitochondrial metabolic activity. Mitochondrial metabolic activity is indirectly proportional to cell viability. The tetrazolium salts are reduced to insoluble purple formazan crystals by mitochondrial dehydrogenases (Fig 2.2). Once the crystals are solubilised with Dimethyl sulfoxide (DMSO), the spectrophotometric reading at 570 nm is used to evaluate cell viability using the following equation:

$$\%\ Cell\ viability = \frac{Average\ sample\ absorbance}{Average\ control\ absorbance} \times 100$$

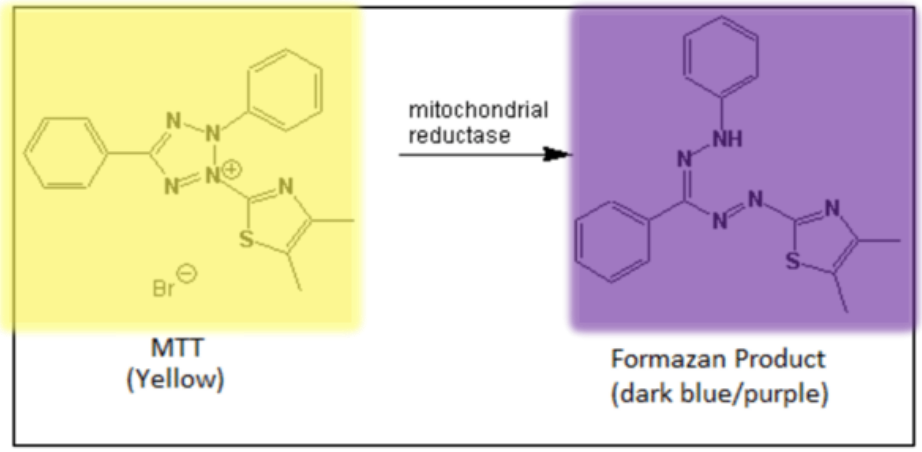

Figure 2.2 The reaction catalysed by mitochondrial reductase to produce formazan products (Karumuri, 2013)

2.4.2. Exposure protocol

HepG2 cells (15,000 cells/well) were seeded in a 96-well microtiter plate and allowed to adhere overnight before incubation (37°C, 5% CO_2,) for 6, 24 and 48 h with various concentrations of KA (0-12.67 mM). MTT salt solution [20 µl; 5 mg/ml in 0.1 M PBS] and CCM (100 µl) was added to the cells and incubated (37ºC, 4 h). Following incubation, the MTT salt was removed, and DMSO (100µl/well) was added to solubilise the formazan crystals. The plate was incubated (37º C, 1 h), and the absorbance was measured using a microplate reader (Biotek µQuant Plate reader, Winooski, VT, USA) at a wavelength of 570 nm with a reference wavelength of 690 nm. Analysis of the absorbance obtained was performed using GraphPad Prism V5.0, and the half-maximum inhibitory concentration (IC_{50}) was obtained.

2.5. Crystal violet assay

2.5.1. Introduction

The crystal violet assay measures cell viability by assessing the ability of cells to adhere to the cell culture vessel. It is based on the principle in which dead cells lose their ability to adhere to cell culture surfaces and are lost from the viable population. The crystal violet dye binds to DNA and proteins in cells (Fig 2.3). When dead cells detach, the number of cells stained with crystal violet staining decreases along with the intensity of the purple colour. The intensity of the purple colour is measured spectrophotometrically and describes the cell survival and growth inhibition potential of the treatment (Feoktistova et al., 2016).

2.5.2. Protocol

Crystal violet assay was performed as per (Feoktistova et al., 2016). HepG2 cells (15,000 cells/well) were adhered to a 96-well microtiter plate and incubated (37°C, 5% CO_2, 24 h) with varying concentrations of KA (0 - 12.67 mM). Following incubation, the cells were washed in dH_2O, and

0.5% crystal violet stain (50 µl) was added. The plates were incubated for 20 min on a bench shaker at 20 oscillations per minute. The cells were washed 4 times in dH_2O and air-dried overnight at RT. Methanol (200 µl) was added to each well, and the plate was incubated at RT for 20 min. The absorbance was read in a microplate reader (Biotek µQuant Plate reader, Winooski, VT, USA) at a wavelength of 570 nm. Cell viability was determined relative to the control.

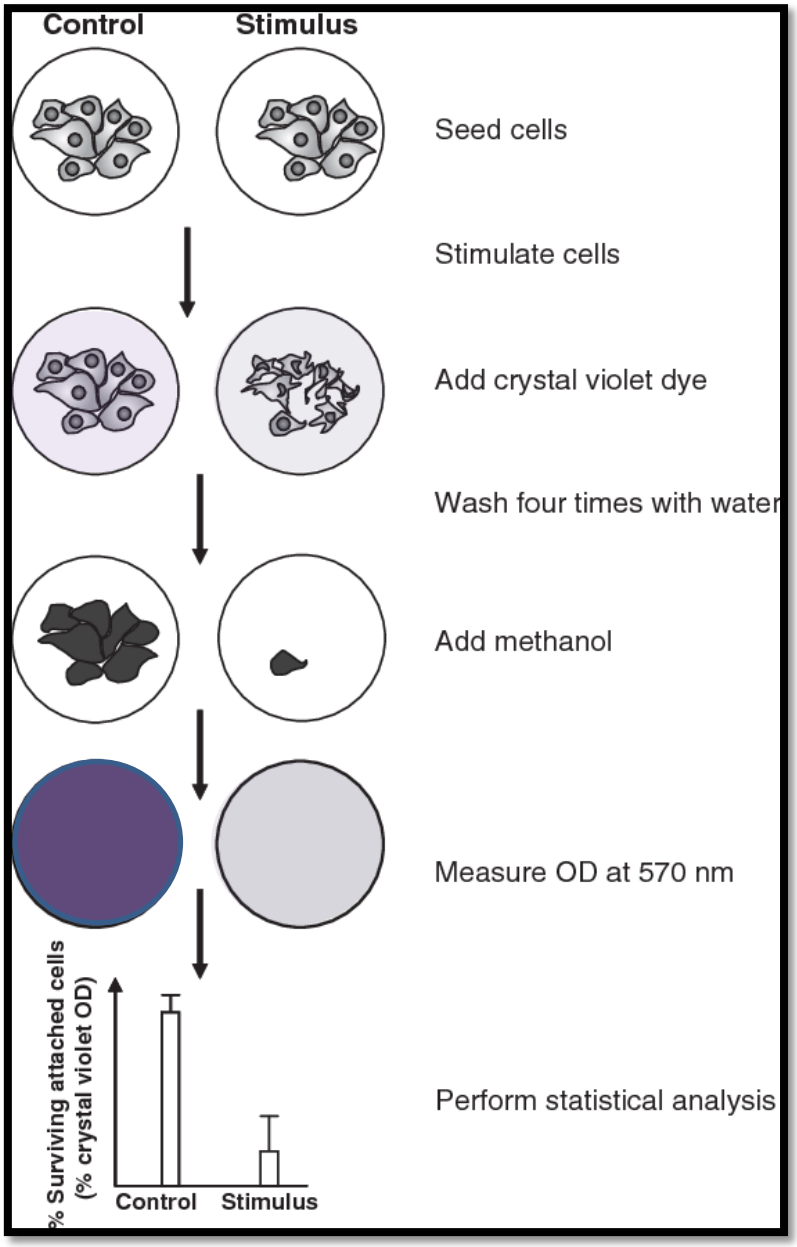

Figure 2.3 Overview of the crystal violet assay (Feoktistova et al., 2016)

2.6. Caspase activity

2.6.1. Introduction

Apoptosis and necrosis are both types of cell death associated with normal and disease states. The Caspase Glo®-3/7, Caspase Glo®-8, and Caspase Glo®-9 assay kits (Promega, Wisconsin, US) were used to measure the activities of caspase 3/7, caspase 8, and caspase 9, respectively. The assay kit contains aminoluciferin substrates which undergo cleavage by caspases. The freed aminoluciferin is catalysed by luciferase to produce luminescent signal. Luminescence is directly proportional to caspase activity.

2.6.2. Protocol

Luminometry was used to determine KA's effect on caspase-3/7, -8, and -9 activities in HepG2 cells. Following treatment with KA for 24 h, HepG2 cells (20,000 cells/well) were seeded in an opaque 96-well microtiter plate with 25 µl of Caspase Glo®-3/7, Caspase Glo®-8, and Caspase Glo®-9 reagents. The plate was incubated for 30 min at RT in the dark and luminescence was measured on a Modulus™ microplate luminometer (Turner Biosystems, Sunnyvale, USA). The results were expressed as relative light units (RLU).

2.7. LDH assay

2.7.1. Introduction

Necrosis of cells displays plasma membrane permeation causing the leakage of intracellular contents into the extracellular matrix (Chan et al., 2013). LDH is an enzyme that plays a role in the glycolytic pathway (Jialal and Sokoll, 2015). The amount of LDH released into the extracellular matrix is correlated with the extent of disruption to the cell membrane (Chan et al., 2013).

LDH catalyses the oxidation of lactate to pyruvate and produces reduced nicotinamide adenine dinucleotide (NADH). Tetrazolium salts are converted into a formazan product using the NADH product in the presence of an electron acceptor (Chan et al., 2013) (Fig 2.4). The spectroscopic reading at 500nm is directly proportional to LDH levels and is used to determine cell membrane damage and hence, is an indicator of necrosis.

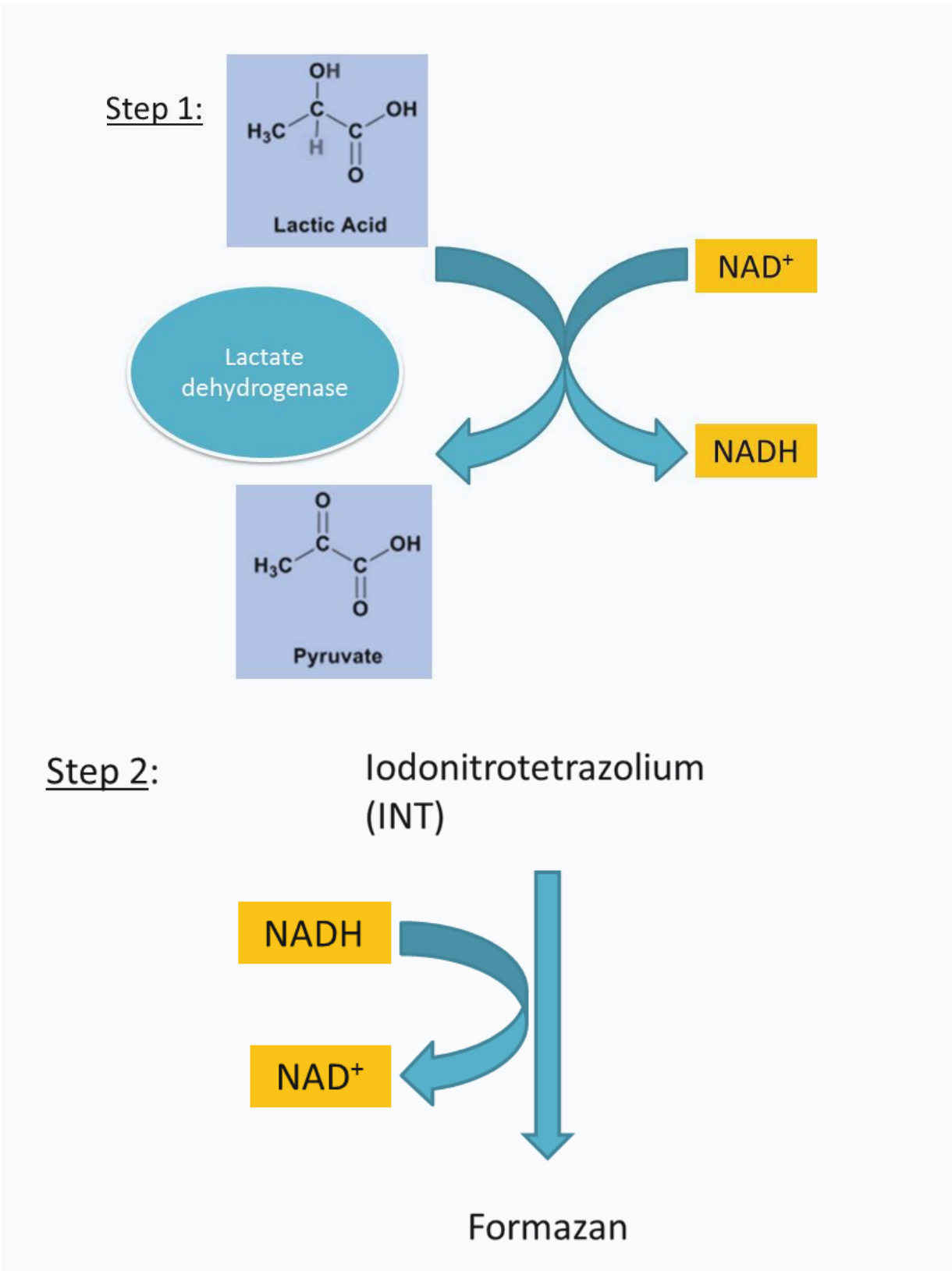

Figure 2.4 Principle of the LDH assay (prepared by author)

2.7.2. Protocol

The LDH cytotoxicity detection kit (Roche, Mannheim, Germany) was used to determine KA's effect on cell membrane integrity. Following the treatment of HepG2 cells with KA for 24 h, supernatants (100 µl) were transferred into a 96-well microtiter plate in triplicate. Thereafter, 100 µl INT/sodium lactate dye solution and diaphorase/NAD^+ catalyst were added to each well, and the plate incubated in the dark for 20 min at RT. Optical density was measured on a spectrophotometer (Biotek µQuant Plate reader, Winooski, VT, USA) at 500 nm. Results were expressed as the concentration of KA (mM) versus optical density.

2.8. ATP Quantification assay

2.8.1. Introduction

The mitochondria produce ATP by the tricarboxylic acid cycle (TCA) enzymes, electron transport chain complexes, and ATP synthase (Zhang et al., 2018). ATP is required for several processes such as intracellular signalling, DNA and RNA synthesis, and active transport. Therefore, ATP synthesis is essential to support cell survival.

The assay uses bioluminescence to measure the ATP concentration in the cell. A key reaction is the luciferase reaction that converts mono-oxygenated luciferin to oxy-luciferin. The reaction requires Mg^+, oxygen, and ATP and results in the release of energy in the form of luminescence (Fig 2.5). The luminescence is directly proportional to ATP and is used to quantify ATP in the cell.

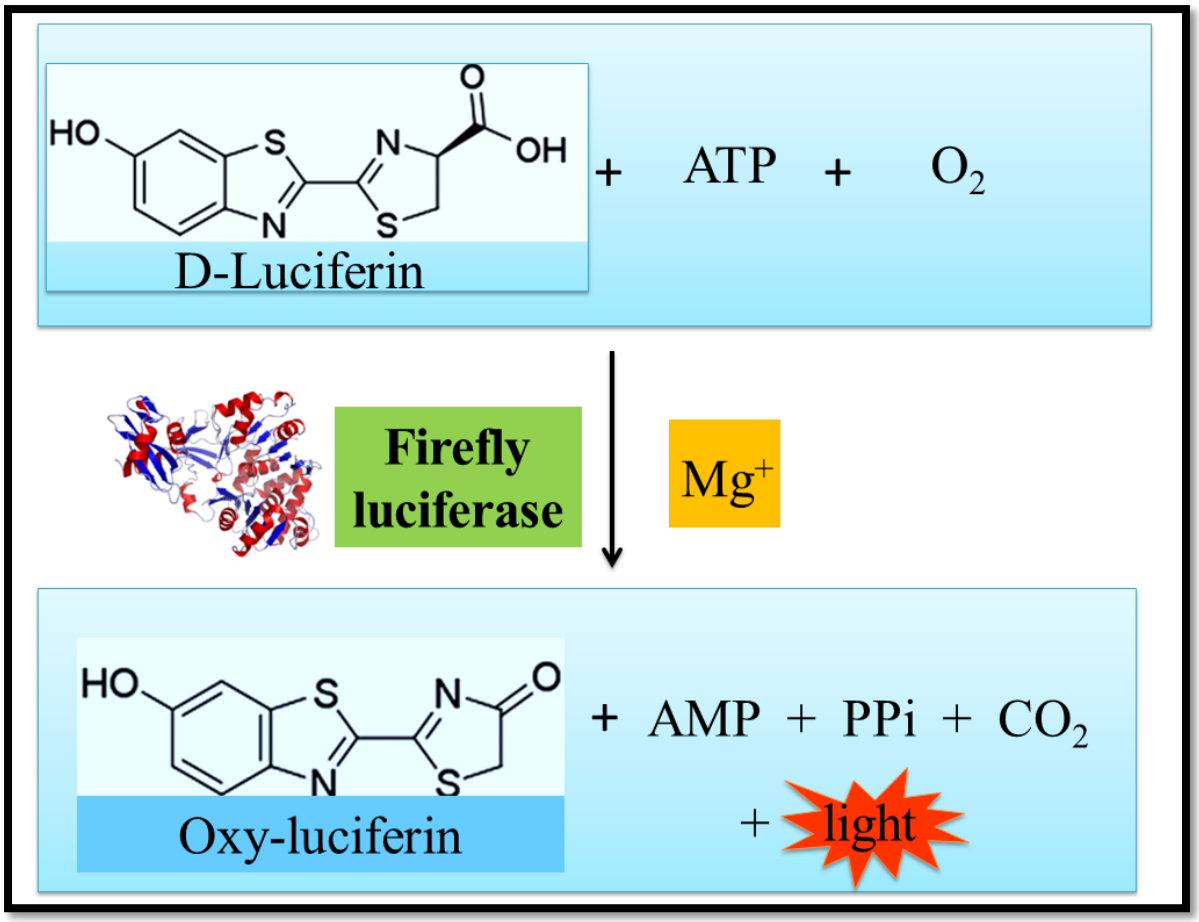

Figure 2.5 The principle reaction of the ATP Cell Titre Glo® assay used to quantify ATP concentration (prepared by author)

2.8.2. Protocol

ATP levels were quantified using the ATP Cell Titre Glo® luminometry assay kit, as previously described (Abdul et al., 2016). HepG2 cells (20,000 cells/well) were seeded in an opaque 96-well microtiter plate and incubated (RT in the dark, 30 min) with 20 µl of ATP Cell Titre Glo® reagent (Promega, Madison, USA). Following incubation, luminescence was measured using the Modulus™ microplate luminometer (Turner Biosystems, Sunnyvale, USA). Luminescence is proportional to the ATP levels and was expressed as relative light units (RLU).

2.9. Lipid peroxidation (TBARS) assay

2.9.1. Introduction

Lipid peroxidation is initiated by hydrogen abstraction from PUFA's due to the presence of excess ROS. A lipid peroxidation chain reaction occurs by the initiation of a three-step mechanism involving an initiation step, a propagation step, and lastly, a termination step (Ayala et al., 2014). The chain reaction produces malondialdehyde (MDA) and 4-Hydroxy-4-nonenal (4-HNE). MDA is used as a

biomarker for lipid peroxidation of omega-3 and -6 fatty acids due to its observed reaction with thiobarbituric acid (TBA) (Ayala et al., 2014). Thiobarbituric acid reactive substances (TBARS) assay is based on the reaction of 2-thiobarbituric acid and one molecule of MDA yielding the chromophoric product MDA-TBA adducts measured at 532 nm (Fig 2.6). The reaction occurs at high temperature and a low pH.

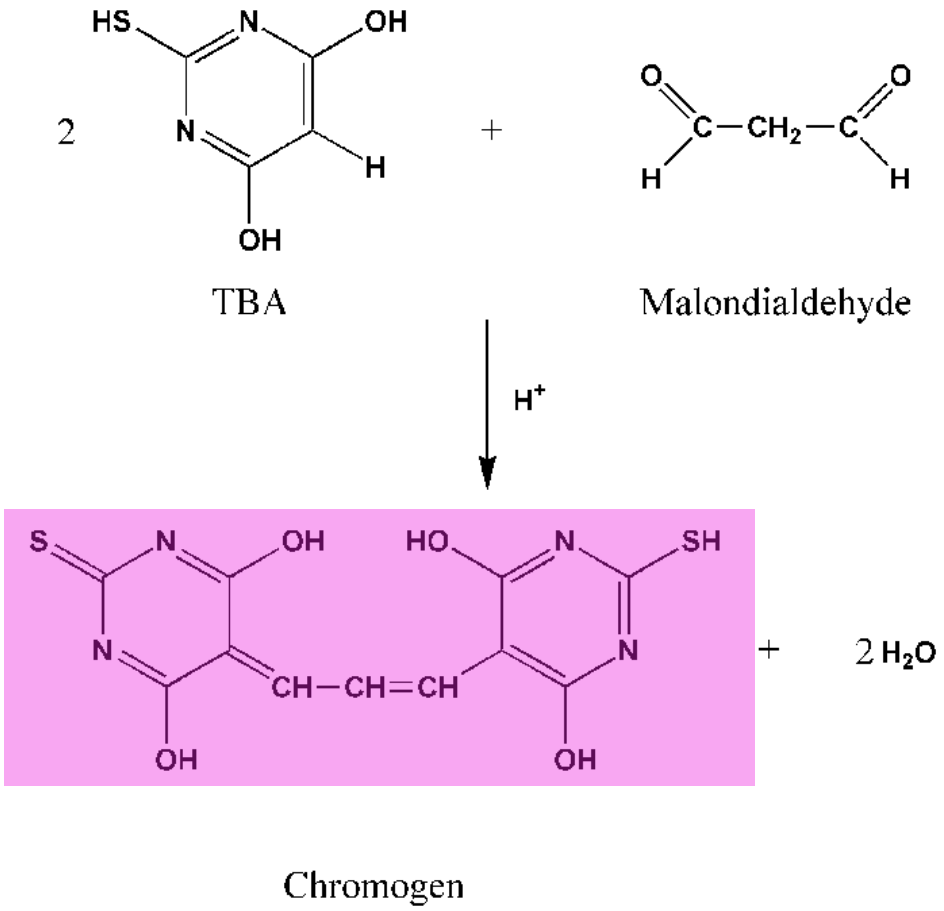

Figure 2.6 Principle reaction in the lipid peroxidation (TBARS) assay, adapted from Antolovich et al. (2002).

2.9.2. Protocol

Briefly, 200 µl of supernatants were added to test tubes along with 2% H_3PO_4 (200 µl), 7% H_3PO_4 (200 µl), and 0.1 M TBA/BHT solution (400 µl). A negative control consisting of 3 mM HCl (400 µl) and a positive control consisting of 1% MDA (1µl) was also prepared. All samples were vortexed, and 1 M HCl (200 µl) added to adjust the pH to 1.5. Samples were heated (100°C, 15 min) and allowed to cool to RT before adding butanol (1500 µl). The samples were vortexed (30 s) and allowed to settle into two distinct phases. The upper butanol phase (100 µl) was transferred into a 96-well microtiter plate in triplicate, and the absorbance was measured using the Biotek µQuant spectrophotometer (Winooski, VT, USA) at a wavelength 532 nm with a reference wavelength of 600 nm. The results

were expressed as MDA concentration (mM), which was calculated using the absorption coefficient (156 mM^{-1}).

2.10. Protein isolation

2.10.1. Introduction

Crude protein was isolated from HepG2 cells using 200 µl Cell Lysis solution (50 mmol/l HEPES, 1% Triton ×100, 10% glycerol, and 50 mmol/l NaCl) for the protein carbonyl assay and 200 µl Cytobuster™ reagent (Novagen, USA) supplemented with protease and phosphatase inhibitors for Western Blot. Cytobuster reagent is a non-ionic detergent that disrupts cell membranes to yield functionally active and expressed proteins when coupled with mechanical scraping. It is supplemented with protease and phosphatase inhibitors to preserve protein integrity (Eslami and Lujan, 2010). The process was carried out on ice to prevent protein degradation.

2.10.2. Protocol

HepG2 was treated with KA for 24 h. The supernatant was removed from flasks, and adhered cells were washed three times with 0.1 M PBS. Isolation of proteins from control and KA-treated HepG2 cells was carried out using the respective lysis solutions (200 µl). Samples were incubated for 30 min on ice before mechanically lysed. The supernatant obtained from the disrupted cells were decanted into 1.5 ml micro-centrifuge tubes. The samples were centrifuged at 13, 000 g for 10 min at 4ºC. Supernatant containing crude protein was decanted into 1.5 ml micro-centrifuge tubes and kept on ice for further quantification and standardization procedures. The pellet was discarded.

2.10.3. Quantification and standardisation of proteins

2.10.3.1. Introduction

The bicinchoninic acid (BCA) assay is used to quantify total crude protein. The method principle reaction is the Biuret reaction. BCA is a water-soluble compound that forms an intense purple complex with cuprous ions (Cu^{+}) in an alkaline environment (Fig 2.7) (Walker, 1996). The stable chromophore BCA-Cu^{2+} complex absorbs light at a 562 nm wavelength (Walker, 1996). The intensity of the purple colour complex is directly proportional to the protein concentration in the sample.

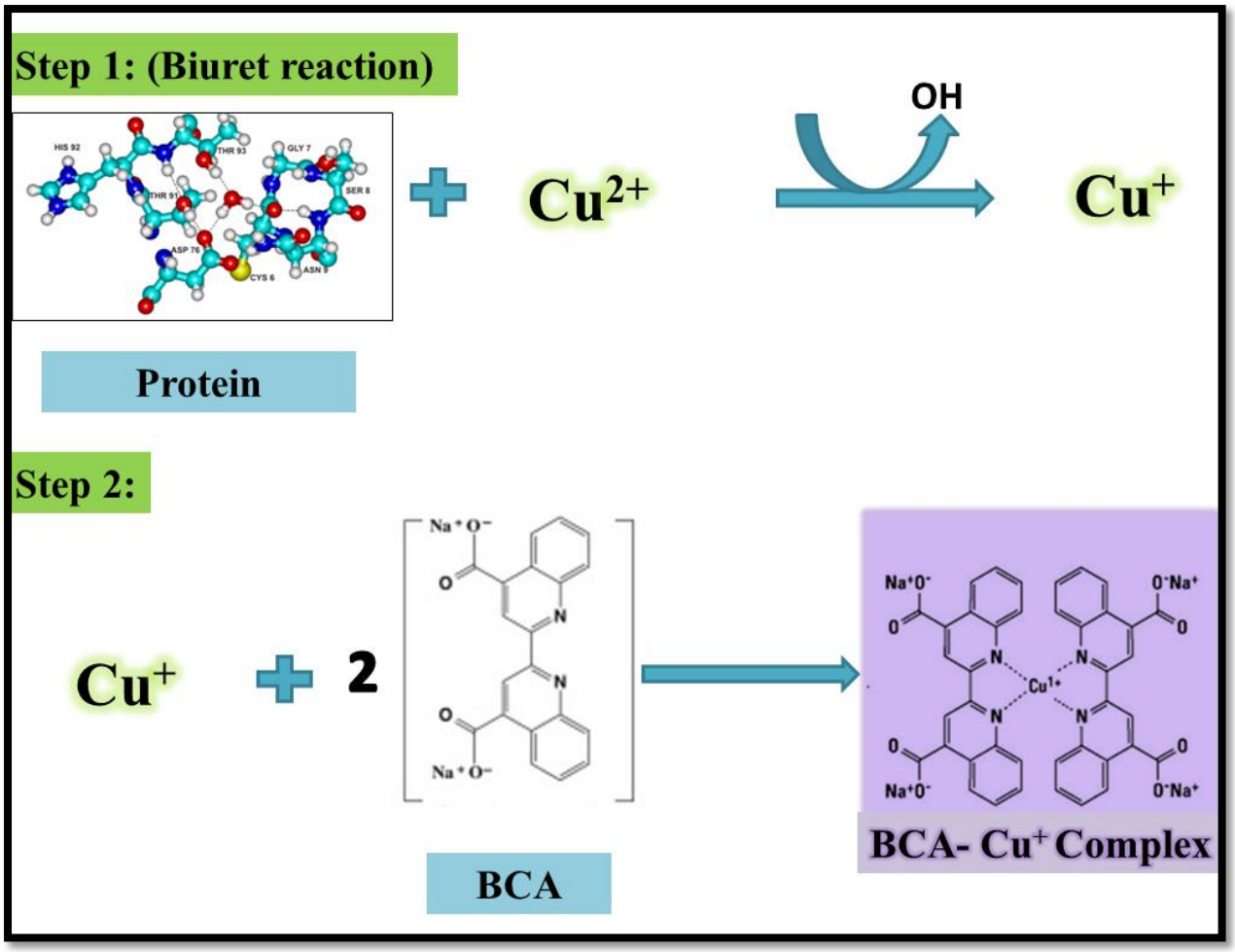

Figure 2.7 The principle reactions in the BCA assay used to quantify protein (prepared by author)

2.10.3.2. Protocol

Bovine serum albumin (BSA) [0, 0.2, 0.4, 0.6, 0.8, and 1 mg/ml], a protein standard, was serially diluted using distilled water and used to construct a standard curve. In a 96-well plate, 25 µl of each standard (triplicate) and protein sample (duplicate) were added into appropriately labelled wells. A working solution (200 µl) containing BCA (198 µl) and $CuSO_4$ (4 µl) was added to each well. The plate was incubated at (37°C, 30 min), to allow the reaction between sample protein and Cu^+ to occur. The absorbance was measured at 562 nm using a spectrophotometer (Bio-tek µQuant Plate Reader). The standard curve was used to determine the concentration of sample proteins (mg/ml) present by extrapolation. The proteins were subsequently standardised to 1 mg/ml for the protein carbonyl assay and 1.5 mg/ml for Western blot.

2.11. Protein oxidation (Protein carbonyl) assay

2.11.1. Introduction

Protein carbonylation occurs when ROS attack side chains of proline, arginine, lysine, and threonine in the presence of transition metals (Fe^{2+} and Cu^{+}) (Celi and Gabai, 2015). The superoxide radicals' mechanism of protein damage involves the oxidation and inactivation of iron-sulphur (Fe-S) proteins. Superoxide radicals target proteins such as complex I NADPH dehydrogenase and succinate dehydrogenase. The Fenton or Haber-Weiss reaction generates hydroxyl radicals and releases Fe^{2+} and H_2O_2.

Primary protein carbonylation is the formation of reactive aldehydes and ketones that can react with 2, 4-dinitrophenylhydrazine (DNPH). Protein oxidation was quantified by measuring the intracellular protein carbonyl groups in the sample at a wavelength of 370 nm.

2.11.2. Protocol

The standardised protein (200 µl) was added to DNPH (800 µl) at RT for 1 h. A blank consisting of the standardised protein (200 µl) and 2.5 M HCl (800 µl) was also prepared. The solution was vortexed after every 15 min interval of the 1h incubation. Following incubation, the protein in each sample was precipitated with 20% Trichloroacetic acid (TCA) (1 ml) on ice and vortexed, followed by centrifugation (2000 g, 10 min, RT). The pellet formed in each sample was washed twice with 1 ml ethanol-ethyl acetate (1:1) and dissolved in 6 mol/l guanidine hydrochloride (500 µl). The samples were incubated (37ºC, 10 min) and centrifuged (2,000 g, 10 min, RT) to remove any insoluble material. The supernatant (100 µl) was added in triplicate into a 96-well microtiter plate (100 µl) and the absorbance was measured at 370 nm with a spectrophotometer. The corrected absorbance was calculated by subtracting the average absorbance obtained from the blank from the sample absorbance. The protein carbonyl concentration was obtained by dividing the corrected absorbance calculated by the 2,4-Dinitrophenol's (DNP's) extinction coefficient (22, 000 $l.M^{-1}.cm^{-1}$). The results were expressed in nanomoles per milligram units.

$$Protein\ carbonyl\ concentration\ (nmol/ml) = \frac{pathway\ (1cm) \times absorbance}{Extinction\ coefficient\ of\ DNP}$$

2.12. Western Blotting

2.12.1. Introduction

Western blot is a molecular-based technique used to identify proteins of interest from a heterogeneous mixture of proteins in the cell. The technique uses sodium dodecyl sulphate polyacrylamide gel electrophoresis (SDS-PAGE) to separate proteins based on their molecular weights (Mahmood and Yang, 2012). The charge of the proteins is exploited to ensure the movement of proteins occurs. The negative charge of the protein migrates towards the positive electrode through the polyacrylamide gel.

The protein's size determines the movement through the gel; the large molecular weight proteins migrate slower through the matrix whereas the smaller molecular weight proteins migrate faster (Mahmood and Yang, 2012). The protein is transferred onto a solid support such as a nitrocellulose or polyvinylidene difluoride (PVDF) membrane. A blocking solution is used to prevent non-specific binding of proteins. The membrane is incubated with antibodies specific to the proteins of interest. The technique used both primary and enzyme-conjugated secondary antibodies to ensure specificity. The membrane is washed and visualised by the reaction between the enzyme conjugated secondary antibody and substrate solution. The protein relative band's density (RBD) is proportional to the amount of protein present (Fig 2.8) (Mahmood and Yang, 2012).

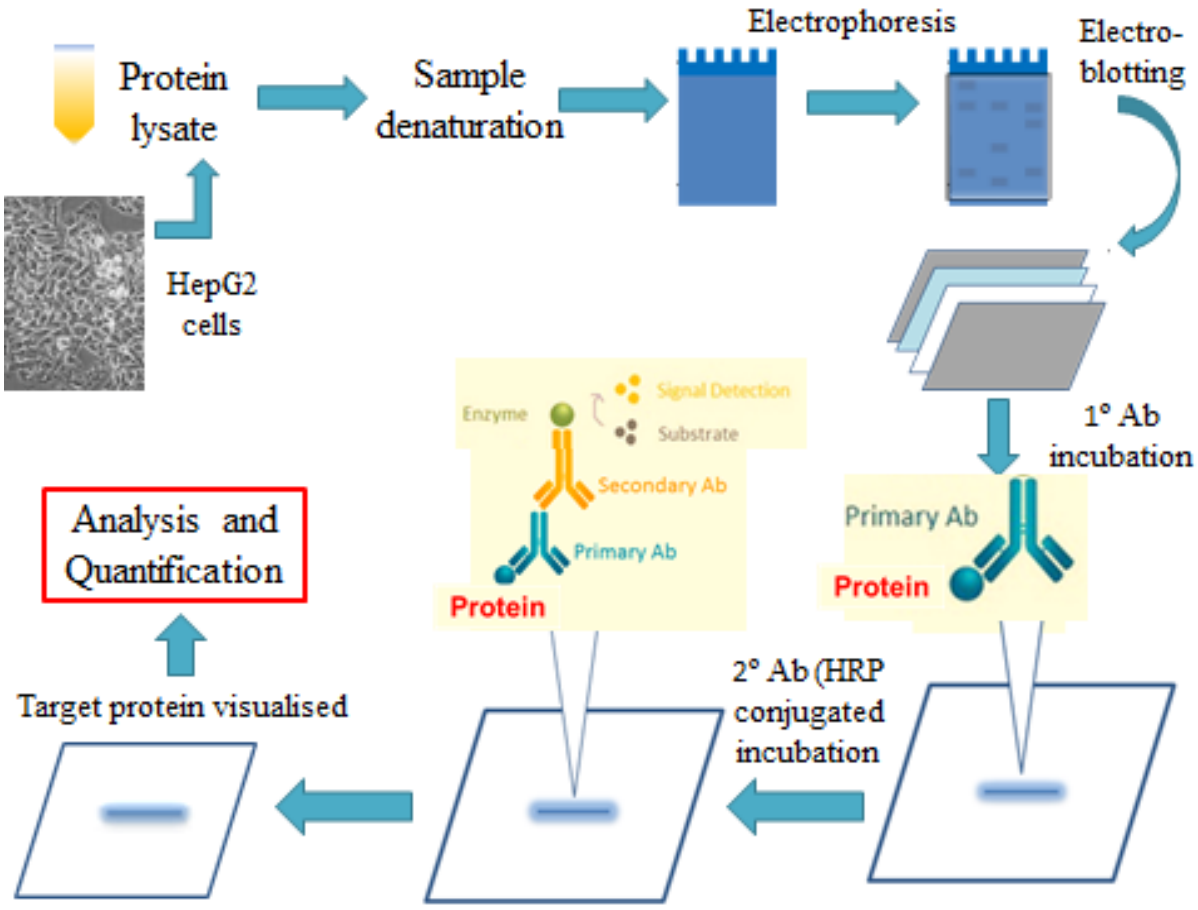

Figure 2.8 Overview of Western blot procedure (prepared by author)

2.12.2. Quantification and standardisation of proteins

2.12.2.1. Protocol

Laemmli buffer (50 µl; dH_2O, 0.5 M Tris-HCl (6.8), bromophenol blue, β- mercaptoethanol, glycerol, and 10% SDS) was added to the standardized protein samples for Western blot and boiled (100ºC) for 5 min. The proteins were allowed to cool at room temperature (RT) and stored at -20°C until the western blot procedure was carried out. The buffer solution components serve specific functions

required for an efficient gel electrophoresis assay. Tris-HCl is required for the pH buffering of the sample solution (Mishra et al., 2017, Bass et al., 2017). Bromophenol blue is a dye used to allow for the visualisation of the protein sample as migration through the gel occurs. β-mercaptoethanol acts as a reducing agent and denatures protein by breaking disulphide bonds, causing the unfolding of proteins (Mahmood and Yang, 2012). Glycerol adds weight to the samples allowing it to sink into the gel wells. SDS has a negative charge and alters the charge of proteins, therefore neutralising their inherent charge. The neutralisation aids in the separation of proteins solely of size and not the charge (Fig 2.9).

2.12.3. SDS-PAGE

2.12.3.1. Introduction

Polyacrylamide is made up of cross-linker N, N'-methylene bis-acrylamide, and acrylamide, which is catalysed by ammonium persulfate (APS). SDS-PAGE comprises of two polyacrylamide gels of differing characteristics: a stacking gel and a resolving gel. The stacking gel is acidic (pH 6.8) and has larger pores due to a lower acrylamide concentration (Mahmood and Yang, 2012). The gel separates proteins poorly and forms thin sharp bands. The resolving gel is basic (pH 8.8) and has narrow pores to separate proteins. The proteins are separated by size, and smaller proteins move more rapidly through the narrower pores, thus migrating further in the polyacrylamide gel towards the positive electrode (Mahmood and Yang, 2012).

2.12.3.2. Protocol

Polyacrylamide gels were prepared, and MINI-PROTEAN 3 SDS-PAGE apparatus (Bio-Rad) were set up according to the manufacturers' guidelines. A 10% resolving gel [Bis-acrylamide, dH_2O, 1.5 M Tris (pH 8.8), 10% SDS, 10% APS, and TEMED] was prepared and allowed to set (RT, 1 h). Once set, the 4% stacking gel [Bis-acrylamide, dH_2O. 0.5 M Tris (pH 6.8), 10% SDS, 10% APS, and TEMED] was added above the resolving gel. A 1cm plastic comb was placed in the stacking gel to form wells to allow for the loading of samples. The gel was allowed to set (RT, 1 h).

The prepared gels was placed into the electrode tank, and the electrode was assembled (mini-PROTEAN Tetra Cell System, Bio-Rad), as per manufacturers guidelines. The samples (25 µl) and molecular weight markers (5 µl) were loaded into the wells of the gel . Once loaded, the electrode tank was filled with running buffer [25 mM Tris, 192 mM glycine, and 0.1% SDS]. The gel was electrophoresed using the Bio-Rad compact power supply (150 V, 1 h).

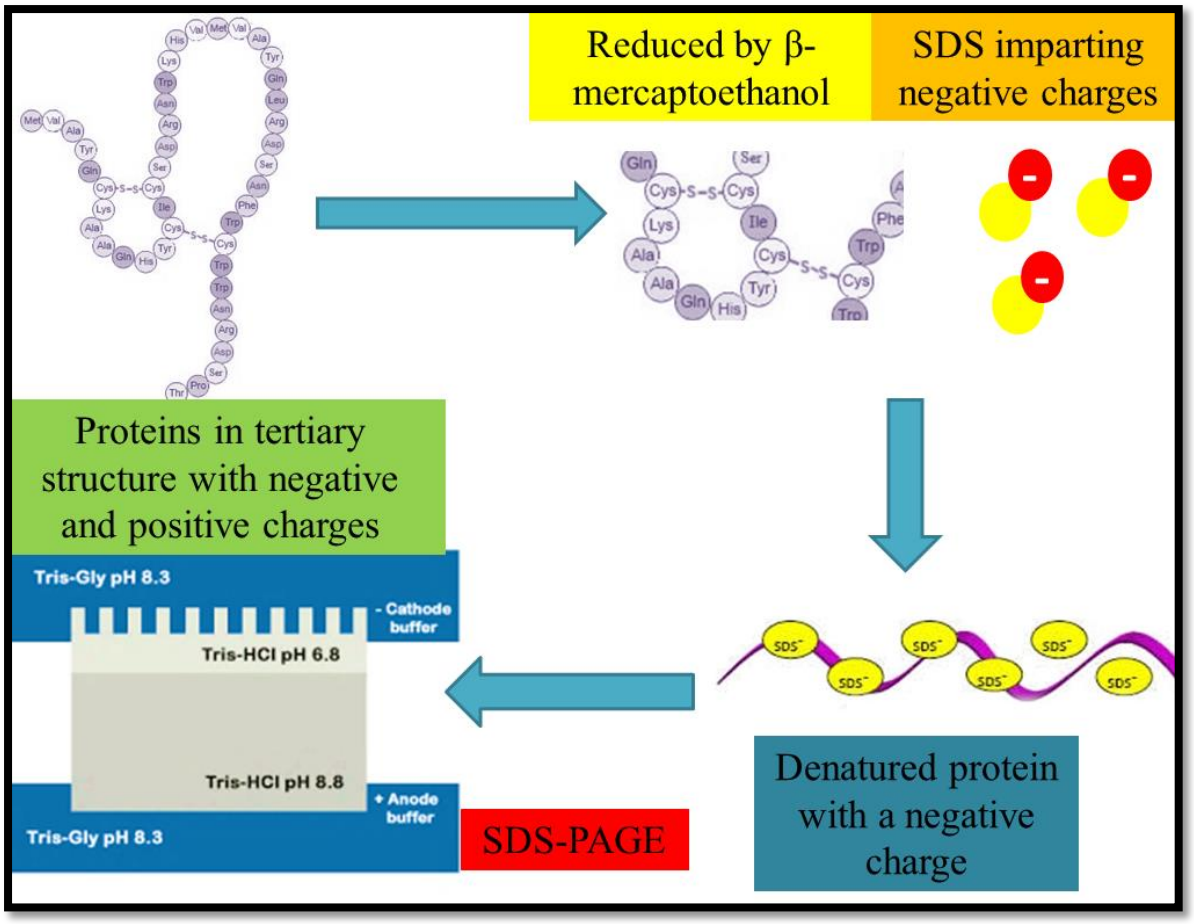

Figure 2.9 Denaturation and alteration of charge of the tertiary structure of proteins by SDS and β-mercaptoethanol (prepared by author)

2.12.4. Protein Transfer (Electro-blotting)

Following electrophoresis, the gel is prepared before transfer onto the nitrocellulose membrane. The stacking gel is removed, and the resolving gel is placed into a gel sandwich assembly. The gel sandwich comprises of two fibre pads, a nitrocellulose membrane, electrophoresed gel, and transfer buffer adjusted to pH 8.3 [25 mM Tris, 192 mM glycine, 20% methanol]. The gel sandwich is assembled between two electrodes, and the separated proteins are transferred to the nitrocellulose membrane using a Bio-Rad Trans-Blot Turbo Transfer System (20 V, 30 min). The protein transfer principle depends on the application of an electric charge that is perpendicular to the surface of the gel. The electric current causes the negatively charged proteins to migrate towards the positively charged electrode resulting in the proteins being embedded onto the nitrocellulose membrane.

2.12.5. Blocking and antibody incubation (Immuno-blotting)

Once the proteins are transferred onto the nitrocellulose membrane, the membrane is incubated in a blocking solution to prevent proteins' non-specific binding. The blocking solution comprises of 5% BSA or 5% non-fat dry milk (NFDM) in Tris buffer saline with 0.05% TWEEN 20 [TTBS, dH_2O,

0.05% TWEEN, 150 mM NaCl, 3 mM KCl, 25 mM Tris, pH 7.5]. Membranes are incubated in the blocking solution with gentle rotation for 1 h at RT. Primary antibodies (Table 1) were used to immunoblot the membranes at RT for 1 h on a shaker. The membranes were then incubated overnight to allow for the binding of primary antibodies to specific proteins. Following incubation, membranes were equilibrated at RT and washed with TTBS at 10 min intervals between washes to remove unbound primary antibodies. The membranes were then incubated in secondary antibodies conjugated with horseradish peroxidase [goat anti-rabbit (Cell Signaling Technology, 7074S) and goat anti-mouse (Cell Signaling Technology, 7076P2) with gentle agitation (1:1,000, 2 h, RT) (Fig 2.12). The secondary antibody facilitates the detection of a specific protein by binding to the primary antibody. Following the incubation, membranes are washed with TTBS five times at 10 min intervals to remove unbound secondary antibodies.

Table 1. Primary antibody dilutions used in Western blot

Antibody	**Catalogue number**	**Dilutions**
Phosphorylated Sirt-1	2314L (Cell Signalling Technology) Rabbit polyclonal	1:5,000
AP-1	A5968 (Sigma Aldrich) Rabbit polyclonal	1:5,000
NFκB	D14E12 (Cell Signalling Technology) Rabbit polyclonal	1:5,000
Phosphorylated-NFκB	3031 (Cell Signalling Technology) Rabbit polyclonal	1:5,000
JNK	SAB 4200176 (Sigma Aldrich) Mouse monoclonal	1:5,000
P38	M8177 (Sigma-Aldrich) Rabbit polyclonal	1:5,000
Nrf-2	12721S (Cell Signalling),	1:5,000

	Rabbit polyclonal	
Phosphorylated Nrf-2	AB76026 (Abcam) Rabbit polyclonal	1:5,000
CAT	CO979 (Sigma Aldrich) Mouse monoclonal	1:5,000

2.12.6. Imaging

Protein bands were visualised using the Bio-Rad Clarity Western ECL Substrate Kit and the ChemiDoc™ XRS + System. The principle reaction that allows visualisation of proteins occurs between the HRP-conjugated secondary antibody and H_2O_2 to free oxygen radicals. The oxygen radicals react with luminol to form aminophtalic acid causing luminescence and enabling the visualisation of protein bands.

2.12.7. Quenching and normalisation

Membranes were quenched in 5% hydrogen peroxide (30 min, 37ºC) and washed once with TTBS (10 min, RT). Membranes were blocked with 5% BSA and incubated in HRP-conjugated antibody for β-actin (Sigma-Aldrich, A3854; 1:5,000; 30 min, RT) as a housekeeping protein. Images were analysed using ImageLab Software™ v6.0 (Bio-Rad). The results were expressed as relative band density (RBD) obtained from the proportion of the RBD of the protein of interest and the RBD of the respective β-actin.

2.13. Quantitative PCR (qPCR)

2.13.1. Introduction

Quantitative polymerase chain reaction (qPCR) involves the amplification and quantification of DNA. The conventional PCR technique only amplifies a target gene, whereas qPCR accurately quantifies the amount of target genes expressed.

The qPCR amplification procedure involves three controlled steps that are performed at different temperatures in repeated cycles. Step 1 involves denaturation of the double-stranded DNA template at (90 - 100°C) to produce single-stranded DNA. The synthesis of cDNA requires various reagents and buffers (Table 2 & Table 3). Step 2 involves the annealing of complimentary primers to the target DNA sequence at temperatures dependent on the primer. Step 3 is extension in which Taq polymerase elongates the annealed primer at 72°C by adding nucleotides. These steps are repeated to produce exponential copies of the original DNA fragment (Table 4 & 5).

The quantity of the target genes expressed is detected using SYBR Green. A SYBR Green dye binds DNA and produces a fluorescent signal that can be detected and quantified (Fig 2.10).

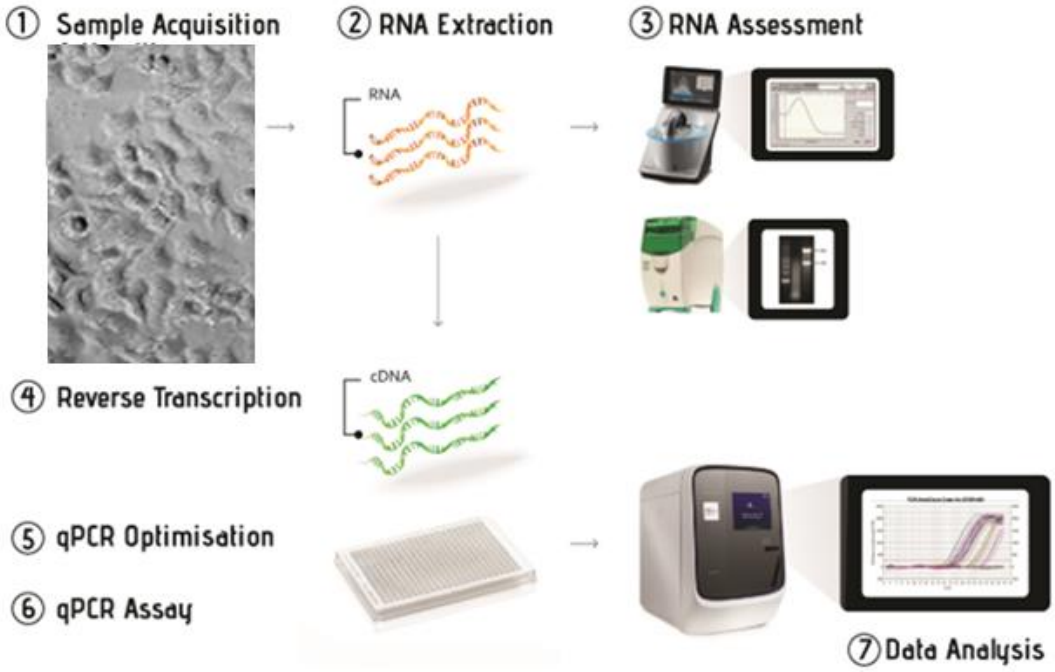

Figure 2.10 Overview of the qPCR steps (Adapted from (Kuang et al., 2018)).

2.13.2. RNA isolation

RNA was isolated from control and KA treated HepG2 cells as per (Chuturgoon et al., 2014). Following 24 h KA-treatment, cells were washed once with PBS and thereafter, 500 µl Qiazol and PBS were added and incubated (5 min, RT). Cells were mechanically scraped and transferred into 1.5 ml microcentrifuge tubes and stored overnight (-80ºC). Chloroform (100 µl) was added, and centrifuged (12,000 x g, 10 min, 4ºC). The supernatant was removed, and to the pellet, isopropanol (250 µl) was added and stored overnight (-80ºC). Thawed samples were centrifuged (12,000 x g, 20 min, 4ºC). The supernatant was discarded, and the pellet was washed with ethanol (75%) and centrifuged (7,400 x g, 15 min, 4ºC). Following the removal of ethanol, RNA pellets were air-dried (30 min, RT). The dried pellets were resuspended in nuclease-free water (15 µl) and stored at -80ºC.

2.13.3. RNA Quantification

The RNA was quantified using the Nanodrop 2000 spectrophotometer (ThermoScientific, Waltham, USA) and standardised to 1000 ng/µl. The A260/A280 absorbance ratio was used to determine RNA purity.

2.13.4. cDNA synthesis for mRNA

For mRNA expression, cDNA was synthesized using the Maxima™ H Minus strand cDNA synthesis kit (ThermoFisher Scientific, K1652) (Table 2). The thermocycler conditions for cDNA synthesis were as follows: 25ºC for 10 min, 50ºC for 15 min, 85ºC for 5 min.

Table 2. Reaction volume and components of the Maxima™ H Minus strand cDNA synthesis kit

Component	One reaction volume
10 mM dNTP mix	1 µl
Oligo (dT) primer (pmol)	0.25 µl
Nuclease-free water	12.75 µl
5× RT buffer	4 µl
Maxima H minus enzyme mix	1 µl
Template DNA	1 µl
TOTAL	**20 µl**

2.13.5 cDNA synthesis for miRNA

For miRNA expression, cDNA was synthesized using the miScript II RT kit (Qiagen, 218161) as per manufacturers' instruction (Table 3). The thermocycler conditions for cDNA synthesis were as follows: 37ºC for 60 min, 95ºC for 5 min, 4ºC for 5 min.

Table 3: Reaction volumes and components of iScript II RT kit used to synthesise cDNA for miRNA expression analysis

Component	One reaction (µl)
5 x miScript HiFlex Buffer	4 µl
10 x miScript Nucleics Mix	2 µl
RNAse free water	11 µl
miScript RT mix	2 µl
RNA template	1 µl

TOTAL	**20 µl**

2.13.6 mRNA expression

The mRNA expressions of *GPx, NFκB, and IκB* were investigated using the PowerUp™ SYBR™ Green Master mix (ThermoFisher Scientific), as per manufacturers instruction. Primers for the forward and reverse sequences are presented in Table 5. Reaction volumes were prepared as follows;

Table 4: qPCR reaction mix (PowerUp™ SYBR™ Green Master mix)

Component	**One reaction volume/ volume per well.**
Sso advanced Universal SYBR Green Supermix	5 µl
RNAse free water	2 µl
Sense primer (25 µM)	1 µl
Anti-sense primer (25 µM)	1 µl
cDNA	1 µl
TOTAL	**10 µl**

CFX96 Touch™ Real-Time PCR Detection System (BioRad) was used to amplify samples. Cycling conditions were as follows: initial denaturation (8 min, 95ºC) followed by 40 cycles of denaturation (15s, 95ºC); annealing (40s, temperature was assessed based on the gene of interest (Table 5)) and extension (30s, 72ºC). Glyceraldehyde-3-Phosphate dehydrogenase (GAPDH), a house-keeping gene, was used to normalise mRNA expression.

Table 5: The primer sequences and annealing temperatures used for mRNA expression

Primer	**Sequence**	**Annealing temperature (ºC)**
GPx	Forward (5'-GACTACACCCAGATGAACGAGC-3') Reverse (5'-AATCCCCAGCAGTGGAATAAGG-3')	58
NFκB (p65)	Forward (5'-ACCAACAACAACCCCTTCCA-3') Reverse (5'-GTAGTCCCCACGCTGCTCTT-3')	60

IκBα	Forward (5'-CACTCCATCCTGAAGGCTACCAAC-3') Reverse(5'-CACACTTCAACAGGAGTGACACCAG-3')	64
GAPDH	Forward (5'-TCCACCACCCTGTTGCTGTA-3') Reverse (5'-ACCACAGTCCATGCCATCAC-3')	Same as gene of interest

2.13.7. miRNA Gene expression

The expression of miR-29a, miR-29b, and miR-155 were analysed using the miScript SYBR Green PCR kit (Qiagen, 218073) and 10X miScript primer assays (Qiagen, Hilden, Germany) as per manufacturers' instruction. The thermocycler conditions were as follows; initial activation (15 min, 95ºC), denaturation (15 sec, 94ºC), annealing (30 sec, 55ºC), and extension (30 sec, 70ºC) for 40 cycles. Human RNU6 (MS000033740) was used as a housekeeping gene to normalise miRNA expression.

2.13.8. Analysis of data for mRNA and miRNA expression

The relative mRNA expression change was assessed using the method described by (Livak and Schmittgen, 2001). The method represents the fold change relative to the control as $2^{-\Delta\Delta Ct}$. All qPCR data were analysed using Bio-Rad CFX Manager™ Software version 3.1.

2.14. 8-OHdG Enzyme-linked immunosorbent assay (ELISA)

2.14.1. DNA isolation

2.14.1.1. Introduction

A cell lysis solution was added to HepG2 cells to obtain crude DNA. The cell lysis solution was made up of EDTA (pH 8), SDS (0.1%), and Tris-Cl. EDTA is a chelation agent used due to its high affinity for divalent cations, which act as co-factors for nucleases. Divalent cations such as Mn^{+}, Ca^{2+}, and Mg^{2+}could inhibit the degradation of DNA. SDS is used as an anionic detergent to lyse the cell membranes and nucleus to enable the release of DNA. The Tris-Cl is positively charged and plays a role in stabilizing the repellent charges present in negatively charged helices (El-Ashram et al., 2016).

2.14.1.2. Protocol

Cells were treated with KA for 24 h, treatments were removed and the cells were washed three times with PBS. The PBS was discarded, and the Cell Lysis solution was added and incubated for 15 min at RT. The cells were mechanically scraped with a cell scraper until a homogenous solution was obtained. In a fume hood, potassium acetate solution (600 µl) was added and the samples were invert mixed for 8 min. The solution was vortexed and centrifuged for 5 min at 13,000 rpm at RT. The supernatant was decanted, and isopropanol (600 µl) was added. The solution was invert mixed and

subsequently centrifuged for 5 min at 13,000 rpm at RT. A white pellet was obtained, and careful consideration was taken not to disturb DNA when removing the isopropanol. Ethanol (300 µl) was added to the pellet and centrifuged at 13,000 rpm for 5 min at RT. The ethanol was decanted and the DNA pellet was air dried (15 min, RT). To the dry pellet, DNA hydration solution (TE buffer) [10 mM EDTA (pH 8), 100mM Tris-Cl (pH 7.4) and dH_2O] was added, and the samples were heated at 65ºC for 15 mins. Once heated, the tubes were allowed to cool for 15 min at RT and stored at -20ºC.

2.14.2. Standardisation and quantification

Crude DNA concentration was quantified using the Nanodrop 2000 spectrophotometer (ThermoScientific, Waltham, USA). All samples were standardised to 100 ng/µl in TE buffer (150 µl) and used for the ELISA procedure.

2.14.3. Enzyme-linked immunosorbent assay (ELISA)

2.14.3.1. Introduction

ELISA is based on the interaction between an antigen and antibody. Antibodies are produced by B-cells in leukocytes and play a crucial role in the body's immune response. Antigens form part of a group that consists of nucleic acids, proteins, peptides, and secondary metabolites (Sakamoto et al., 2018). ELISA exploits this characteristic of antibodies and antigens in a highly specific and selective technique. ELISA is a five-step procedure (Fig 2.11). The method relies on the adsorption of antigens or antibodies onto a solid phase. The first step involves antigens or antibodies coating on a polystyrene plate. The second step is the addition of samples to the wells to be captured by the antibodies. The third step requires the detection of antibody-antigen reaction is visualised using enzymes linked to antibodies such as horseradish peroxidase (HRP) (Sakamoto et al., 2018). The fourth step involves the addition of the HRP substrate (3,3',5,5'- Tetramethylbenzidine, TMB), which forms a coloured complex with HRP which is visualised using a spectrophotometer. The last step stops the reaction using a stop solution (sulfuric acid) and data is analysed to determine the concentration of target molecule in the samples.

2.14.3.2. Protocol

Preparation of 8-OHdG standards were prepared by completing a serial dilution of 7 concentrations [60, 30, 15, 7.5, 3.75, 1.875, and 0.94 ng/ml]. To a micrcentrifuge tube, 500 µl sample diluent is added and 250 µl into a second microcentrifuge tube. To the first microcentrifuge, 3 µl of 8-OHdG standard stock (10 µg/ml) was added. The samples were serially diluted to obtain the required concentrations.

Briefly, standards (50 µl), zero standard, and isolated DNA samples (100 ng/ml) were added in duplicate in the 96-well microtiter plate. The anti-8-OHdG was diluted in antibody diluent, and 50 µl was added in the appropriate wells except for the blank. The plates were covered and incubated at RT for 1 h. The individual wells were aspirated and washed five times with wash buffer (300 µl) and

inverted on an absorbent paper to remove excess liquid. A working solution comprises of the anti-mouse antibody and diluted in HRP diluent as per manufacturers' instruction. The working solution (100 µl) was pipetted into each well, and incubated (1 h, RT). Each well was aspirated and washed five times (300 µl, RT) and inverted to remove excess liquid. TMB substrate solution (100 µl) was added to each well and incubated (15 min, RT) in the dark. Following incubation, stop solution (100 µl) was added to each well. The absorbance was read at a wavelength of 450 nm on a spectrophotometer.

The average net optical density (OD) was calculated as follows;

$$Average\ net\ OD = average\ sample\ OD - average\ blank\ OD$$

Absorbances were used to for the construction of a standard curve (average net OD standards versus concentration standards) from which the concentration of 8-OHdG was calculated.

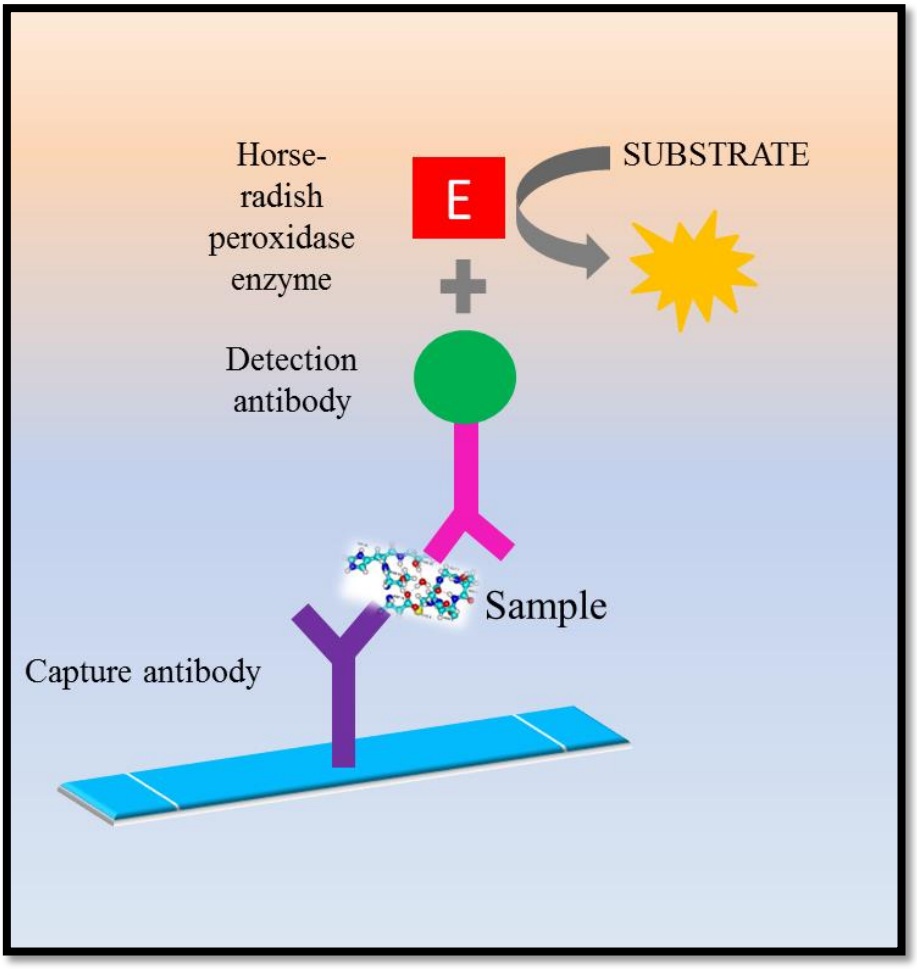

Figure 2.11 The principle of ELISA (prepared by author)

2.15. Statistical analysis

The data were analysed using GraphPad Prism V5.0 Software (GraphPad Prism Software Inc.). One-way analysis of variance (ANOVA) followed by Tukey multiple comparison tests (95% CI) was used to present data to determine statistical significance. The data was represented as mean ± standard deviation (SD) (n = 3), unless otherwise stated. Significant data obtained a p-value of below 0.05.

CHAPTER 3

RESULTS

3.1. Mitochondrial output in HepG2 cells

MTT and crystal violet assay was used to determine cell viability and mitochondrial output (0-12.67 mM KA). KA dose-dependently decreased HepG2 cell viability with half a maximal inhibitory concentration (IC_{50}) of 8.02 mM (Fig 3.1A). Furthermore, a significant decline in cell viability was observed at 4.22 and 12.67 mM KA (Figure 3.1B, $p < 0.0001$); these concentrations were used for all subsequent assays.

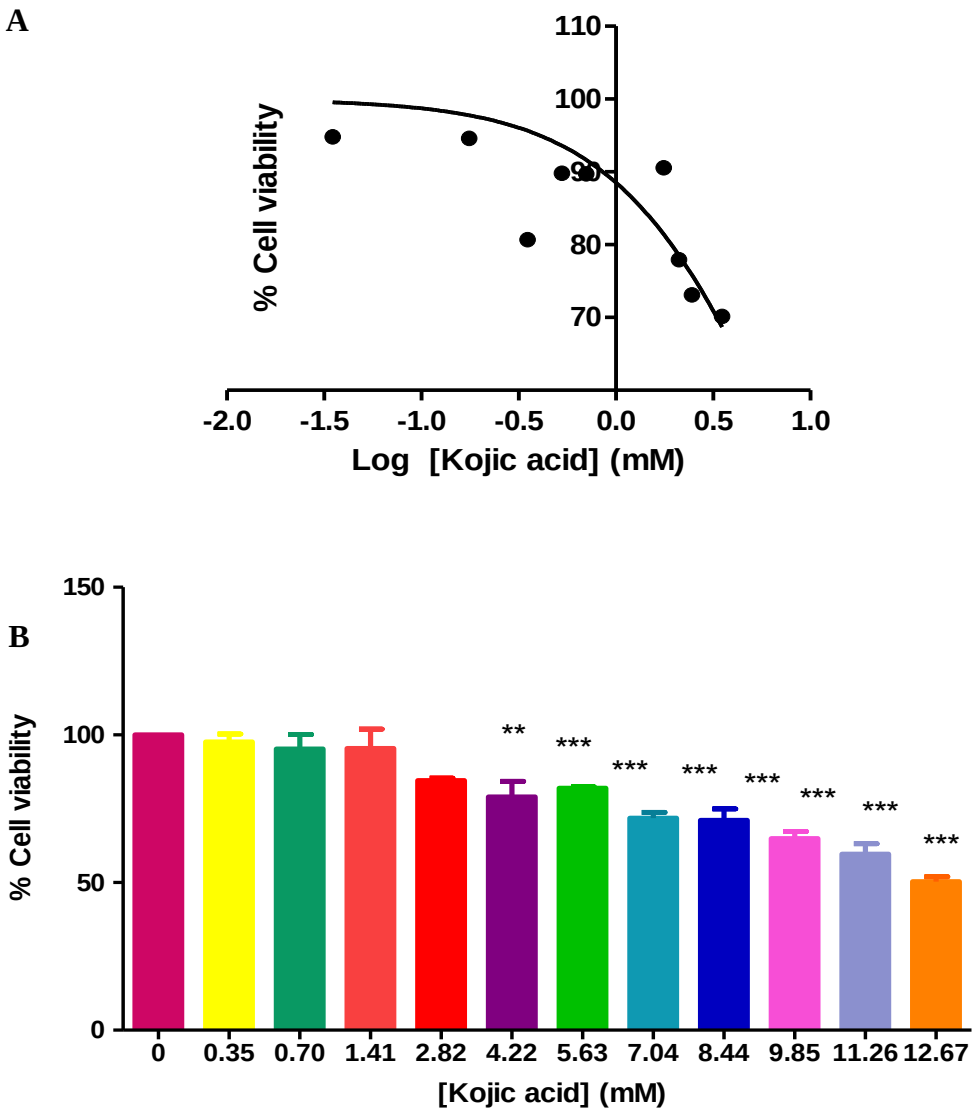

Figure 3.1 KA dose-dependently decreased HepG2 cell viability as depicted using the MTT assay (A) and crystal violet assay (B) (n = 3)

3.2. Kojic acid induced cell death in HepG2 cells

The activities of caspases 9, 8, and 3/7 and LDH leakage were assessed to determine cell death in HepG2 cells. KA upregulated the activity of the initiator caspase 9 ($p < 0.0001$, Fig 3.2A) and caspase 8 ($p = 0.0003$, Fig 3.2B) at all concentrations compared to the control. The activity of the executioner caspase 3/7 was significantly increased by the 4.22 mM KA but decreased by the 12.67 mM treatment ($p < 0.0001$, Fig 3.2C). The LDH results indicate that KA at 4.22mM was decreased and 8.02 mM was significantly decreased whereas, 12.67 mM KA caused significant membrane damage ($p < 0.0001$, Fig 3.3). The decrease in caspase 3/7 activity, as well as the increase in LDH leakage/membrane damage strongly suggests that necrosis is the mode of cell death.

A

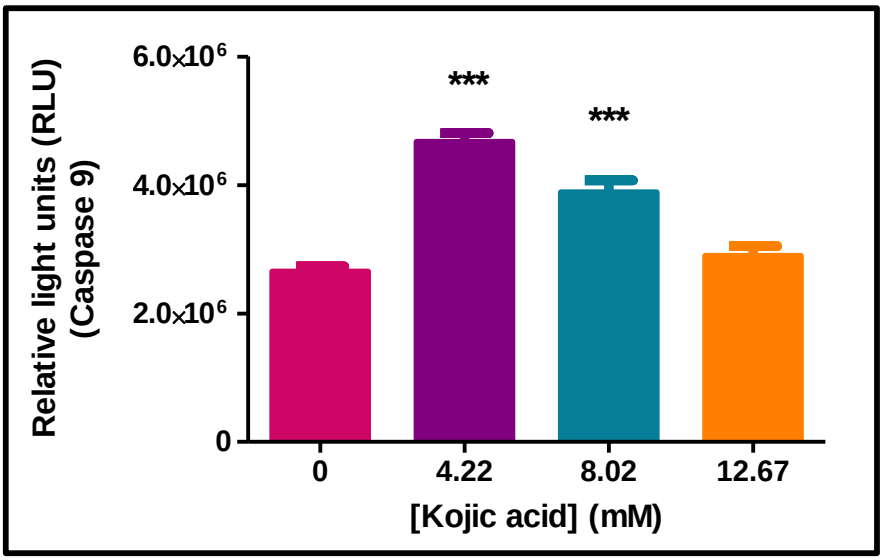

B

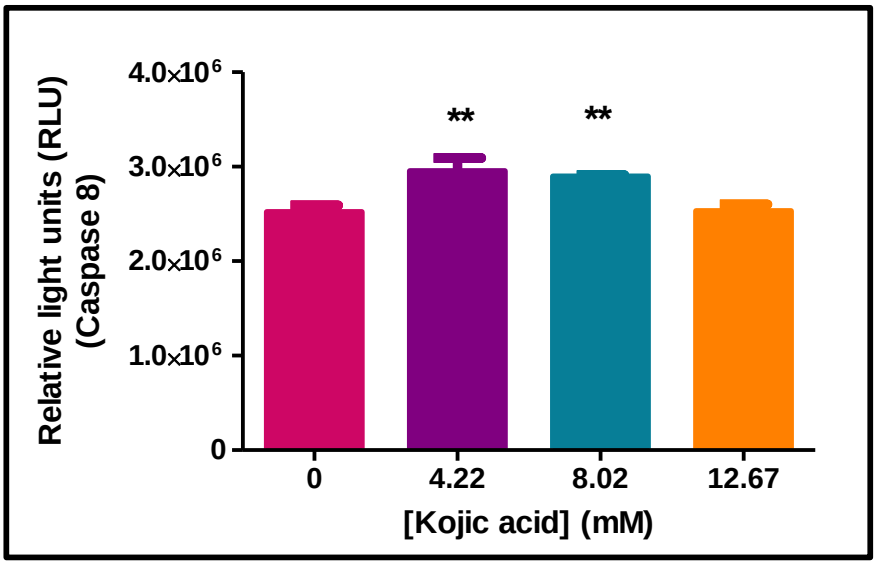

C

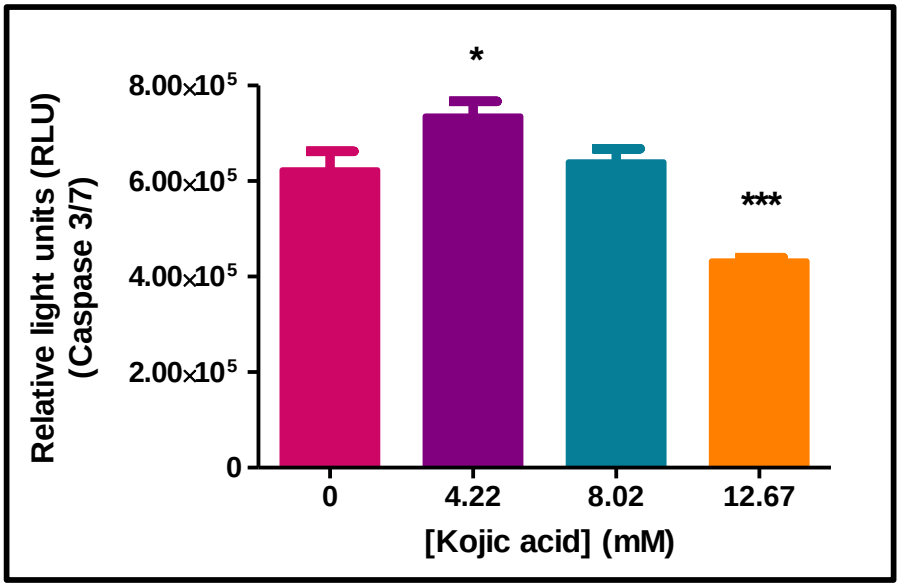

Figure 3.2 The effect of KA treatment on caspase activities of 9 (A), 8 (B), and 3/7 (C) in HepG2 cells (*p<0.05, **p<0.001, ***p<0.0001) (n = 3)

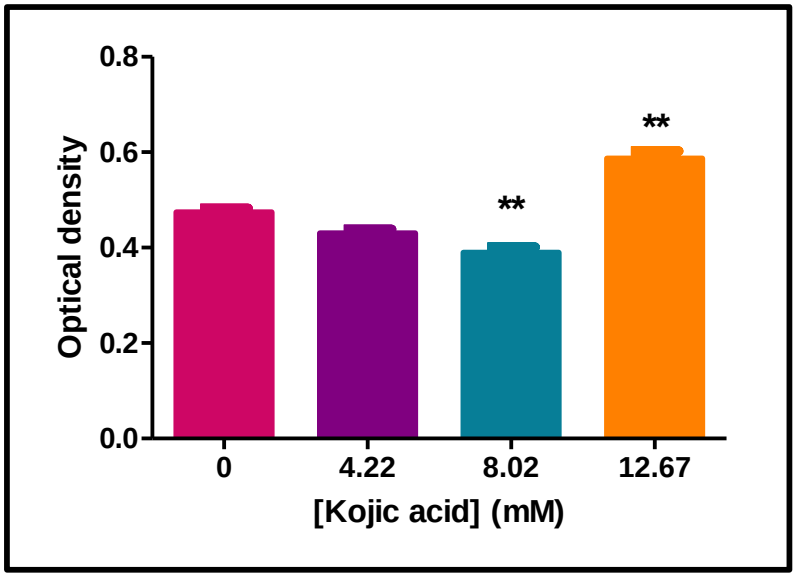

Figure 3.3 The effect of KA on LDH leakage/membrane integrity in HepG2 cells (p < 0.001) (n = 3)**

3.3. Assessment of oxidative stress

To confirm cell death induction due to stress responses, macromolecules, and ATP were assessed in HepG2 cells following KA treatment. ATP levels were not increased at 4.22 mM and 8.02 mM however, ATP was significantly increased at 12.67 mM KA relative to the control ($p < 0.0001$, Fig 3.4).

KA treatment altered the antioxidant status in HepG2 cells. KA significantly increased extracellular MDA production- a by-product of lipid peroxidation ($p < 0.0001$, Fig 3.5A) relative to the control. The increase of lipid peroxidation suggests the presence of oxidative stress. The markers of lipid peroxidation, such as 4-HNE, have the ability to form an adduct with DNA resulting in DNA breaks. Although lipid peroxidation markers were upregulated, it was found that KA did not induce a significant increase in 8-OHdG ($p = 0.0025$, Fig 3.5B). Protein carbonyls were assessed in KA-exposed cells compared to the control. Protein oxidation was significantly decreased in KA-exposed cells ($p < 0.0001$, Fig 3.5C).

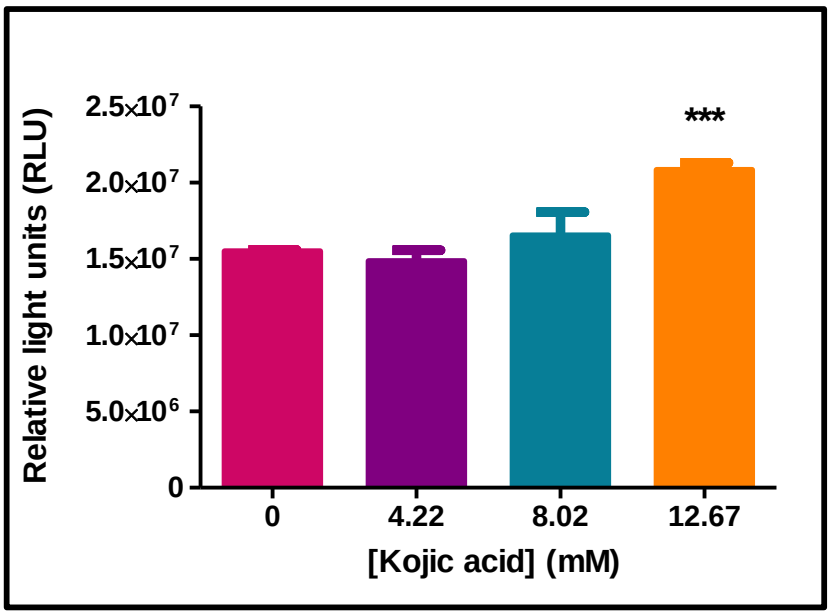

Figure 3.4 Intracellular ATP levels in HepG2 cells for 24h (*p<0.0001) (n = 3)**

A

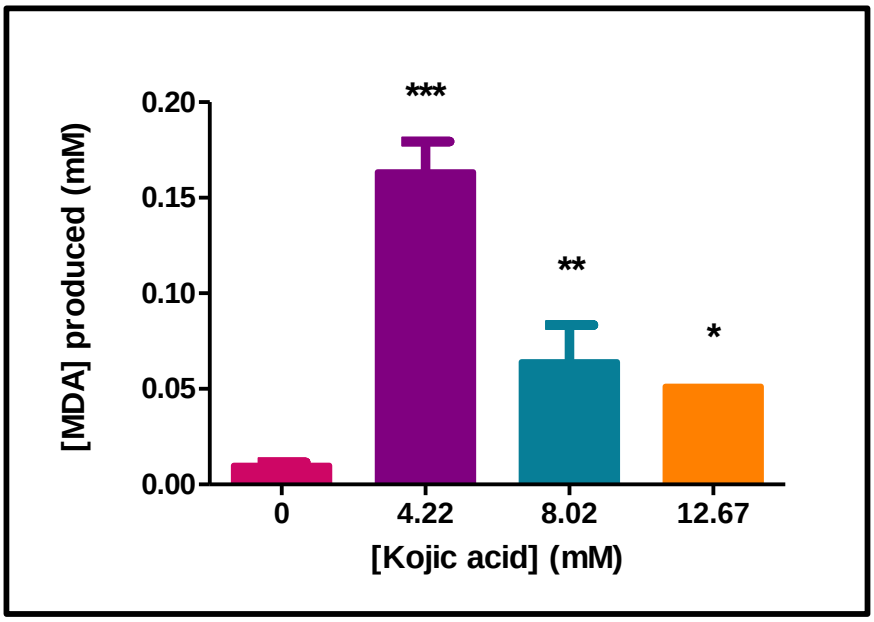

B

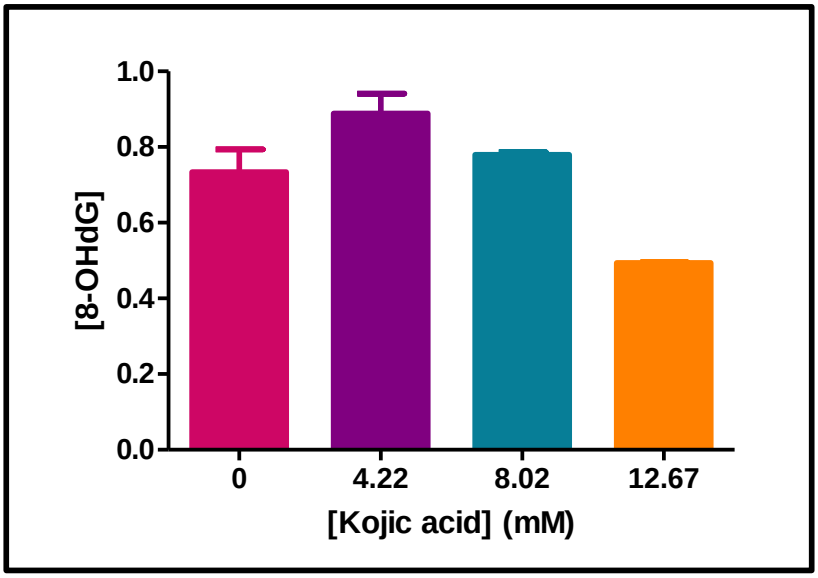

C

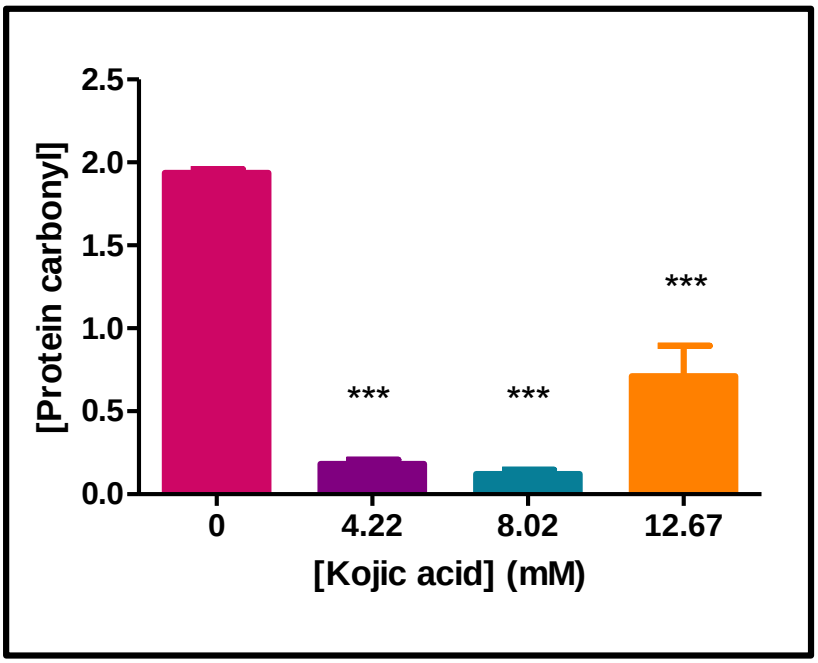

Figure 3.5 The effect of KA on cellular oxidation in HepG2 cells. KA increased (A) extracellular MDA concentration, and decreased (B) 8-OHdG and (C) Protein carbonyl concentrations after 24 h treatment (*p<0.05, **p<0.001, ***p<0.0001) (n = 3)

3.4. Antioxidant responses

Antioxidant response factors, Nrf 2 and p-Nrf 2 were downregulated significantly by KA (12.67 mM). At concentrations of 4.22 and 8.02 mM KA, Nrf 2 (p = 0.0002, Fig 3.6A) and p-Nrf2 (p < 0.0001, Fig 3.6B) expression was increased by KA in response to oxidative stress.

CAT, which aids in detoxification of peroxides, was downregulated following KA treatment (p = 0.0002, Fig 3.6C). The expression of *GPx* was investigated using qPCR to validate the occurrence of oxidative stress. *GPx* transcript levels were upregulated at 4.22 mM (1.51 fold) and 8.02 mM (1.07 fold); however, at 12.67 mM (1.02 fold), there was no change in expression relative to the control (Fig 3.6D).

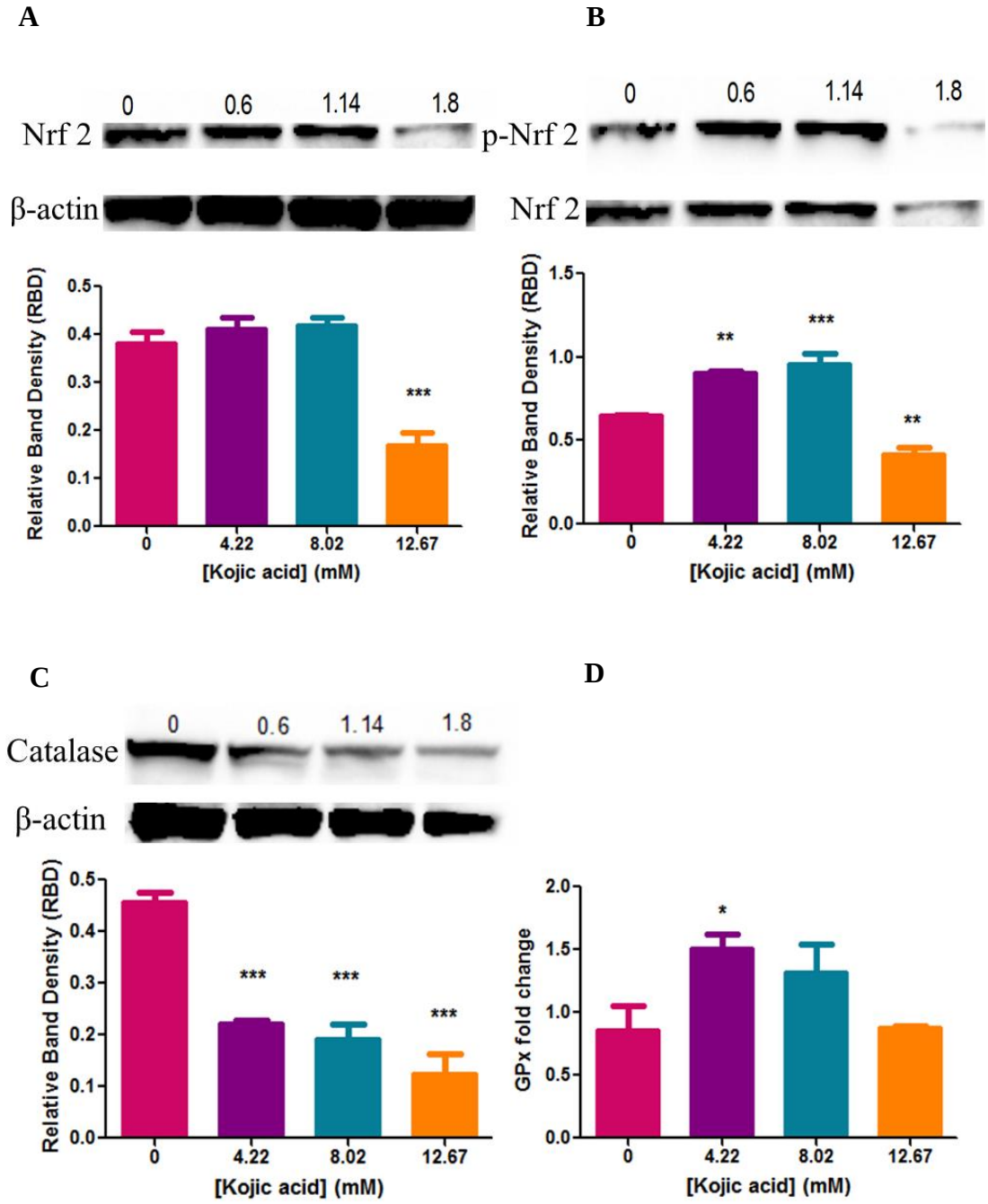

Figure 3.6 The effect of KA on antioxidant expression of total Nrf2 (A), p-Nrf2 (B), CAT (C), *GPx* mRNA in HepG2 cells (*p<0.05, **p<0.001, ***p<0.0001) (n = 3)

3.5. Immune response by MAPK proteins

JNK1/2 and p38 are stress-activated protein kinases (SAPK) and play a role in cell regulation, inflammation, and apoptosis. MAPK proteins were assessed using Western blot to determine the immune response to KA. The expression of JNK1/2 was downregulated by KA relative to the control (p < 0.0001, Fig 3.7A & B). The protein expression of p38 was significantly increased at concentrations 4.22 and 8.02 mM but remained unchanged at 12.67 mM (p = 0.0011, Fig 3.7C).

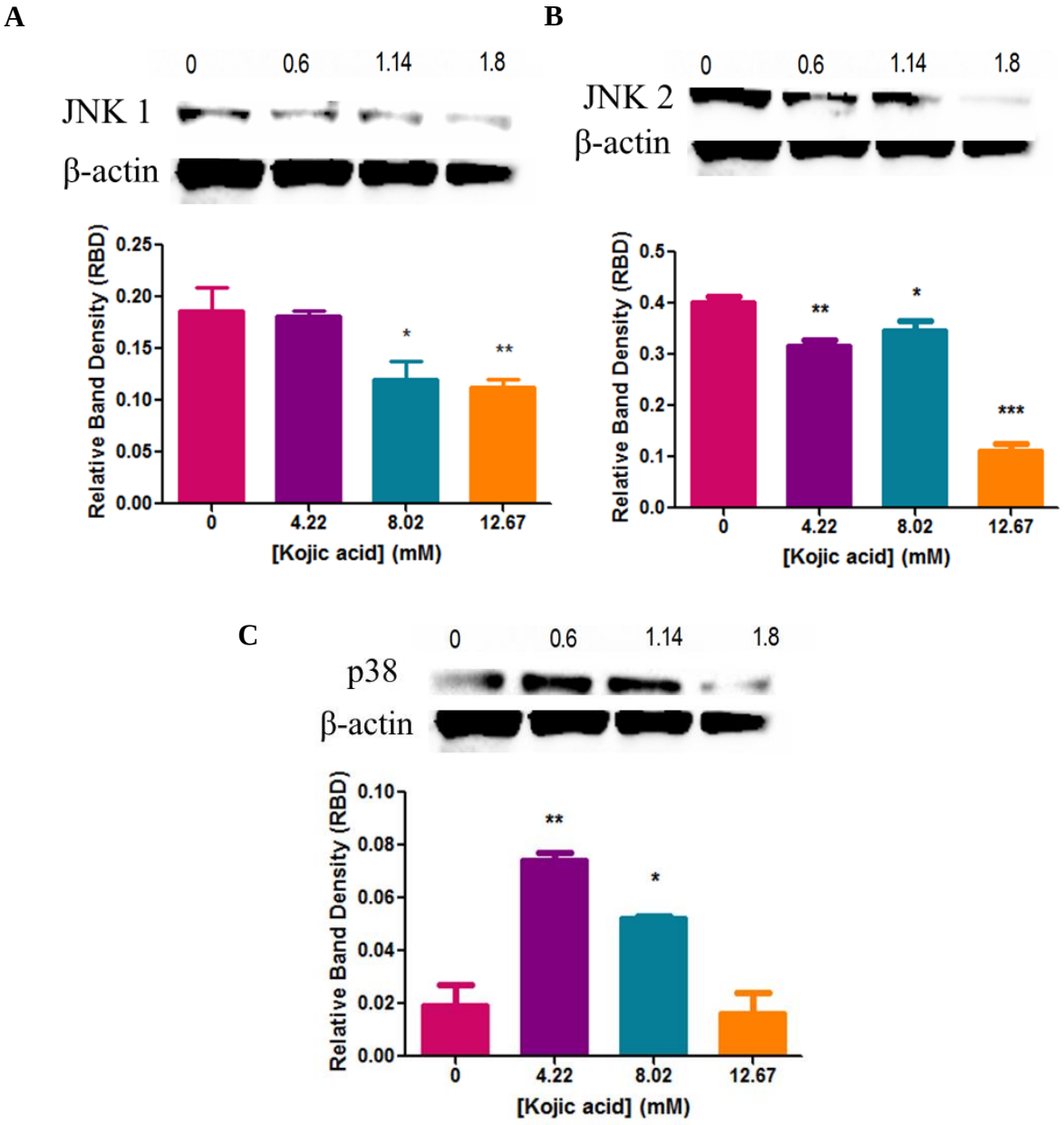

Figure 3.7 Immune response by MAPK proteins following KA-exposure (*p<0.05, **p<0.001, ***p<0.0001). A. JNK1, B. JNK2, C. p38 (n = 3)

3.6. Inflammatory response in HepG2 cells

In the presence of toxic insults, inflammatory markers play a key role in cell regulation. Sirt1 acts as an inhibitor of inflammation by decreasing NFκB and AP-1 expression. Phosphorylated - Sirt1 expression was significantly downregulated by KA relative to the control ($p < 0.0001$, Fig 3.8A). AP-1 expression was elevated by KA ($p = 0.0003$, Fig 3.8 B).

Decrease in p-Sirt1 expression resulted in the increase of total NFκB protein expression ($p < 0.0001$, Fig 3.8C). However, NFκB pathway was not activated reflected in a decrease in phosphorylated-NFκB expression. The decrease of activated NFκB was proportional to dose concentration ($p < 0.0001$, Fig 3.8D). qPCR was carried out to validate KA's anti-inflammatory potential. *NFκB* gene

expression was decreased at 4.22 mM (0.82 fold), 8.02 mM (0.24 fold); however, at 12.67 mM (1.02 fold) was unchanged relative to the control (Fig 3.9A). Notably, both protein and gene expression showed a significant decrease in *NFκB* expression at 8.02 mM. Similarly, *IκB* expression was decreased at 8.02mM. *IκB* expression was increased relative to the control at 4.22 and 12.67 mM ($p < 0.0001$, Fig 3.9B)

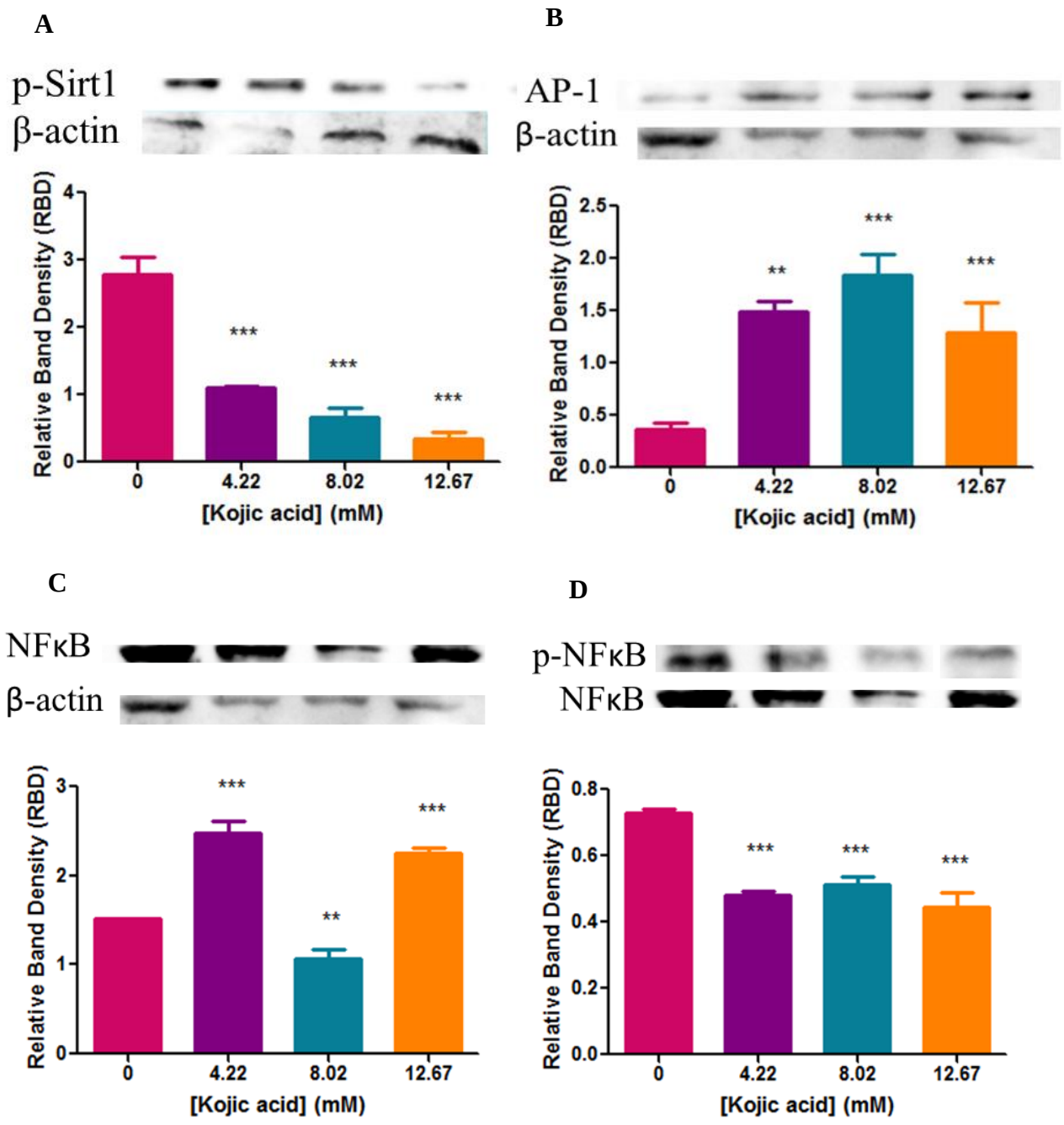

Figure 3.8 Protein expression of inflammatory markers, p-Sirt1 (A), AP-1 (B), NFκB (C) and p-NFκB (D) in HepG2 cells following KA treatment (p<0.001, ***p<0.0001) (n = 3)**

A

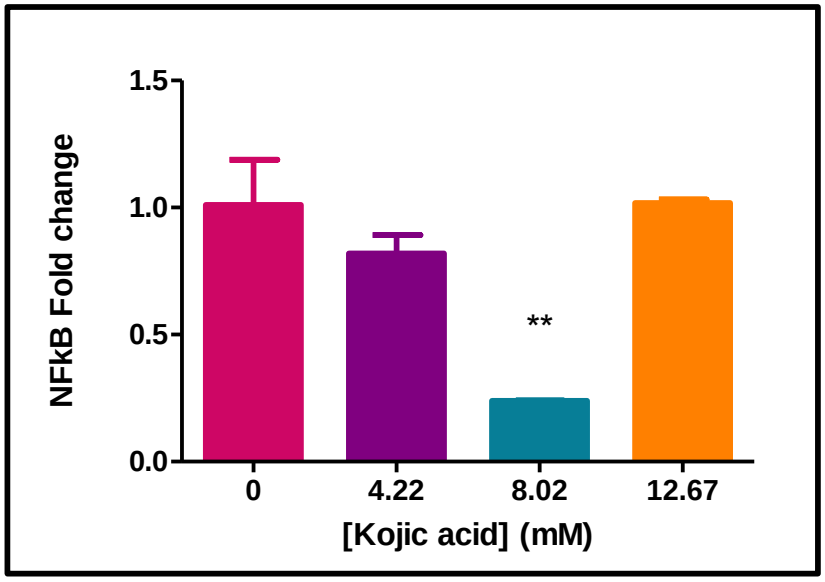

B

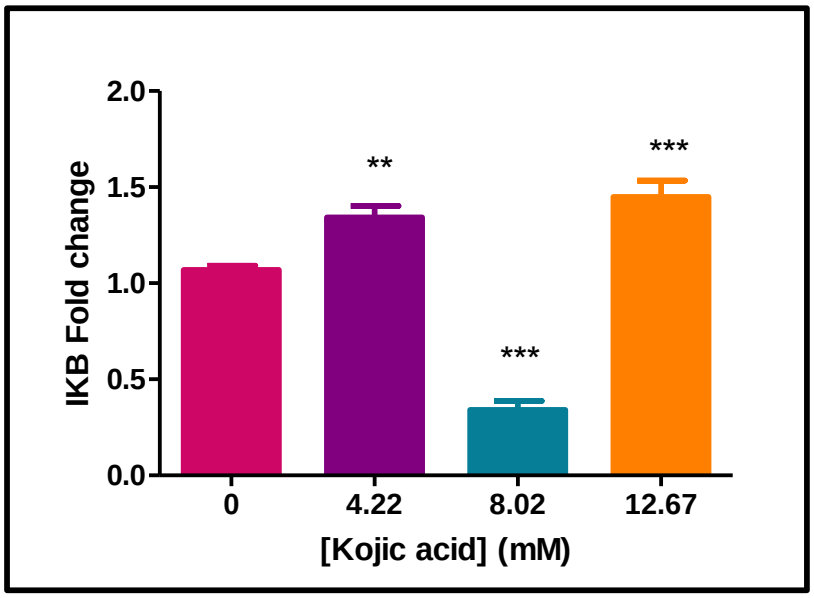

Figure 3.9 Gene expression of inflammatory markers *NFκB and IκB* in HepG2 cells following KA-treatment (p<0.001, ***p<0.0001) (n = 3)**

3.7. MiRNA expression involved in oxidative stress and immune response in HepG2 cells

Following treatment, the gene expression of *miRNA-29a* was upregulated significantly at 12.67 mM (p = 0.0002, Fig 3.10A). *MiRNA-29b* expression was increased following KA-treatment (p = 0.0009, Fig 3.10B). *MiRNA-155* was upregulated significantly at 4.22 mM (p = 0.0018, Fig 3.10C).

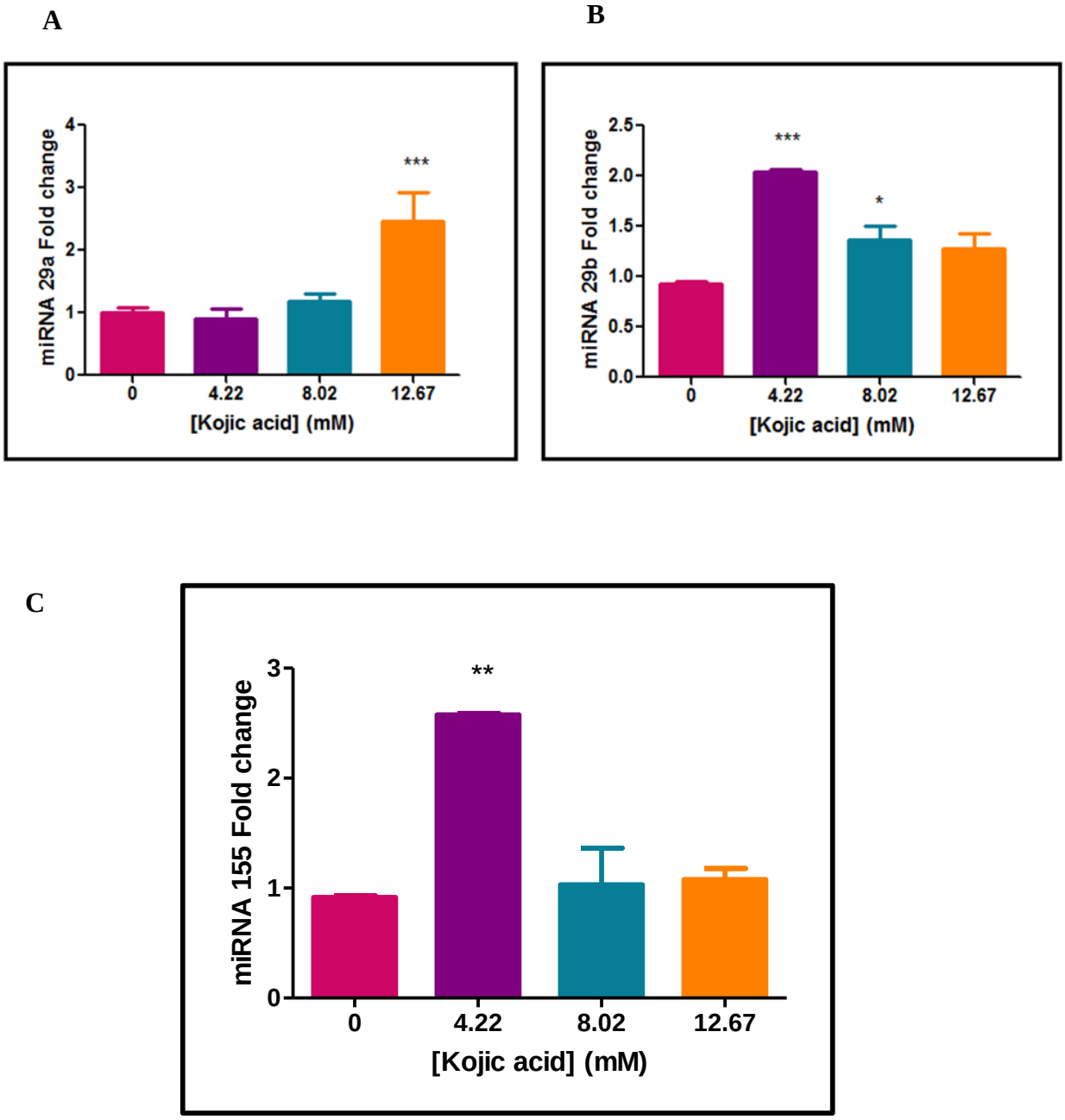

Figure 3.10 MiRNA expression in HepG2 cells following KA-treatment (*p<0.05, **p<0.001, ***p<0.0001) (n = 3)

CHAPTER 4

DISCUSSION

KA is found in a many food and beauty products. According to the U.S. Food and Drug Administration (FDA), *A. oryzae* (koji) is classified as generally regarded as safe (GRAS), although the nutritional benefit has not been thoroughly studied (Hamajima et al., 2016). In terms of skin-lightening purposes, the FDA has not approved KA for use in pharmaceutical products (Belsito et al., 2009). Studies pertaining to the toxicity of KA in the human liver are limited. The applications of KA in skin lightening have drawn attention to its toxicity on skin cells in humans and animals (Kim et al., 2003, Lajis et al., 2012). KA is ingested in fermented food products, and therefore organs involved in the metabolism and excretion of toxins need to be further studied. The present study evaluated the effect of KA in key biochemical processes on HepG2 cells.

Cell viability assays were carried out to determine the effect of KA on human liver cells. KA decreased cell viability in a dose-dependent manner, more significantly at high doses (12.67 mM) (Fig 3.1A & B). The MTT assay did not show a significant decrease in cell viability; however, significant cell death was observed in the Crystal Violet assay. The result suggests no significant mitochondrial dysregulation (MTT assay) due to KA treatment, with the exception of 12.67 mM. Weak acids, such as KA, are known to inhibit growth by lowering the cellular pH. In the cytoplasm, the un-dissociated acid molecules pass through the plasma membrane by diffusion, depending on the molecule's lipophilicity. The acids dissociate into charged anions and protons. Some acids cannot pass through the plasma membrane and accumulate in the cytoplasm. The cytoplasm's acidification inhibits processes such as metabolism, leading to a decrease in cell viability (Stratford and Anslow, 1998, Kundukad et al., 2020).

To confirm cell death, apoptosis activating caspases -9, -8, and 3/7 and LDH leakage/membrane integrity were assessed. Positive results for apoptosis initiation were reflected by an upregulation of caspase-8, -9, and -3/7 (Fig 3.2). In agreement with previous studies, KA-induced apoptosis in HeLa cells in response to oxidative stress stimulated by copper-induced apoptotic agents (Chen et al., 2013). KA derivatives have copper-chelating properties that initiate apoptosis in HepG2 cells (Oncul et al., 2019). However, in the present study, KA itself has shown increased caspase -3/7, -8, and -9 activity at lower concentrations (4.22 and 8.02 mM), leading to cell apoptosis. It was also observed that there was a significant decrease in LDH levels suggesting no leakage and damage to cellular membranes (Fig 3.3). Interestingly at 12.67 mM, caspase -8 and -9 and executioner caspase -3/7 was not activated. However, LDH levels were increased, suggesting a decrease in cell viability due to the high concentration of KA damaging to the cellular membrane leading to necrosis.

Cellular metabolism efficiency is reliant on the supply of ATP that is produced in the mitochondria. The mitochondria are organelles responsible for the generation of ATP via the OxPHOS (Zhang et al., 2018). A high density of mitochondria is essential for the high metabolic activity of the liver. A decline in cell viability suggests possible dysregulation on the mitochondrial level. The majority of ROS production occurs during mitochondrial respiration, making the mitochondria susceptible to damage (Ott et al., 2007). KA significantly increased ATP production (Fig 3.4). "Stress signals" are interpreted by the increase of ATP that mediates for downstream signalling. KA is known to increase ATP in the case of injury in *Hypsizygus marmoreus* (Zhang et al., 2017). Necrosis is an ATP-independent mode of cell death however, cancer cells have the ability to utilise LDH to aerobically metabolise ATP. This could account for the increase of ATP at 12.67 KA. To date, there has been no study evaluating the change in ATP levels following exposure to KA treatment in human cells.

KA increased MDA production in HepG2 cells, indicative of the occurrence of oxidative stress (Fig 3.5A). KA elevated MDA levels significantly in the liver of iron-loaded Wistar rats and did not show any protective effect attributed to KA's chelating ability (Kotyzova et al., 2004). The alteration in pH results in enzyme activity changes, reaction rates, protein stability, and nucleic acid structure (Kundukad et al., 2020).

Due to KA's weak acid properties, protein and DNA damage was assessed. DNA plays an important role in information transfer; hence mutations can lead to pathologies such as cancer (Yin et al., 1995). An analysis on the most common DNA lesion, 8-OHdG was investigated. The data suggests a slight increase in the concentration of oxidative lesions; however, the result was statistically insignificant (Fig 3.5B). Genotoxic studies *in vivo* found that 8-OHdG oxidative adducts were not significantly increased in the thyroid of rats. The liver, colon, and stomach were further analysed to confirm the result and found no significant increase in the concentration of oxidative lesions *in vivo* correlating with the *in vitro* results obtained (Higa et al., 2007, Tamura et al., 2006). Studies into KA concerning its ability to form tumours in *in vivo* and *in vitro* models have displayed conflicting results. However, an attribute of KA highlighted by research is its anti-carcinogenic properties. DNA lesions have been found to be a factor leading to carcinogenesis. The highest treatment concentration decreased 8-OHdG levels relative to the control, correlating with this deduction. Protein carbonyl concentrations were investigated to determine KA's ability to oxidise proteins. A significant decrease in protein carbonyls (Fig 3.5C) relative to the control was observed. KA did not exert toxic effects on DNA and protein.

Mammalian cells have defence mechanisms to ensure homeostasis of the intracellular environment by scavenging ROS (Basak et al., 2017). The production of ROS initiates the activation of regulatory proteins to minimise cellular damage. Nrf2 is responsible for cellular defence mechanisms by the

induction of the phase 2 responses. This process is dependent on the dissociation of KEAP-1, a repressor that contains zinc bound to reactive cysteine thiols and facilitates the detection of ROS and electrophiles. The phosphorylation of Nrf2 (p-Nrf2) leads to an increase in stability and activity (Nguyen et al., 2009). KA has the potential to target the zinc found between Nrf2 and KEAP-1, hence facilitating the release of Nrf2. Results showed an increase in Nrf2 and p-Nrf2 expression (Fig 3.6A & B), suggesting KA chelation properties may play a role in the release of Nrf2 from KEAP-1. Nrf2 is a mediator of the anti-apoptotic protein Bcl 2 in stress-induced apoptosis. The increased in p-Nrf2 expression by KA may have occurred due to persistent oxidative stress. However, the increase in Nrf2 expression could have been insufficient due to apoptotic proteins being initiated, resulting in the release of cytochrome c into the cytosol and encouraging apoptosome formation.

Nrf2 is a transcription factor that activates ARE, a protein found in antioxidants such as CAT and SOD_2 (Nguyen et al., 2009). The cell's defence is the neutralisation of free radicals by reducing peroxides to water and oxygen facilitated by antioxidant enzymes, namely, CAT and SOD_2 (Basak et al., 2017, Zhang et al., 2017). The protein expression of CAT was downregulated following treatment with KA, but more significantly at 12.67 mM. The amount of MDA-TBA adducts produced correlates with the hindrance of cellular antioxidant response and lipid peroxidation (Fig 3.6C). This is in agreement with previous studies in which KA deactivated regulatory proteins, CAT, in the liver and kidney of rats (Kotyzova et al., 2004). *GPx* functions in reducing peroxides and oxidises glutathione to glutathione disulphide. Gene expression of *GPx* revealed an increase at KA concentrations with high MDA levels (4.22 and 8.02 mM) (Fig 3.6D).

Cells respond to stimuli by the activation of the MAPK signalling pathway in order to facilitate for an antioxidant response, inflammation, cell survival, and cell death (Cuenda and Rousseau, 2007, Shaulian and Karin, 2002, Weston and Davis, 2002, Kammeyer and Luiten, 2015). KA's role in the inhibition of tyrosinase activity by copper's chelation draws attention to the MAPK kinase proteins. The expression of MAPK proteins that mediates for cellular regulation, namely JNK1/2 and p38, were investigated to elucidate the cell's response to KA toxicity. The MAPK p38 and JNK1/2 proteins play a role in apoptosis, inflammation, and cytokine production (Morrison, 2012). JNK1/2 molecules are activated by DNA damage and oxidative stress (Sun et al., 2009). Additionally, JNK regulates the anti-apoptotic protein, Bcl-2 (Dhanasekaran and Reddy, 2008). The relationship is in agreement with the present study results as shown by the decrease of JNK1/2 ineffectively inhibiting Bcl-2 hence encouraging apoptosis (Fig 3.7A & B). p38 is a stress-activated protein kinase initiated by upstream MAPK signalling. KA was found to upregulate MAPK expression in HeLa cells (Chen et al., 2013), which is in agreement with the results obtained for p38 in HepG2 cells (Fig 3.7C). Prolonged activation of this pathway can lead to cell death due to the presence of ROS (Redza-Dutordoir and Averill-Bates, 2016, Ott et al., 2007). Stress signal detection is carried out by JNK1/2 and p38, which

initiate cell death activation and decrease cell proliferation (Ayala et al., 2014). This suggests the involvement of the MAPK pathway in response to ROS following KA treatment in HepG2 cells.

Inflammation has been implicated in the initiation and progression of diseases. Key biomarkers involved in the NFκB pathway were evaluated to determine the effect of KA-treatment on inflammation in HepG2 cells (Fig. 3.8 & 3.9). Sirt1 possesses protective properties against oxidative stress by inhibiting NFκB and AP-1 expression (Becatti et al., 2018, Xie et al., 2013a). The expression of phosphorylated-Sirt1 was downregulated by KA (Fig 3.8A). AP-1 is made up of several proteins, namely Fos, Jun, Maf, and ATF. Sirt-1 decreases c-fos/c-Jun acetylation resulting in decreased transcription of AP-1. Therefore decreased Sirt-1 expression will cause an increase in AP-1 and NFκB expression. The study found an increase in AP-1 expression (Fig 3.8B). AP-1 plays a role in COX-2 inflammatory responses (Xie et al., 2013a). Total NFκB expression was increased following KA-treatment with the exception of 8.02 mM; however, phosphorylated-NFκB expression was decreased (Fig 3.8C & D). Despite the increase in NFκB expression, activation of NFκB and transcription of inflammatory genes was decreased by KA. The results correlate with KA anti-inflammatory properties illustrated in *in vitro* studies in other cell lines (Moon et al., 2001, Ahn et al., 2003). Similarly, gene expression of NFκB was decreased at 8.02 mM (Fig 3.9A). Gene expression of IκB was increased with the exception of 8.02 mM (Fig 3.9B). Due to the trend observed, the results suggest a potent inhibition of the inflammation pathway NFκB by KA at 8.02 mM.

MicroRNA (miRNA) is a class of post-transcriptional repressors of gene expression (Reinhart et al., 2000). KA significantly increased miRNA-29a expression at the 12.67 mM concentration. At 12.67mM KA apoptosis and inflammation did not occur (Fig 3.10A). The result is in agreement with literature which states miRNA-29a exerts anti-apoptotic effects on cells and downregulates NFκB expression in miRNA-29a transgenic mice.

MiRNA-29b dysregulation plays a role in fibrosis pathogenesis in C57BL/6 mice (Su et al., 2019). Moreover, miRNA-29b regulates oxidative stress, decreases cell viability, and increased apoptosis (Hou et al., 2017, Engedal et al., 2018). MiRNA-29b was shown to negatively regulate Sirt1 in ovarian cancer cells (Hou et al., 2017). MiRNA-29b has pro-apoptotic properties. The miRNA-29b expression was increased at concentrations shown to undergo apoptosis (Fig 3.10B).

The miRNA control of oxidative stress and apoptosis was assessed by analysing miRNA-155 expression in treated HepG2 cells. MiRNA-155 suppresses antioxidant response by SOD_2 and CAT, promoting ROS generation. Regulation of miRNA-155 expression was found to be carried out by NFκB and MAPK signalling (Wang et al., 2015). However, NFκB is also a target of miRNA-155 by controlling IKKβ and IKKε expression (Ma et al., 2011). This results in the repression of NFκB activation which is consistent with the increased miRNA-155 expression and decreased NFκB expression. MiRNA-155 also stimulated cell proliferation in pancreatic cancer cells (T-rex and K-ras

cells) by the inhibition of FOXO3a (Wang et al., 2015). Hence KA upregulated miRNA-155 expression at 4.22 mM; however, at higher concentrations, no significant changes were observed (Fig 3.10C). Notably, the most significant elevation in MDA levels and miRNA-155 occurred at 4.22 mM correlating the oxidative stress results with miRNA expression.

CHAPTER 5

CONCLUSION

From the data obtained, it can be determined that KA has cytotoxic potential in HepG2 cells. Studies show that KA at very low concentrations acts as an antioxidant (Saeedi et al., 2019). The concentrations found to cause oxidative stress was much higher than the KA content in cosmetics. HepG2 cells were susceptible to KA toxicity by inducing oxidative stress. The study found no significant DNA and protein damage at treated concentrations. On the contrary, KA has shown potential hepatic protective properties. MAPK proteins activate inflammatory pathways in the presence of oxidative stress. KA elevated stress-activated protein kinase p38 and decreased inflammatory biomarkers.

The evaluation of cosmetic products was found to contain KA concentrations between 1-2%. The European Commission's Scientific Committee on Scientific Products (SCCP) determined a maximum allowed concentration of 1% in skincare products due to health concerns reflected in published work on the effect of thyroid and skin sensitisation (SCCP, 2008). KA use as a food preservative in seafood was found to have an approximate concentration of 0.25%-0.6% KA.

In terms of ingestion, KA is a fermentation by-product in food and is found in small quantities. Previous research has found the LD_{50} dose in mammals to be 1g/kg (Brtko et al., 2004). The absorption and distribution of KA were found to be negligible from dermal penetration. Therefore metabolism of KA will significantly lower the distributed concentration of KA.

In conclusion, the study illustrated that although oxidative stress and apoptosis was elevated, the effect on liver health in terms of DNA damage, protein oxidation and inflammation was minimal. Notably, the concentrations of the KA used to exert such effects were much larger than the average use and require further research through dermal and oral exposures.

CHAPTER 6

LIMITATIONS OF THE STUDY

KA's use in the beauty industry suggests varying exposure periods. The present study investigated cell viability due to KA exposures for 6h, 24h, and 48h. The study was carried out on an immortalised cell line *in vitro*; therefore, future studies need to be carried in an *in vivo* model to validate the *in vitro* study results.

KA has weak acid properties that have a potential mitochondrial effect. HepG2 cell lines are a cancer cell line that minimizes dependence on the mitochondria; therefore, the mitochondrial output cannot conclusively be deduced until further studies are carried out.

REFERENCES

ABDUL, N. S., NAGIAH, S. & CHUTURGOON, A. A. 2016. Fusaric acid induces mitochondrial stress in human hepatocellular. *Toxicon,* 119 336-344.

ABOU SEIF, H. S. 2016. Physiological changes due to hepatotoxicity and the protective role of some medicinal plants. *Beni-Suef University Journal of Basic and Applied Sciences,* 5**,** 134-146.

AHN, K. S., MOON, K. Y., LEE, J. & KIM, Y. S. 2003. Downregulation of NF-kappaB activation in human keratinocytes by melanogenic inhibitors. *Journal of Dermatological Science,* 31**,** 193-201.

ALCENDOR, R. R., GAO, S., ZHAI, P., ZABLOCKI, D., HOLLE, E., YU, X., TIAN, B., WAGNER, T., VATNER, S. F. & SADOSHIMA, J. 2007. Sirt1 Regulates Aging and Resistance to Oxidative Stress in the Heart. *Circulation Research,* 100**,** 1512-1521.

AYALA, A., MUNOZ, M. F. & ARGUELLES, S. 2014. Lipid peroxidation: production, metabolism, and signaling mechanisms of malondialdehyde and 4-hydroxy-2-nonenal. *Oxidative Medicine and Cellular Longevity,* 2014**,** 1-31.

AZAMI, F., TAZIKEH-LEMESKI, E. & MAHMOOD-JANLOU, M.-A. 2017. Kojic Acid Effect on the Inhibitory Potency of Tyrosinase. *Journal of Chemical Health Risks,* 7**,** 147-155.

BANDYOPADHYAY, D. 2009. Topical treatment of melasma. *Indian journal of dermatology,* 54**,** 303-309.

BASAK, P., SADHUKHAN, P., SARKAR, P. & SIL, P. C. 2017. Perspectives of the Nrf-2 signaling pathway in cancer progression and therapy. *Toxicology Reports,* 4**,** 306-318.

BASS, J. J., WILKINSON, D. J., RANKIN, D., PHILLIPS, B. E., SZEWCZYK, N. J., SMITH, K. & ATHERTON, P. J. 2017. An overview of technical considerations for Western blotting applications to physiological research. *Scandanavian Journal of Medicine and Science in Sports,* 27**,** 4-25.

BEARD, R. L. & WALTON, G. S. 1969. Kojic acid as an insecticidal mycotoxin. *Journal of Invertebrate Pathology,* 14**,** 53-59.

BECATTI, M., BARYGINA, V., MANNUCCI, A., EMMI, G., PRISCO, D., LOTTI, T., FIORILLO, C. & TADDEI, N. 2018. Sirt1 Protects against Oxidative Stress-Induced Apoptosis in Fibroblasts from Psoriatic Patients: A New Insight into the Pathogenetic Mechanisms of Psoriasis. *International Journal of Molecular Sciences,* 19**,** 1572.

BEELIK, A. 1956. Kojic acid. *Adv Carbohydr Chem,* 48**,** 145-83.

BELSITO, D. V., HILL, R. A., KLAASSEN, C. D. & LIEBLER, D. C. TENTATIVE SAFETY ASSESSMENT Kojic Acid as Used in Cosmetics 2009. 1-68.

BENTLEY, R. 2006. From miso, saké and shoyu to cosmetics: a century of science for kojic acid. *Natural Products Reports,* 23**,** 1046-62.

BRENNER, M. & HEARING, V. J. 2008. The protective role of melanin against UV damage in human skin. *Photochemistry and photobiology,* 84**,** 539-549.

BRTKO, J., RONDAHL, L., FICKOVÁ, M., HUDECOVÁ, D., EYBL, V. & UHER, M. 2004. Kojic acid and its derivatives: history and present state of art. *Central European Journal of Public Health,* 12 Suppl**,** S16-8.

BURDOCK, G. A., SONI, M. G. & CARABIN, I. G. 2001. Evaluation of health aspects of kojic acid in food. *Regulatory Toxicology and Pharmacology,* 33**,** 80-101.

BURNETT, C. L., BERGFELD, W. F., BELSITO, D. V., HILL, R. A., KLAASSEN, C. D., LIEBLER, D. C., MARKS, J. G., SHANK, R. C., SLAGA, T. J., SNYDER, P. W. & ANDERSEN, F. A. 2010. Final Report of the Safety Assessment of Kojic Acid as Used in Cosmetics. *International Journal of Toxicology,* 29**,** 244S-273S.

CARÈ, A., CATALUCCI, D., FELICETTI, F., BONCI, D., ADDARIO, A., GALLO, P., BANG, M. L., SEGNALINI, P., GU, Y., DALTON, N. D., ELIA, L., LATRONICO, M. V., HØYDAL, M., AUTORE, C., RUSSO, M. A., DORN, G. W., 2ND, ELLINGSEN, O., RUIZ-LOZANO, P., PETERSON, K. L., CROCE, C. M., PESCHLE, C. & CONDORELLI, G. 2007. MicroRNA-133 controls cardiac hypertrophy. *Nature Medicine,* 13**,** 613-8.

CASAS-GRAJALES, S. & MURIEL, P. 2015. Antioxidants in liver health. *World Journal of Gastrointestinal Pharmacology and Therapeutics,* 6**,** 59-72.

CELI, P. & GABAI, G. 2015. Oxidant/Antioxidant Balance in Animal Nutrition and Health: The Role of Protein Oxidation. *Frontiers in Veterinary Science,* 2**,** 1-13.

CHAN, F. K.-M., MORIWAKI, K. & DE ROSA, M. J. 2013. Detection of necrosis by release of lactate dehydrogenase activity. *Methods in Molecular Biology (Clifton, N.J.),* 979**,** 65-70.

CHANG, T.-S. 2009. An updated review of tyrosinase inhibitors. *International journal of molecular sciences,* 10**,** 2440-2475.

CHEN, J., ZHANG, Z. & CAI, L. 2014. Diabetic cardiomyopathy and its prevention by nrf2: current status. *Diabetes & Metabolism Journal,* 38**,** 337-345.

CHEN, J. S., WEI, C. I. & MARSHALL, M. R. 1991. Inhibition mechanism of kojic acid on polyphenol oxidase. *Journal of Agricultural and Food Chemistry,* 39**,** 1897-1901.

CHEN, L., DENG, H., CUI, H., FANG, J., ZUO, Z., DENG, J., LI, Y., WANG, X. & ZHAO, L. 2017. Inflammatory responses and inflammation-associated diseases in organs. *Oncotarget,* 9**,** 7204-7218.

CHEN, Y.-H., LU, P.-J., HULME, C. & SHAW, A. Y. 2013. Synthesis of kojic acid-derived copper-chelating apoptosis inducing agents. *Medicinal Chemistry Research,* 22**,** 995-1003.

CHOI, H., KIM, K., HAN, J., CHOI, H., JIN, S. H., LEE, E. K., SHIN, D. W., LEE, T. R., LEE, A.-Y. & NOH, M. 2012. Kojic acid-induced IL-6 production in human keratinocytes plays a role in its anti-melanogenic activity in skin. *Journal of Dermatological Science,* 66**,** 207-215.

CHOUDHARY, D., SAHAY, G. & SINGH, J. 1992. Effect of some mycotoxins on reproduction in pregnant albino rats. *Journal of Food Science and Technology (Mysore),* 29**,** 264-265.

CHUTURGOON, A. A., PHULUKDAREE, A. & MOODLEY, D. 2014. Fumonisin B1 modulates expression of human cytochrome P450 1b1 in human hepatoma (Hepg2) cells by repressing Mir-27b. *Toxicology Letters,* 227**,** 50-55.

COHEN, G. M. 1997. Caspases: the executioners of apoptosis. *Biochemical Journal,* 326 (Pt 1)**,** 1-16.

COOKE, M. S., EVANS, M. D., DIZDAROGLU, M. & LUNEC, J. 2003. Oxidative DNA damage: mechanisms, mutation, and disease. *The FASEB Journal,* 17**,** 1195-1214.

COUPLAND, K. & NIEHAUS, W. G. 1987a. Effect of nitrogen supply, Zn2+, and salt concentration on kojic acid and versicolorin biosynthesis by *Aspergillus parasiticus*. *Experimental Mycology,* 11**,** 206-213.

COUPLAND, K. & NIEHAUS, W. G. 1987b. Effect of nitrogen supply, Zn2+, and salt concentration on kojic acid and versicolorin biosynthesis byAspergillus parasiticus. *Experimental Mycology,* 11**,** 206-213.

CRUZAT, V., MACEDO ROGERO, M., NOEL KEANE, K., CURI, R. & NEWSHOLME, P. 2018. Glutamine: Metabolism and Immune Function, Supplementation and Clinical Translation. *Nutrients,* 10**,** 1564.

CUENDA, A. & ROUSSEAU, S. 2007. p38 MAP-Kinases pathway regulation, function and role in human diseases. *Biochimica et Biophysica Acta (BBA) - Molecular Cell Research,* 1773**,** 1358-1375.

DALLE-DONNE, I., ROSSI, R., GIUSTARINI, D., MILZANI, A. & COLOMBO, R. 2003. Protein carbonyl groups as biomarkers of oxidative stress. *Clinica Chimica Acta,* 329**,** 23-38.

DEBACQ-CHAINIAUX, F., BOILAN, E., LE MOUTIER, J. D., WEEMAELS, G. & TOUSSAINT, O. 2010. p38MAPK in the Senescence of Human and Murine Fibroblasts. 694.

DEHN, P. F., WHITE, C. M., CONNERS, D. E., SHIPKEY, G. & CUMBO, T. A. 2004. Characterization of the Human Hepatocellular Carcinoma (HEPG2) Cell Line as an in vitro Model for Cadmium Toxicity Studies. *In Vitro Cellular & Developmental Biology. Animal,* 40**,** 172-182.

DERI, B., KANTEEV, M., GOLDFEDER, M., LECINA, D., GUALLAR, V., ADIR, N. & FISHMAN, A. 2016. The unravelling of the complex pattern of tyrosinase inhibition. *Scientific reports,* 6**,** 1-10.

DHANASEKARAN, D. N. & REDDY, E. P. 2008. JNK signaling in apoptosis. *Oncogene,* 27**,** 6245-6251.

DONATO, M. T., TOLOSA, L. & GÓMEZ-LECHÓN, M. J. 2015a. Culture and Functional Characterization of Human Hepatoma HepG2 Cells. *Methods Mol Biol,* 1250**,** 77-93.

DONATO, M. T., TOLOSA, L. & GÓMEZ-LECHÓN, M. J. 2015b. Culture and Functional Characterization of Human Hepatoma HepG2 Cells. *Methods of Molecular Biology,* 1250**,** 77-93.

EL-ASHRAM, S., AL NASR, I. & SUO, X. 2016. Nucleic acid protocols: Extraction and optimization. *Biotechnology reports (Amsterdam, Netherlands)*, 12**,** 33-39.

EL-KADY, I. A., ZOHRI, A. N. A. & HAMED, S. R. 2014. Kojic acid production from agro-industrial by-products using fungi. *Biotechnology Research International*, 2014**,** 1-10.

ELMORE, S. 2007. Apoptosis: a review of programmed cell death. *Toxicologic pathology*, 35**,** 495-516.

ENGEDAL, N., ŽEROVNIK, E., RUDOV, A., GALLI, F., OLIVIERI, F., PROCOPIO, A. D., RIPPO, M. R., MONSURRÒ, V., BETTI, M. & ALBERTINI, M. C. 2018. From Oxidative Stress Damage to Pathways, Networks, and Autophagy via MicroRNAs. *Oxidative Medicine and Cellular Longevity*, 2018**,** 4968321.

ESLAMI, A. & LUJAN, J. 2010. Western blotting: sample preparation to detection. *Journal of visualized experiments : JoVE***,** 2359.

FEOKTISTOVA, M., GESERICK, P. & LEVERKUS, M. 2016. Crystal Violet Assay for Determining Viability of Cultured Cells. *Cold Spring Harbor Protocol*, 2016**,** 343-346.

FINDLAY, G. H., MORRISON, J. G. & SIMSON, I. W. 1975. Exogenous ochronosis and pigmented colloid milium from hydroquinone bleaching creams. *British Journal of Dermatology*, 93**,** 613-22.

FISHER, G. J. A. & VOORHEES, J. J. 1998. Molecular Mechanisms of Photo aging and its Prevention by Retinoic Acid: Ultraviolet Irradiation Induces MAP Kinase Signal Transduction Cascades that Induce Ap-l-Regulated Matrix Metalloproteinases that Degrade Human Skin In Vivo. *ID SYMPOSIUM PROCEEDINGS*, 3**,** 61-68.

FUJIMOTO, N., ONODERA, H., MITSUMORI, K., TAMURA, T., MARUYAMA, S. & ITO, A. 1999. Changes in thyroid function during development of thyroid hyperplasia induced by kojic acid in F344 rats. *Carcinogenesis*, 20**,** 1567-71.

GALLUZZI, L., VITALE, I., AARONSON, S. A., ABRAMS, J. M., ADAM, D., AGOSTINIS, P., ALNEMRI, E. S., ALTUCCI, L., AMELIO, I., ANDREWS, D. W., ANNICCHIARICO-PETRUZZELLI, M., ANTONOV, A. V., ARAMA, E., BAEHRECKE, E. H., BARLEV, N. A., BAZAN, N. G., BERNASSOLA, F., BERTRAND, M. J. M., BIANCHI, K., BLAGOSKLONNY, M. V., BLOMGREN, K., BORNER, C., BOYA, P., BRENNER, C., CAMPANELLA, M., CANDI, E., CARMONA-GUTIERREZ, D., CECCONI, F., CHAN, F. K. M., CHANDEL, N. S., CHENG, E. H., CHIPUK, J. E., CIDLOWSKI, J. A., CIECHANOVER, A., COHEN, G. M., CONRAD, M., CUBILLOS-RUIZ, J. R., CZABOTAR, P. E., D'ANGIOLELLA, V., DAWSON, T. M., DAWSON, V. L., DE LAURENZI, V., DE MARIA, R., DEBATIN, K.-M., DEBERARDINIS, R. J., DESHMUKH, M., DI DANIELE, N., DI VIRGILIO, F., DIXIT, V. M., DIXON, S. J., DUCKETT, C. S., DYNLACHT, B. D., EL-DEIRY, W. S., ELROD, J. W., FIMIA, G. M., FULDA, S., GARCÍA-SÁEZ, A. J., GARG, A. D., GARRIDO, C., GAVATHIOTIS, E., GOLSTEIN, P.,

GOTTLIEB, E., GREEN, D. R., GREENE, L. A., GRONEMEYER, H., GROSS, A., HAJNOCZKY, G., HARDWICK, J. M., HARRIS, I. S., HENGARTNER, M. O., HETZ, C., ICHIJO, H., JÄÄTTELÄ, M., JOSEPH, B., JOST, P. J., JUIN, P. P., KAISER, W. J., KARIN, M., KAUFMANN, T., KEPP, O., KIMCHI, A., KITSIS, R. N., KLIONSKY, D. J., KNIGHT, R. A., KUMAR, S., LEE, S. W., LEMASTERS, J. J., LEVINE, B., LINKERMANN, A., LIPTON, S. A., LOCKSHIN, R. A., LÓPEZ-OTÍN, C., LOWE, S. W., LUEDDE, T., LUGLI, E., MACFARLANE, M., MADEO, F., MALEWICZ, M., MALORNI, W., MANIC, G., et al. 2018. Molecular mechanisms of cell death: recommendations of the Nomenclature Committee on Cell Death 2018. *Cell Death & Differentiation,* 25**,** 486-541.

GAO, B., NING, S., LI, J., LIU, H., WEI, W., WU, F., TANG, Y., FENG, Y., LI, K. & ZHANG, L. 2015. Integrated analysis of differentially expressed mRNAs and miRNAs between hepatocellular carcinoma and their matched adjacent normal liver tissues. *Oncology Reports,* 34**,** 325-333.

GASCHLER, M. M. & STOCKWELL, B. R. 2017. Lipid peroxidation in cell death. *Biochemical and Biophysical Research Communications,* 482**,** 419-425.

GILLBRO, J. M. & OLSSON, M. J. 2011. The melanogenesis and mechanisms of skin-lightening agents – existing and new approaches. *International Journal of Cosmetic Science,* 33**,** 210-221.

GIROIR, L. E., HUFF, W. E., KUBENA, L. E., HARVEY, R. B., ELISSALDE, M. H., WITZEL, D. A., YERSIN, A. G. & IVIE, G. W. 1991. Toxic Effects of Kojic Acid in the Diet of Male Broilers1. *Poultry Science,* 70**,** 499-503.

GSTRAUNTHALER, G., LINDL, T. & VAN DER VALK, J. 2013. A plea to reduce or replace fetal bovine serum in cell culture media. *Cytotechnology,* 65**,** 791-793.

HAMAJIMA, H., MATSUNAGA, H., FUJIKAWA, A., SATO, T., MITSUTAKE, S., YANAGITA, T., NAGAO, K., NAKAYAMA, J. & KITAGAKI, H. 2016. Japanese traditional dietary fungus koji Aspergillus oryzae functions as a prebiotic for Blautia coccoides through glycosylceramide: Japanese dietary fungus koji is a new prebiotic. *Springerplus,* 5**,** 1-10.

HANAHAN, D. & WEINBERG, R. A. 2000. The hallmarks of cancer. *Cell,* 100**,** 57-70.

HENGARTNER, M. O. 2000. The biochemistry of apoptosis. *Nature,* 407**,** 770-776.

HIGA, Y., KAWABE, M., NABAE, K., TODA, Y., KITAMOTO, S., HARA, T., TANAKA, N., KARIYA, K. & TAKAHASHI, M. 2007. Kojic acid -absence of tumor-initiating activity in rat liver, and of carcinogenic and photo-genotoxic potential in mouse skin. *The Journal of Toxicological Sciences,* 32**,** 143-59.

HIGA, Y., OHKUBO, A., KITAJIMA, S., HATORI, A. & KARIYA, K. 2000. STUDIES ON THYROID FUNCTION IN RATS SUBJECTED TO REPEATED ORAL ADMINISTRATION WITH KOJIC ACID. *The Journal of Toxicological Sciences,* 25**,** 167-175.

HIRA, Y., OHYAMA, Y., KAIMI, K., MISHIMA, Y. & FURUKAWA, T. 1985. Inhibitory effect of kojic acid contained cream in UV-induced pigmentationin human skin. *Japanese Cosmetic Science Society,* 9**,** 109.

HODGKINSON, C. A., MOORE, K. J., NAKAYAMA, A., STEINGRÍMSSON, E., COPELAND, N. G., JENKINS, N. A. & ARNHEITER, H. 1993. Mutations at the mouse microphthalmia locus are associated with defects in a gene encoding a novel basic-helix-loop-helix-zipper protein. *Cell,* 74**,** 395-404.

HOU, M., ZUO, X., LI, C., ZHANG, Y. & TENG, Y. 2017. Mir-29b Regulates Oxidative Stress by Targeting SIRT1 in Ovarian Cancer Cells. *Cellular Physiology and Biochemistry,* 43**,** 1767-1776.

HUGHES, M. J., LINGREL, J. B., KRAKOWSKY, J. M. & ANDERSON, K. P. 1993. A helix-loop-helix transcription factor-like gene is located at the mi locus. *Journal of Biological Chemistry,* 268**,** 20687-90.

IARC KOJIC ACID. *IARC MONOGRAPHS,* 79**,** 607-618.

IMOSE, J., NONOMURA, S. & TATSUMI, C. 1970. Studies on Kojic Acid Metabolism by Microorganisms. *Agricultural and Biological Chemistry,* 34**,** 1443-1456.

ISHIKAWA, S., SASAKI, Y. F., KAWAGUCHI, S., MOCHIZUKI, M. & NAGAO, M. 2006. Characterization of Genotoxicity of Kojic Acid by Mutagenicity in Salmonella and Micronucleus Induction in Rodent Liver. *Genes and Environment,* 28**,** 31-37.

JIALAL, I. & SOKOLL, L. J. 2015. Clinical Utility of Lactate Dehydrogenase: A Historical Perspective. *American Journal of Clinical Pathology,* 143**,** 158-159.

JING, X., YANG, J., JIANG, L., CHEN, J. & WANG, H. 2018. MicroRNA-29b Regulates the Mitochondria-Dependent Apoptotic Pathway by Targeting Bax in Doxorubicin Cardiotoxicity. *Cellular Physiology and Biochemistry,* 48**,** 692-704.

JUNTTILA, M. R., LI, S. P. & WESTERMARCK, J. 2008. Phosphatase-mediated crosstalk between MAPK signaling pathways in the regulation of cell survival. *The FASEB Journal,* 22**,** 954-965.

KAKKAR, P. & SINGH, B. K. 2007. Mitochondria: a hub of redox activities and cellular distress control. *Molecular and Cellular Biochemistry,* 305**,** 235-53.

KALRA, A., YETISKUL, E., WEHRLE, C. & TUMA, F. I. 2020 Physiology, Liver.

KAMMERER, S. & KÜPPER, J.-H. 2018. Human hepatocyte systems for in vitro toxicology analysis. *Journal of Cellular Biotechnology,* 3**,** 85-93.

KAMMEYER, A. & LUITEN, R. M. 2015. Oxidation events and skin aging. *Ageing Research Reviews,* 21**,** 16-29.

KARIMIAN, A., AHMADI, Y. & YOUSEFI, B. 2016. Multiple functions of p21 in cell cycle, apoptosis and transcriptional regulation after DNA damage. *DNA Repair,* 42**,** 63-71.

KARUMURI, B. 2013. *Metabolic Assay Based Validation of Cell Viability to Inflammatory Stimuli and Anti-Cancer Drugs in Normal and Tumor Brain Glia*.

KATOH, S., TOYAMA, J., KODAMA, I., KAMIYA, K., AKITA, T. & ABE, T. 1992. Protective action of iron-chelating agents (catechol, mimosine, deferoxamine, and kojic acid) against ischemia-reperfusion injury of isolated neonatal rabbit hearts. *European Surgical Research,* 24**,** 349-55.

KAWAI, Y., GARDUÑO, L., THEODORE, M., YANG, J. & ARINZE, I. J. 2011. Acetylation-deacetylation of the transcription factor Nrf2 (nuclear factor erythroid 2-related factor 2) regulates its transcriptional activity and nucleocytoplasmic localization. *Journal of Biological Chemistry,* 286**,** 7629-40.

KIM, D., PARK, G. B. & HUR DAE, Y. 2014. Apoptotic signaling through reactive oxygen species in cancer cells. *World Journal of Immunology,* 4**,** 158-173.

KIM, D. H., HWANG, J. S., BAEK, H. S., KIM, K. J., LEE, B. G., CHANG, I., KANG, H. H. & LEE, O. S. 2003. Development of 5-[(3-aminopropyl)phosphinooxy]-2-(hydroxymethyl)-4H-pyran-4-one as a novel whitening agent. *Chemical and Pharmaceutical Bulletin* 51**,** 113-6.

KIM, J. H., CHANG, P.-K., CHAN, K. L., FARIA, N. C. G., MAHONEY, N., KIM, Y. K., MARTINS, M. D. L. & CAMPBELL, B. C. 2012. Enhancement of commercial antifungal agents by Kojic Acid. *International Journal of Molecular Sciences,* 13**,** 13867-13880.

KLEIN, J. R. & OLSEN, N. S. 1947. Inhibition of d-amino acid oxidase by kojic acid. *Fed Proc,* 6**,** 267.

KOOYERS, T. J. & WESTERHOF, W. 2004. [Toxicological aspects and health risks associated with hydroquinone in skin bleaching formula]. *Ned Tijdschr Geneeskd,* 148**,** 768-71.

KOTYZOVA, D., EYBL, V., KOUTENSKY, J., BRTKO, J. & GLATTRE, E. 2004. Effects of kojic acid on oxidative damage and on iron and trace element level in iron-overloaded mice and rats. *Central European Journal of Public Health,* 12 Suppl**,** S41-4.

KROEMER, G., DALLAPORTA, B. & RESCHE-RIGON, M. 1998. The mitochondria death/life regulator in apoptosis and necrosis. Annu Rev Physiol 60: 619-642. *Annual Review of Physiology,* 60**,** 619-42.

KUANG, J., YAN, X., GENDERS, A. J., GRANATA, C. & BISHOP, D. J. 2018. An overview of technical considerations when using quantitative real-time PCR analysis of gene expression in human exercise research. *PLoS ONE* 13**,** 1-27.

KUNDUKAD, B., UDAYAKUMAR, G., GRELA, E., KAUR, D., RICE, S. A., KJELLEBERG, S. & DOYLE, P. S. 2020. Weak acids as an alternative anti-microbial therapy. *Biofilm,* 2**,** 100019.

LAJIS, A. F. B., HAMID, M. & ARIFF, A. B. 2012. Depigmenting effect of Kojic acid esters in hyperpigmented B16F1 melanoma cells. *Journal of Biomedicine & Biotechnology,* 2012**,** 1-9.

LEE, H. F., BOLTJES, B. & EISENMAN, W. 1950. Kojic Acid as an Inhibitor of Tubercle Bacilli. *American Review of Tuberculosis and Pulmonary Diseases,* 61**,** 738-41.

LIGUORI, I., RUSSO, G., CURCIO, F., BULLI, G., ARAN, L., DELLA-MORTE, D., GARGIULO, G., TESTA, G., CACCIATORE, F., BONADUCE, D. & ABETE, P. 2018. Oxidative stress, aging, and diseases. *Clinical Interventions in Aging,* 13**,** 757-772.

LIN, J. Y. & FISHER, D. E. 2007. Melanocyte biology and skin pigmentation. *Nature,* 445**,** 843-50.

LIVAK, K. J. & SCHMITTGEN, T. D. 2001. Analysis of Relative Gene Expression Data Using Real-Time Quantitative PCR and the 2−ΔΔCT Method. *Methods,* 25**,** 402-408.

LORETO, C., LA ROCCA, G., ANZALONE, R., CALTABIANO, R., VESPASIANI, G., CASTORINA, S., RALPH, D. J., CELLEK, S., MUSUMECI, G., GIUNTA, S., DJINOVIC, R., BASIC, D. & SANSALONE, S. 2014. The role of intrinsic pathway in apoptosis activation and progression in Peyronie's disease. *Biomed Research International,* 2014**,** 1-10.

LUKIW, W. J., ZHAO, Y. & CUI, J. G. 2008. An NF-kappaB-sensitive micro RNA-146a-mediated inflammatory circuit in Alzheimer disease and in stressed human brain cells. *The Journal of Biological Chemistry,* 283**,** 31315-31322.

LUNA, C., LI, G., QIU, J., EPSTEIN, D. L. & GONZALEZ, P. 2009. Role of miR-29b on the regulation of the extracellular matrix in human trabecular meshwork cells under chronic oxidative stress. *Molecular vision,* 15**,** 2488-2497.

MA, X., BECKER BUSCAGLIA, L. E., BARKER, J. R. & LI, Y. 2011. MicroRNAs in NF-kappaB signaling. *Journal of Molecular Cell Biology,* 3**,** 159-166.

MAHMOOD, T. & YANG, P.-C. 2012. Western blot: technique, theory, and trouble shooting. *North American journal of medical sciences,* 4**,** 429-434.

MASUM, M. N., YAMAUCHI, K. & MITSUNAGA, T. 2019. Tyrosinase Inhibitors from Natural and Synthetic Sources as Skin-lightening Agents. *Reviews in Agricultural Science,* 7**,** 41-58.

MAURER, B., STANCZYK, J., JÜNGEL, A., AKHMETSHINA, A., TRENKMANN, M., BROCK, M., KOWAL-BIELECKA, O., GAY, R. E., MICHEL, B. A., DISTLER, J. H., GAY, S. & DISTLER, O. 2010. MicroRNA-29, a key regulator of collagen expression in systemic sclerosis. *Arthritis Rheum,* 62**,** 1733-43.

MAYER, A. M. 1986. Polyphenol oxidases in plants-recent progress. *Phytochemistry,* 26**,** 11-20.

MESSADI, D. V., DOUNG, H. S., ZHANG, Q., KELLY, A. P., TUAN, T. L., REICHENBERGER, E. & LE, A. D. 2004. Activation of NFkappaB signal pathways in keloid fibroblasts. *Arch Dermatol Res,* 296**,** 125-33.

MISHRA, M., TIWARI, S. & GOMES, A. V. 2017. Protein purification and analysis: next generation Western blotting techniques. *Expert review of proteomics,* 14**,** 1037-1053.

MOHAMAD, R., MOHAMED, M., SUHAILI, N., SALLEH, M. & ARIFF, A. 2010. Kojic acid: Applications and development of fermentation process for production. *Biotechnology and Molecular Biology Reviews,* 5**,** 24-37.

MOON, K. Y., AHN, K. S., LEE, J. & KIM, Y. S. 2001. Kojic acid, a potential inhibitor of NF-kappaB activation in transfectant human HaCaT and SCC-13 cells. *Archives of Pharmacal Research,* 24**,** 307-11.

MORRISON, D. K. 2012. MAP kinase pathways. *Cold Spring Harbor perspectives in biology,* 4**,** a011254.

MOTO, M., MORI, T., OKAMURA, M., KASHIDA, Y. & MITSUMORI, K. 2006. Absence of liver tumor-initiating activity of kojic acid in mice. *Arch Toxicol,* 80**,** 299-304.

MURPHY, M. P. 2009. How mitochondria produce reactive oxygen species. *Biochem J,* 417**,** 1-13.

NAKAGAWA, M., KAWAI, K. & KAWAI, K. 1995. Contact allergy to kojic acid in skin care products. *Contact Dermatitis,* 32**,** 9-13.

NAKAYAMA, H. 1982. Treatment of chloasma with topical Kojic Acid. *Jap. J. Clin. Dermatol.,* 36**,** 715-722.

NAWARAK, J., HUANG-LIU, R., KAO, S.-H., LIAO, H.-H., SINCHAIKUL, S., CHEN, S.-T. & CHENG, S.-L. 2008. Proteomics Analysis of Kojic Acid Treated A375 Human Malignant Melanoma Cells. *Journal of Proteome Research,* 7**,** 3737-3746.

NGUYEN, T., NIOI, P. & PICKETT, C. B. 2009. The Nrf2-antioxidant response element signaling pathway and its activation by oxidative stress. *Journal of Biological Chemistry,* 284**,** 13291-5.

NIWA, Y. & AKAMATSU, H. 1991. Kojic acid scavenges free radicals while potentiating leukocyte functions including free radical generation. *Inflammation,* 15**,** 303-315.

O'BRIEN, J., HAYDER, H., ZAYED, Y. & PENG, C. 2018. Overview of MicroRNA Biogenesis, Mechanisms of Actions, and Circulation. *Frontiers in Endocrinology,* 9.

OGIWARA, Y., SUGIURA, M., WATANABE, K., TAWARA, J., ENDO, E., MARUYAMA, H., TSUJI, S., MATSUE, K., YAMADA, H., WAKO, Y. & KAWASAKO, K. 2015. Evaluation of the repeated-dose liver, bone marrow and peripheral blood micronucleus and comet assays using kojic acid. *Mutation Research/Genetic Toxicology and Environmental Mutagenesis,* 780-781**,** 111-116.

ONCUL, S., KARAKAYA, G., DILSIZ AYTEMIR, M. & ERCAN, A. 2019. A kojic acid derivative promotes intrinsic apoptotic pathway of hepatocellular carcinoma cells without incurring drug resistance. *Chemical Biology and Drug Design***,** 1-10.

OTT, M., GOGVADZE, V., ORRENIUS, S. & ZHIVOTOVSKY, B. 2007. Mitochondria, oxidative stress and cell death. *Apoptosis,* 12**,** 913-922.

PARRISH, F. W., WILEY, B. J., SIMMONS, E. G. & LONG, L., JR. 1966. Production of aflatoxins and kojic acid by species of Aspergillus and Penicillium. *Applied microbiology,* 14**,** 139-139.

PAWELEK, J. M. & KÖRNER, A. M. 1982. The biosynthesis of mammalian melanin. *Am Sci,* 70**,** 136-45.

PEKKARINEN, S. S., HEINONEN, I. M. & HOPIA, A. I. 1999. Flavonoids quercetin, myricetin, kaemferol and (+)-catechin as antioxidants in methyl linoleate. *Journal of the Science of Food and Agriculture,* 79**,** 499-506.

PIZZINO, G., IRRERA, N., CUCINOTTA, M., PALLIO, G., MANNINO, F., ARCORACI, V., SQUADRITO, F., ALTAVILLA, D. & BITTO, A. 2017. Oxidative Stress: Harms and Benefits for Human Health. *Oxidative medicine and cellular longevity,* 2017**,** 8416763-8416763.

PLATTNER, F. & BIBB, J. A. 2012. Chapter 25 - Serine and Threonine Phosphorylation. *In:* BRADY, S. T., SIEGEL, G. J., ALBERS, R. W. & PRICE, D. L. (eds.) *Basic Neurochemistry (Eighth Edition).* New York: Academic Press.

RAMANA, K. V., SRIVASTAVA, S. & SINGHAL, S. S. 2013. Lipid Peroxidation Products in Human Health and Disease. *Oxidative Medicine and Cellular Longevity,* 2013**,** 583438.

REDZA-DUTORDOIR, M. & AVERILL-BATES, D. A. 2016. Activation of apoptosis signalling pathways by reactive oxygen species. *Biochimica et Biophysica Acta (BBA) - Molecular Cell Research,* 1863**,** 2977-2992.

REINHART, B. J., SLACK, F. J., BASSON, M., PASQUINELLI, A. E., BETTINGER, J. C., ROUGVIE, A. E., HORVITZ, H. R. & RUVKUN, G. 2000. The 21-nucleotide let-7 RNA regulates developmental timing in Caenorhabditis elegans. *Nature,* 403**,** 901-6.

RODRIGUES, A. P., CARVALHO, A. S., SANTOS, A. S., ALVES, C. N., DO NASCIMENTO, J. L. & SILVA, E. O. 2011. Kojic acid, a secondary metabolite from Aspergillus sp., acts as an inducer of macrophage activation. *Cell Biol Int,* 35**,** 335-43.

SAEEDI, M., ESLAMIFAR, M. & KHEZRI, K. 2019. Kojic acid applications in cosmetic and pharmaceutical preparations. *Biomedicine and Pharmacotherapy,* 110**,** 582-593.

SAKAMOTO, S., PUTALUN, W., VIMOLMANGKANG, S., PHOOLCHAROEN, W., SHOYAMA, Y., TANAKA, H. & MORIMOTO, S. 2018. Enzyme-linked immunosorbent assay for the quantitative/qualitative analysis of plant secondary metabolites. *Journal of natural medicines,* 72**,** 32-42.

SALMINEN, A., KAARNIRANTA, K. & KAUPPINEN, A. 2013. Crosstalk between Oxidative Stress and SIRT1: Impact on the Aging Process. *International journal of molecular sciences,* 14**,** 3834-3859.

SANSHO SEIYAKU CO., L. 2001. Absorption, distribution, metabolism, and excretion (ADME) of kojic acid in the rat. *Unpublished*.

SAUER, H., WARTENBERG, M. & HESCHELER, J. 2001. Reactive oxygen species as intracellular messengers during cell growth and differentiation. *Cell Physiol Biochem,* 11**,** 173-86.

SCCP, S. C. O. C. P. 2008. Opinion on Kojic acid.

SCHMILZ, M. L. 1995. Function and activation of the transcription factor NF-KB in the response to toxins and pathogens. *Toxicology Letters,* 82-83**,** 407-411.

SHALINI, S., DORSTYN, L., DAWAR, S. & KUMAR, S. 2015. Old, new and emerging functions of caspases. *Cell Death & Differentiation,* 22**,** 526-539.

SHAULIAN, E. & KARIN, M. 2002. AP-1 as a regulator of cell life and death. *Nature Cell Biology,* 4**,** E131-6.

SINGH, G., PACHOURI, U. C., KHAIDEM, D. C., KUNDU, A., CHOPRA, C. & SINGH, P. 2015. Mitochondrial DNA Damage and Diseases. *F1000Research,* 4**,** 176-176.

SOUZA, M. D. L. M. D., SULYOK, M., FREITAS-SILVA, O., COSTA, S. S., BRABET, C., MACHINSKI JUNIOR, M., SEKIYAMA, B. L., VARGAS, E. A., KRSKA, R. & SCHUHMACHER, R. 2013. Cooccurrence of Mycotoxins in Maize and Poultry Feeds from Brazil by Liquid Chromatography/Tandem Mass Spectrometry. *The Scientific World Journal,* 2013**,** 427369.

STANCZYK, J., PEDRIOLI, D. M., BRENTANO, F., SANCHEZ-PERNAUTE, O., KOLLING, C., GAY, R. E., DETMAR, M., GAY, S. & KYBURZ, D. 2008. Altered expression of MicroRNA in synovial fibroblasts and synovial tissue in rheumatoid arthritis. *Arthritis Rheum,* 58**,** 1001-9.

STRATFORD, M. & ANSLOW, P. 1998. Evidence that sorbic acid does not inhibit yeast as a classic 'weak acid preservative'. *Letters in Applied Microbiology,* 27**,** 203-206.

STROBER, W. 2015. Trypan Blue Exclusion Test of Cell Viability. *Current protocols in immunology,* 111**,** A3.B.1-A3.B.3.

SU, W.-H., WANG, C.-J., HUNG, Y.-Y., LU, C.-W., OU, C.-Y., TSENG, S.-H., TSAI, C.-C., KAO, Y.-T. & CHUANG, P.-C. 2019. MicroRNA-29a Exhibited Pro-Angiogenic and Anti-Fibrotic Features to Intensify Human Umbilical Cord Mesenchymal Stem Cells-Renovated Perfusion Recovery and Preventing against Fibrosis from Skeletal Muscle Ischemic Injury. *International Journal of Molecular Sciences,* 20**,** 1-24.

SUN, Z., HUANG, Z. & ZHANG, D. D. 2009. Phosphorylation of Nrf2 at Multiple Sites by MAP Kinases Has a Limited Contribution in Modulating the Nrf2 Dependent Antioxidant Response. *Plos One,* 4**,** 1-9.

TAMURA, T., MITSUMORI, K., TOTSUKA, Y., WAKABAYASHI, K., KIDO, R., KASAI, H., NASU, M. & HIROSE, M. 2006. Absence of *in vivo* genotoxic potential and tumor initiation activity of Kojic acid in the rat thyroid. *Toxicology,* 222**,** 213-224.

TIAO, M.-M., WANG, F.-S., HUANG, L.-T., CHUANG, J.-H., KUO, H.-C., YANG, Y.-L. & HUANG, Y.-H. 2014. MicroRNA-29a protects against acute liver injury in a mouse model of obstructive jaundice via inhibition of the extrinsic apoptosis pathway. *Apoptosis,* 19**,** 30-41.

UHER, M., KONECNY, V. & RAJNIAKOVA, O. 1994. Synthesis of 5-hydroxy-2-hydroxymethyl-4H-pyran-4-one derivatives with pesticide activity. *Chem. Pap.,* 48**,** 282-284.

VALAVANIDIS, A., VLACHOGIANNI, T. & FIOTAKIS, C. 2009. 8-hydroxy-2′ -deoxyguanosine (8-OHdG): A Critical Biomarker of Oxidative Stress and Carcinogenesis. *Journal of*

environmental science and health. Part C, Environmental carcinogenesis & ecotoxicology reviews, 27**,** 120-39.

WALKER, J. M. 1996. The Bicinchoninic Acid (BCA) Assay for Protein Quantitation. *In:* WALKER, J. M. (ed.) *The Protein Protocols Handbook.* Totowa, NJ: Humana Press, 11-14.

WANG, P., ZHU, C.-F., MA, M.-Z., CHEN, G., SONG, M., ZENG, Z.-L., LU, W.-H., YANG, J., WEN, S. & CHIAO, P. J. 2015. Micro-RNA-155 is induced by K-Ras oncogenic signal and promotes ROS stress in pancreatic cancer. *Oncotarget,* 6**,** 21148-21158.

WANG, Y., BRANICKY, R., NOË, A. & HEKIMI, S. 2018. Superoxide dismutases: Dual roles in controlling ROS damage and regulating ROS signaling. *The Journal of cell biology,* 217**,** 1915-1928.

WATANABE, T., MORI, T., KITAMURA, Y., UMEMURA, T., OKAMURA, M., KASHIDA, Y., NISHIKAWA, A., HIROSE, M. & MITSUMORI, K. 2005 Lack of Initiating Activity of Kojic Acid on Hepatocarcinogenesis in F344 Rats. *J Toxicol Pathol* 18**,** 79–84.

WEI, X., LUO, D., YAN, Y., YU, H., SUN, L., WANG, C., SONG, F., GE, H., QIAN, H., LI, X., TANG, X. & LIU, P. 2019. Kojic acid inhibits senescence of human corneal endothelial cells via NF-κB and p21 signaling pathways. *Experimental Eye Research,* 180**,** 174-183.

WESTON, C. R. & DAVIS, R. J. 2002. The JNK Signal Transduction Pathway. *Current Opinion in Genetics & Development,* 12**,** 14-21.

WIEMER, E. A. 2007. The role of microRNAs in cancer: no small matter. *Eur J Cancer,* 43**,** 1529-44.

WIESMÜLLER, L., FORD, J. M. & SCHIESTL, R. H. 2002. DNA Damage, Repair, and Diseases. *Journal of biomedicine & biotechnology,* 2**,** 45-45.

WILSON, B. J. 1966. Toxins other than aflatoxins produced by Aspergillus flavus. *Bacteriological reviews,* 30**,** 478-484.

WONG, R. S. 2011. Apoptosis in cancer: from pathogenesis to treatment. *J Exp Clin Cancer Res,* 30**,** 87.

WU, Y., SHI, Y. G., ZENG, L. Y., PAN, Y., HUANG, X. Y., BIAN, L. Q., ZHU, Y. J., ZHANG, R. R. & ZHANG, J. 2019. Evaluation of antibacterial and anti-biofilm properties of kojic acid against five food-related bacteria and related subcellular mechanisms of bacterial inactivation. *Food Sci Technol Int,* 25**,** 3-15.

XIE, J., ZHANG, X. & ZHANG, L. 2013a. Negative regulation of inflammation by SIRT1. *Pharmacological Research,* 67**,** 60-7.

XIE, J., ZHANG, X. & ZHANG, L. 2013b. Negative regulation of inflammation by SIRT1. *Pharmacol Res,* 67**,** 60-7.

YAKES, F. M. & VAN HOUTEN, B. 1997. Mitochondrial DNA damage is more extensive and persists longer than nuclear DNA damage in human cells following oxidative stress. *Proceedings of the National Academy of Sciences,* 94**,** 514.

YANG, H., ZHANG, W., PAN, H., FELDSER, H. G., LAINEZ, E., MILLER, C., LEUNG, S., ZHONG, Z., ZHAO, H., SWEITZER, S., CONSIDINE, T., RIERA, T., SURI, V., WHITE, B., ELLIS, J. L., VLASUK, G. P. & LOH, C. 2012. SIRT1 Activators Suppress Inflammatory Responses through Promotion of p65 Deacetylation and Inhibition of NF-κB Activity. *PLOS ONE,* 7**,** e46364.

YEUNG, F., HOBERG, J. E., RAMSEY, C. S., KELLER, M. D., JONES, D. R., FRYE, R. A. & MAYO, M. W. 2004. Modulation of NF-kappaB-dependent transcription and cell survival by the SIRT1 deacetylase. *Embo j,* 23**,** 2369-80.

YIN, B., WHYATT, R. M., PERERA, F. P., RANDALL, M. C., COOPER, T. B. & SANTELLA, R. M. 1995. Determination of 8-hydroxydeoxyguanosine by an Immunoaffinity Chromatography-Monoclonal antibody-based ELISA. *Free Radical Biology and Medicine,* 18**,** 1023-1032.

ZEKE, A., MISHEVA, M., REMÉNYI, A. & BOGOYEVITCH, M. A. 2016. JNK Signaling: Regulation and Functions Based on Complex Protein-Protein Partnerships. *Microbiology and Molecular Biology Reviews,* 80**,** 793.

ZHANG, J., CHEN, H., CHEN, M., WANG, H., WANG, Q., SONG, X., HAO, H. & FENG, Z. 2017. Kojic acid-mediated damage responses induce mycelial regeneration in the basidiomycete Hypsizygus marmoreus. *PLoS One,* 12**,** 1-20.

ZHANG, J., HAN, X. & LIN, Y. 2018. Dissecting the regulation and function of ATP at the single-cell level. *PLOS Biology,* 16**,** 1-7.

ZHANG, J., WANG, X., VIKASH, V., YE, Q., WU, D., LIU, Y. & DONG, W. 2016. ROS and ROS-Mediated Cellular Signaling. *Oxidative Medicine and Cellular Longevity,* 2016**,** 4350965.

ZHAO, R. Z., JIANG, S., ZHANG, L. & YU, Z. B. 2019. Mitochondrial electron transport chain, ROS generation and uncoupling (Review). *Int J Mol Med,* 44**,** 3-15.

ZOLGHADRI, S., BAHRAMI, A., HASSAN KHAN, M. T., MUNOZ-MUNOZ, J., GARCIA-MOLINA, F., GARCIA-CANOVAS, F. & SABOURY, A. A. 2019. A comprehensive review on tyrosinase inhibitors. *Journal of enzyme inhibition and medicinal chemistry,* 34**,** 279-309.

APPENDIX A

KA increased cell viability at concentrations (0-4.22 mM) following a 6h KA-treatment with the highest increase in cell viability at 4.22 mM (170.65%). A decrease in cell viability in comparison to 4.22 mM, was observed at 5.63 -12.7 mM with the lowest cell viability percentage at 126.8% (Fig 4). There was no inhibition of cell viability observed relative to the control (p =0.0006).

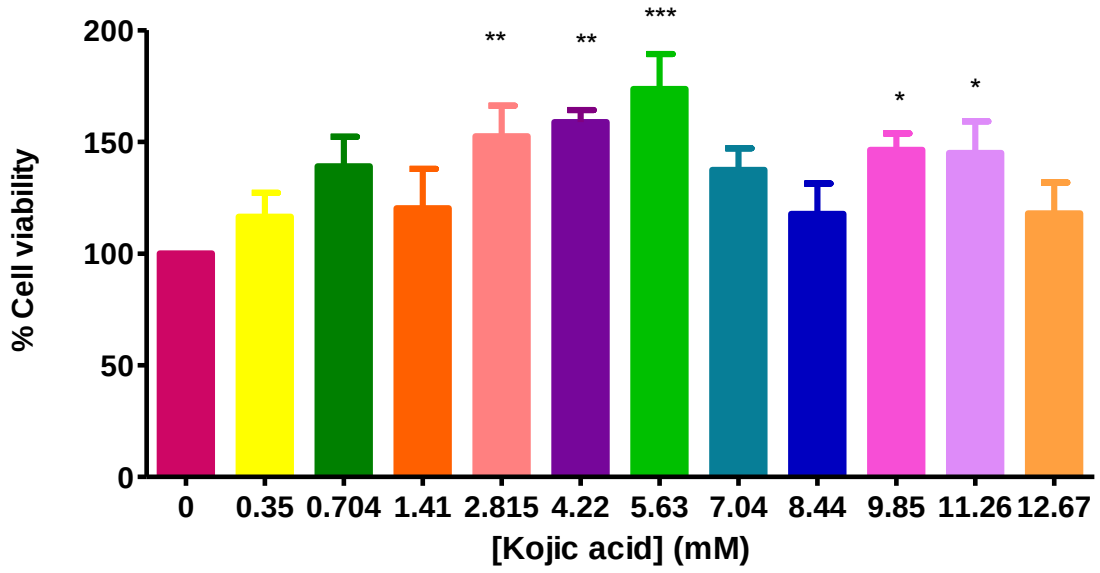

Figure 4.1 KA increased cell viability as depicted using the MTT assay in HepG2 cells for 6h (*p<0.05, **p<0.001, ***p<0.0001) (n = 3)

APPENDIX B

KA dose-dependently decreased cell viability of HepG2 cells following a 48h treatment (Fig 5). The data illustrates that KA is cytotoxic to cells with an IC_{50} = 7.2 mM. The IC_{50} was determined to be similar to that of the 24h treatment. Therefore, subsequent treatments were carried out at the determined 50% cell death concentrations for 24h.

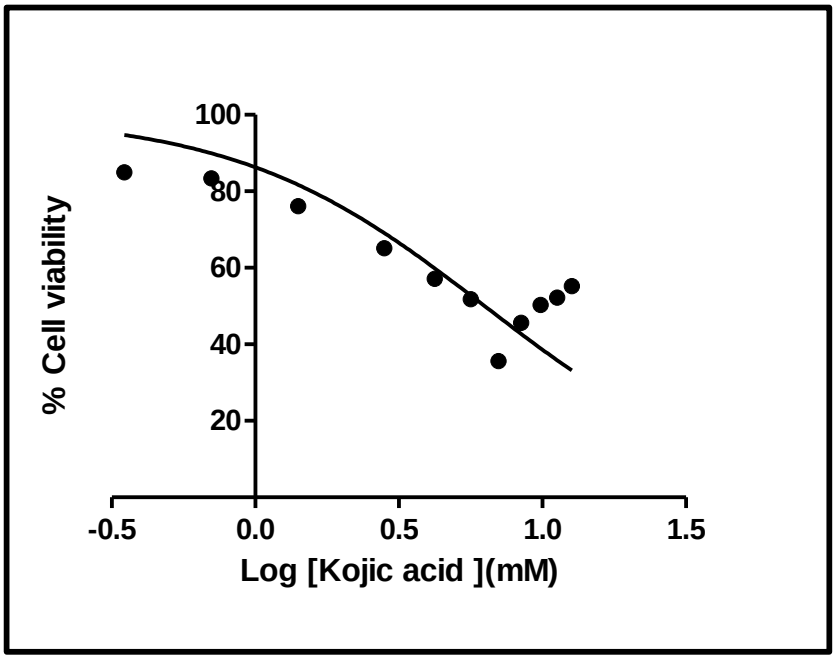

Figure 5.1 KA dose-dependently decreased HepG2 cell viability as depicted using the MTT assay for 48h (IC_{50}= 7.2 mM)

APPENDIX C

BCA assay (Western Blot protein preparation)

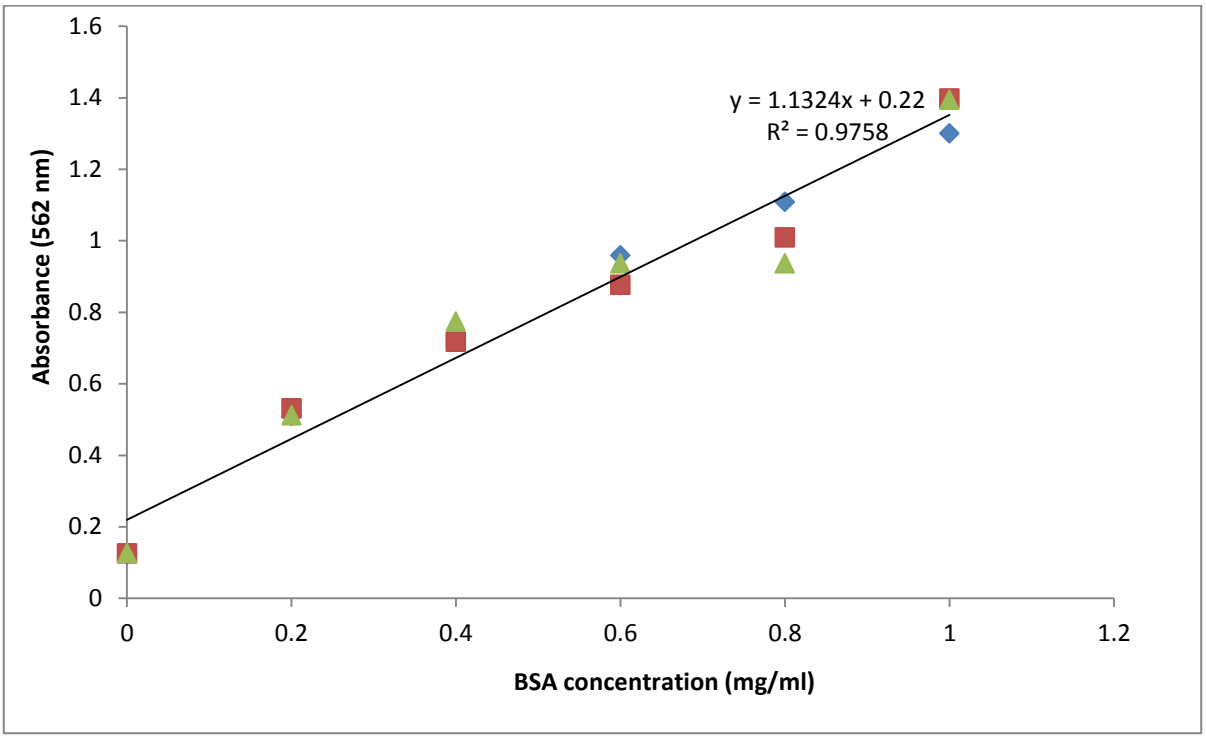

Figure 6.1 Standard curve obtained from BSA protein standard to determine the unknown concentrations of protein in samples

Table 6. Standardisation of proteins used for Western Blot (Final volume = 200µl; concentration = 1.5 mg/ml)

Sample (mM)	Mean absorbance	Protein concentration (mg/ml)	Volume of Protein stock (µl)	CytoBuster (µl)	Volume of Laemmli buffer (µl)
0	1.976	1.550689	129.03	70.97	200
4.22	2.2995	1.836365	108.7	91.3	200
8.02	2.0945	1.655334	121.21	78.79	200
12.67	1.9215	1.502561	133.33	66.67	200

APPENDIX D

BCA assay (Protein carbonyl preparation)

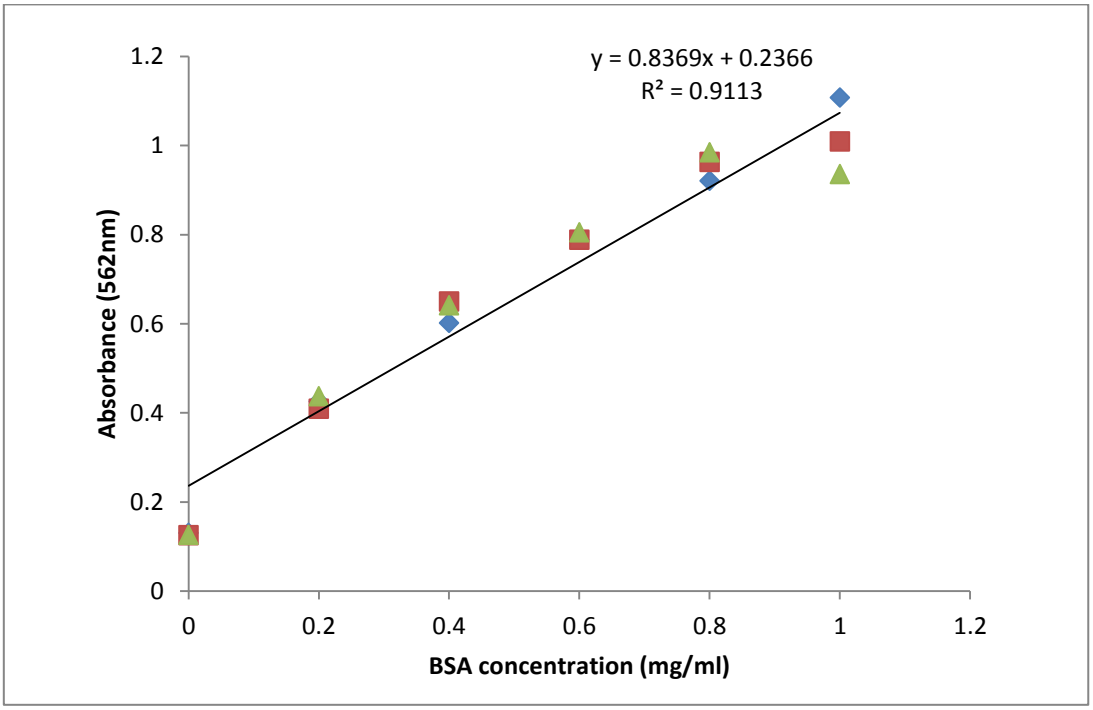

Figure 7.1 Standard curve obtained from BSA protein standard to determine the unknown concentrations of protein in samples

Table 7. Standardisation of proteins used for the protein carbonyl assay (Final volume = 300µl; concentration = 1.0 mg/ml)

Sample (mM)	Mean absorbance	Protein concentration (mg/ml)	Volume of Protein stock (µl)	Cell Lysis solution (µl)	Volume of Laemmli buffer (µl)
0	2.291	2.00829	149.3808	150.6192	300
4.22	2.079	1.79629	167.0109	132.9891	300
8.02	2.0855	1.80279	166.4087	133.5913	300
12.67	2.1005	1.81779	165.0356	134.9644	300

APPENDIX E

DNA isolation standardisation

Table 8. Standardisation of DNA used for ELISA (Final volume = 150µl; concentration = 100 ng/ml)

Concentrations (mM)	DNA stock (µl)	TE buffer (µl)
0	18.32	131.68
4.22	11.34	138.66
8.02	13.98	136.02
12.67	13.21	136.79

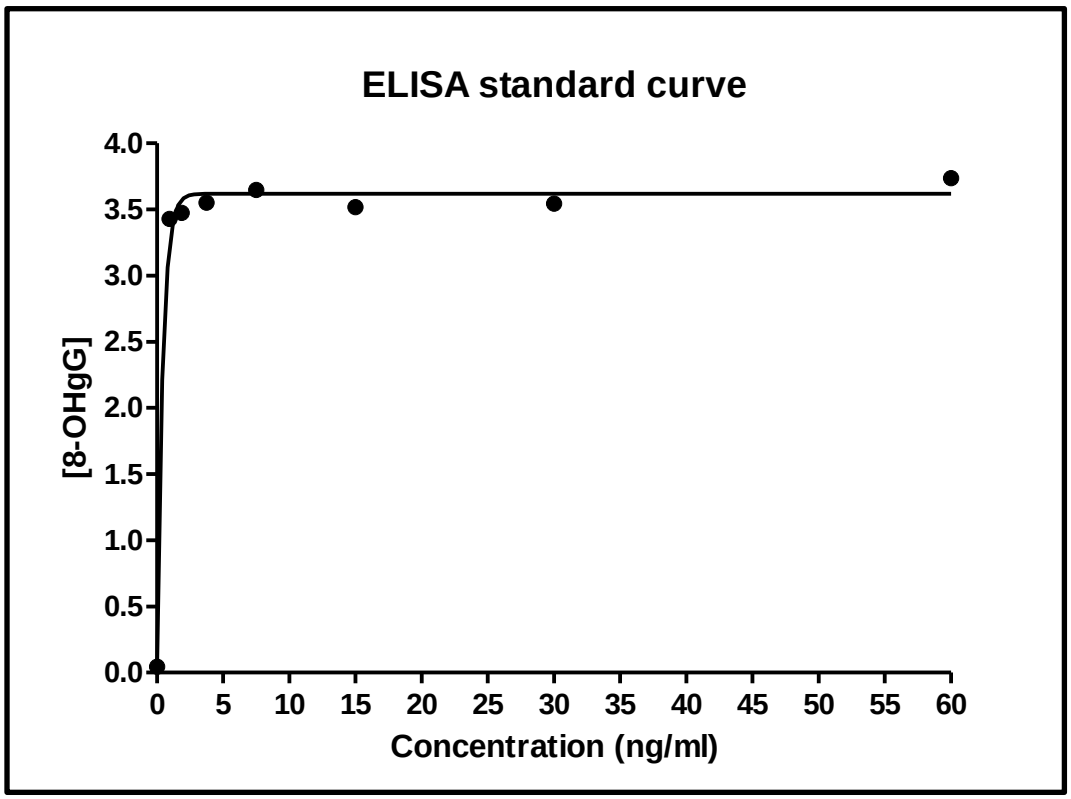

Figure 8 The 8-OHdG concentrations standards obtained from ELISA to extrapolate unknown concentration of DNA adducts in treatment samples

Table 9: Concentrations extrapolated from the 8-OHdG standard concentration graph

Concentration of Treatment (mM)	Concentration of DNA damage (ng/ml)
0	0.7315
4.22	0.8872
8.02	1.1702
12.67	0.4937

APPENDIX F

Turnitin Report

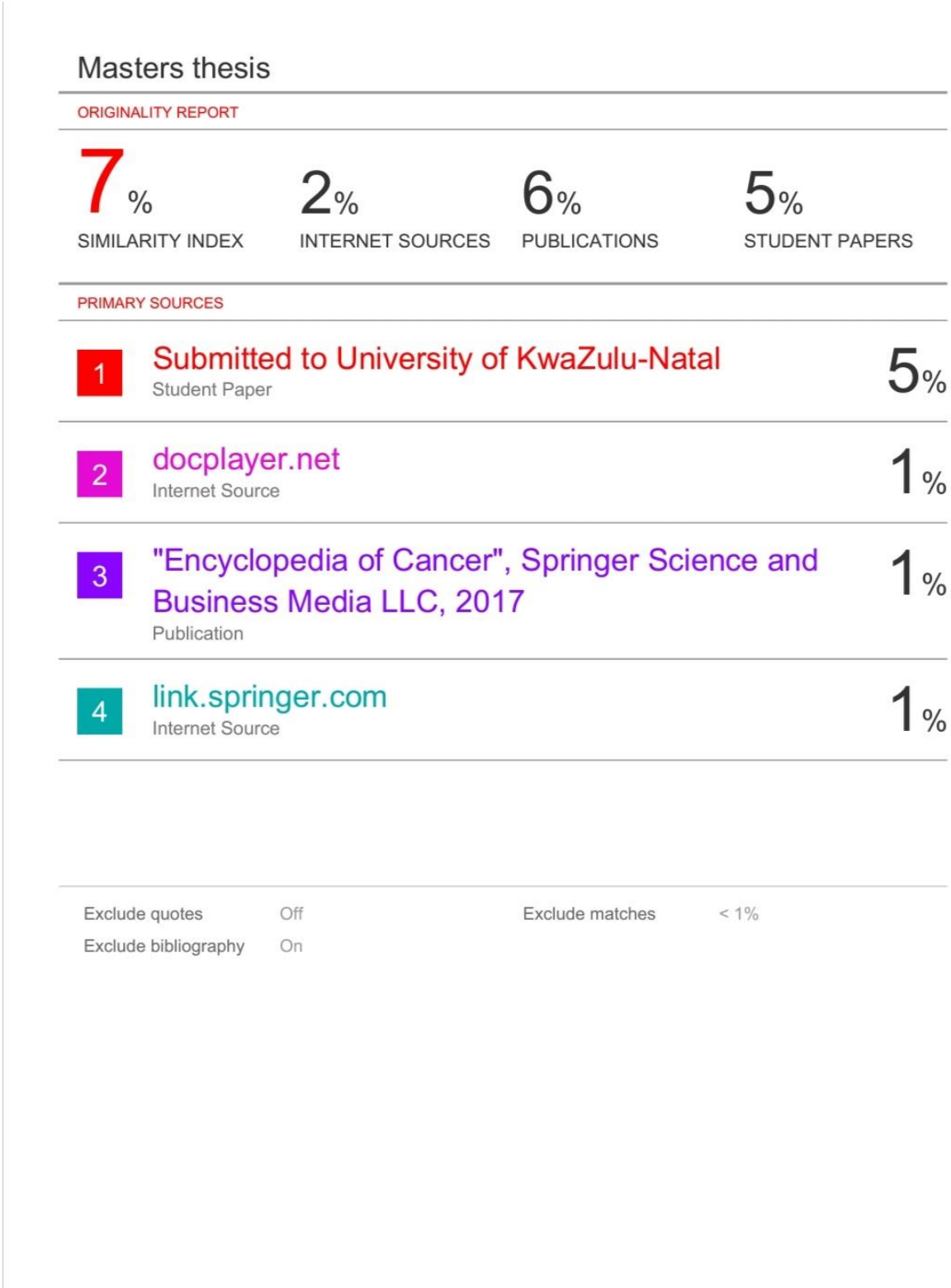

Masters thesis

ORIGINALITY REPORT

7%	2%	6%	5%
SIMILARITY INDEX	INTERNET SOURCES	PUBLICATIONS	STUDENT PAPERS

PRIMARY SOURCES

1	Submitted to University of KwaZulu-Natal Student Paper	5%
2	docplayer.net Internet Source	1%
3	"Encyclopedia of Cancer", Springer Science and Business Media LLC, 2017 Publication	1%
4	link.springer.com Internet Source	1%

Exclude quotes	Off	Exclude matches	< 1%
Exclude bibliography	On		